TRANSPORTATION RESEARCH RECORD 860

Snow Control, Traffic Effects on New Concrete, and Corrosion

TRANSPORTATION RESEARCH BOARD

NATIONAL RESEARCH COUNCIL

NATIONAL ACADEMY OF SCIENCES
WASHINGTON, D.C. 1982

Transportation Research Record 860
Price $7.20
Edited for TRB by Naomi Kassabian

mode
1 highway transportation

subject areas
25 structures design and performance
32 cement and concrete
34 general materials
40 maintenance
64 soil science

Library of Congress Cataloging in Publication Data
National Research Council. Transportation Research Board.
Snow control, traffic effects on new concrete, and corrosion.

(Transportation research record; 860)
1. Roads–Snow and ice control–Addresses, essays, lectures. 2. Pavements, Concrete–Addresses, essays, lectures. 3. Concrete–Corrosion–Addresses, essays, lectures. 4. Traffic engineering–Addresses, essays, lectures. I. National Research Council (U.S.). Transportation Research Board. II. Series.
TE7.H5 no. 860 [TE220.5] 380.5 625.7'63] 82-19019
ISBN 0-309-03363-2 ISSN 0361-1981

Sponsorship of the Papers in This Transportation Research Record

GROUP 3–OPERATION AND MAINTENANCE OF TRANSPORTATION FACILITIES
Patricia F. Waller, University of North Carolina at Chapel Hill, chairman

Committee on Structures Maintenance
Roland H. Berger, Byrd, Tallamy, MacDonald & Lewis, chairman
Jimmy D. Lee, North Carolina Department of Transportation, secretary
Bernard R. Appleman, Myron G. Brown, William G. Byers, Robert C. Donnaruma, Al J. Dunn, Ian J. Dussek, Nicholas M. Engleman, Stanley Gordon, Robert N. Kamp, Henry L. Kinnier, L. A. Kuhlmann, Gayle E. Lane, David G. Manning, R. J. Posthauer, John G. Risch, Jack W. Roberts, George P. Romack, Steven J. Shecter, Charles Slavis, James Allen Tavenner, Marilyn H. Tobey, Robert G. Tracy, Alden L. West

Committee on Winter Maintenance
L. David Minsk, U.S. Army CRREL, chairman
Franklin S. Adams, Robert R. Blackburn, Francis H. Carr, Jr., John C. Cook, Robert A. Crawford, Henri DeLannoy, William E. Dickinson, Charles E. Dougan, Karl H. Dunn, Henry W. Farrell, Gerald P. Fitzgerald, Brice E. Horwell, John G. Irving, Edward J. Kehl, James F. Kelley, Henry W. Kirchner, John M. Kirtland, Byron N. Lord, William J. O'Brien, Warren M. Reeves, T. Ray Ringer, George R. Russell, Ronald D. Tabler, Ross G. Wilcox

Committee on Corrosion
Harold J. Fromm, Ministry of Transportation & Communications, chairman
Kenneth J. Boedecker, Jr., E. J. Breckwoldt, Kenneth C. Clear, Seymour K. Coburn, Carl F. Crumpton, Richard J. Kessler, Walter Kilareski, David G. Manning, A. P. Moser, Arnold M. Rosenberg, Gary T. Satterfield, Herbert J. Schmidt, Jr., Robert G. Tracy, Frank O. Wood

Adrian G. Clary, Transportation Research Board staff

Sponsorship is indicated by a footnote at the end of each report. The organizational units, officers, and members are as of December 31, 1981.

Contents

Authors of the Papers in This Record

Crumpton, Carl F., Kansas Department of Transportation, Bureau of Materials and Research, 2300 Van Buren Street, Topeka, KS 66611
Donnelly, Denis, Colorado Department of Highways, 4201 East Arkansas Avenue, Denver, CO 80222
Esch, David C., State of Alaska Department of Transportation and Public Facilities, 2301 Peger Road, Fairbanks, AK 99701
Fouad, Fouad H., School of Engineering and Department of Civil Engineering, University of Alabama in Birmingham, University Station, Birmingham, AL 35294
Fromm, H.J., Ontario Ministry of Transportation and Communications, 1201 Wilson Avenue, Downsview, Ontario, Canada M3M 1J8
Furnish, Richard P., Traffic Operations Branch, Wyoming State Highway Department, P.O. Box 1708, Cheyenne, WY 82002
Furr, Howard L., Department of Civil Engineering, Texas A&M University, College Station, TX 77843
Griffin, Richard, Colorado Department of Highways, 4201 East Arkansas Avenue, Denver, CO 80222
Gustafson, Kent, Statens vag-och trafikinstitut, Fack, S-581 01, Linköping, Sweden
Jayaprakash, G.P., Kansas Department of Transportation, Bureau of Materials and Research, 2300 Van Buren Street, Topeka, KS 66611
Korfhage, Glenn R., Minnesota Department of Transportation, Room B-9, Transportation Building, St. Paul, MN 55155
Nydahl, John, College of Engineering, University of Wyoming, University Station, Box 3295, Laramie, WY 82071
Pell, Kynric M., University of Wyoming, P.O. Box 3295, Laramie, WY 82071
Pianca, F., Ontario Ministry of Transportation and Communications, 1201 Wilson Avenue, Downsview, Ontario, Canada M3M 1J8
Swanson, Herbert, Colorado Department of Highways, 4201 East Arkansas Avenue, Denver, CO 80222
Tabler, Ronald D., Rocky Mountain Forest and Range Experiment Station, Forest, Range, and Watershed Laboratory, 222 South 22nd Street, Laramie, WY 82070

Geothermal Heating of Highway Structures

JOHN NYDAHL, KYNRIC M. PELL, DENIS DONNELLY, HERBERT SWANSON, AND RICHARD GRIFFIN

A report is given on the Colorado Department of Highways feasibility study to incorporate geothermal heating systems at critical locations in the proposed Interstate through Glenwood Canyon. The investigation was prompted by the concern that the proximity of the Colorado River and the extensive shading by the canyon walls may cause significant icing and preferential freezing problems on portions of the elevated structures. The direct application of the locally available geothermal water in the bridge decks to reduce these hazards was precluded primarily due to the possibility of freezing but also because of fouling and corrosion problems. The use of heat pipes as intermediate heat exchangers between the water and the deck was proposed to eliminate the possibility of water freezing in the deck and because of its effectiveness in similar applications. Ammonia-charged gravity-operated heat pipes were constructed by using two different evaporator designs and several condenser spacings in order to experimentally determine the performance of these heating systems. The snow-cover duration above all these heat exchangers relative to the unheated control was reduced by 96 percent or more even though the modules were extremely fouled by the geothermal water. The water-flow rate and temperature were 35 gal/min (133 L/min) and 25°C (77°F), respectively, over much of the 1980-1981 winter test. It appears that a fairly large number of these units could have been run in series before an appreciable degradation in the performance of the latter units would have occurred. In cases requiring minimal snow-melting capability or involving preferential icing problems, the water temperature could possibly be as low as 10° C (50° F), which means that well water or municipal water supplies would be feasible water sources.

An 11-mile (17.6-km) section of mountainous highway in Colorado is currently scheduled for improvement to Interstate standards. The existing two-lane road is confined by the Colorado River and the scenic but sheer walls of Glenwood Canyon. Roadway ice has been a persistent problem in this canyon because of the lack of direct winter sunlight and the river's proximity, which causes a high local humidity. This icing problem is expected to be magnified on certain segments of the proposed highway because it incorporates several tunnels and a significant length of elevated structures, some of which will be superelevated.

Since the area is endowed with considerable geothermal activity, a feasibility study of incorporating geothermal snow- and ice-melting systems at these critical locations was undertaken. A project panel formed by the Colorado Department of Highways (CDOH) divided this study into three phases. The initial phase included a literature search, identification of known geothermal waters in the area, and a preliminary engineering and cost analysis. The literature search indicated that only one small section of roadway in the United States has been geothermally heated. Even though this system has operated effectively since 1948 in Klamath Falls, Oregon, no useful engineering design data have been developed. The Japanese have also operated several snow-melting systems for roads with "natural thermal water," but they are just beginning to quantify the performance of these systems (1).

The second phase of the feasibility study involved exploratory drilling in the canyon to determine the local thermal gradient and hopefully to discover new geothermal sources near the proposed structures. The preliminary results obtained from these two phases are given in a CDOH report by Swanson (2). This paper will summarize the results obtained from the final phase of the study, which entailed the design, fabrication, instrumentation, and subsequent performance of a prototype geothermal bridge-heating system (3).

EXPERIMENTAL FACILITY

It was predetermined that the geothermal water should not flow through pipes embedded in the deck since the freezing of the water during a system failure could irreparably damage the heating system and fracture the deck. The geothermal water also contains both corrosive and fouling materials, which cause maintenance to be required on the exposed plumbing elements. It was therefore decided to use ammonia-charged gravity-operated heat pipes as intermediate heat exchangers to prevent these problems from occurring within the deck slab itself. Ammonia heat pipes were chosen because of their simplicity and success in similar applications (4-7).

The heat pipes employed on this project are illustrated schematically in Figures 1 and 2. Any time that the flowing water is warmer than the deck, energy from the geothermal water is conducted through the walls of the evaporator pipe and vaporizes a portion of the liquid ammonia within the evaporator. The ammonia vapor rises into the condenser tubes where it condenses to give up the heat of vaporization to the deck; the condensate then returns to the evaporator under the influence of gravity. Since the energy transport is in the form of the latent heat of vaporization, the temperature drop along the heat pipe is extremely small.

The two different heat-pipe designs depicted in Figures 1 and 2 were provided by the SETA Corporation of Laramie, Wyoming, and Energy Engineering, Incorporated (EEI) of Albuquerque, New Mexico. The SETA Corporation provided three manifolds with condenser element spacings of 0.15 m (6 in), 0.30 m (12 in), and 0.46 m (18 in). These three units will be referred to as the SETA 6-in, SETA 12-in, and SETA 18-in modules, respectively. EEI provided heat-pipe manifolds of an alternate design with 0.15-m and 0.20-m (8-in) condenser-pipe spacings (EEI 6-in and EEI 8-in).

To test these heat pipes in situ, a structure that will eventually be used as a parking garage by CDOH was erected in the Glenwood Springs Maintenance Yard from two twin-T slabs placed on abutments 2 m (6.5 ft) high. Longitudinal and transverse layers of reinforcing steel that supported the heat-pipe manifolds were placed on the 15x5-m (50x16-ft) deck formed by the twin-T's. This deck was then overlaid with 0.15 m of concrete with the top of all the condenser elements located approximately 6.4 cm (2.5 in) below the surface. The entire deck was heated with the exception of a 2.5x5-m (8x16-ft) control section located in the center of the deck. The bottom of the deck was insulated with 5 cm (2 in) of urethane foam except under the unheated control.

The geothermal water was obtained from a dammed ditch that drained through the maintenance yard. Some of this water had to be recirculated when the system was operated at the higher flow rates since the spring's output was not adequate.

In order to quantify the performance of each heat-pipe system, a variety of transducers were employed. The water-flow rate through the system was monitored in addition to the water temperature at the entrance and exit of each heat-pipe manifold. An array of thermistors was used in each deck section to trace the thermal responses of the upper and lower deck surfaces, of a few condenser pipes, and of several locations midway between the condenser pipes. In addition, the local environment was quantified in terms of ambient air temperature, wind speed, wind direction, relative humidity, barometric

Figure 1. SETA heat-pipe design for Glenwood Springs geothermally heated bridge.

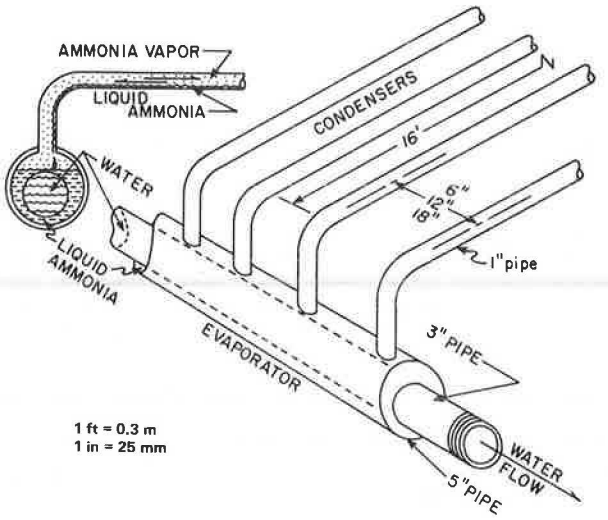

Figure 2. EEI heat-pipe design for Glenwood Springs geothermally heated bridge.

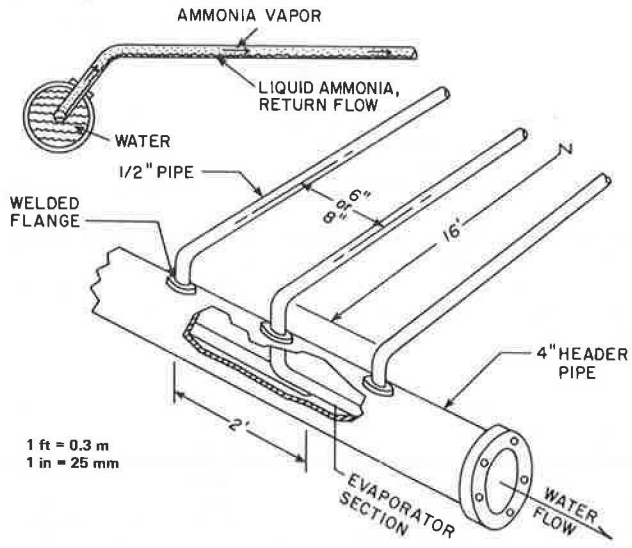

pressure, and incoming solar radiation. These data were recorded by a 100-channel data acquisition supplied by the Department of Mechanical Engineering at the University of Wyoming. The various surface conditions on the deck were also photographed on a 24-h basis by using a time-lapse camera activated at 10-min intervals.

SYSTEM PERFORMANCE

The geothermal heating system was activated on March 18, 1980, shut down on April 11 for the summer, reactivated on September 19, 1980, and permanently disabled in June 1981. The monthly averaged climatic record for the 1980-1981 winter (8) is compared in Table 1 with the long-term climatological averages. Table 1 also tabulates the percentage of each month for which experimental data were obtained. The 1980-1981 winter was relatively mild in that the two traditionally coldest months, December and January, were approximately 4°C warmer than normal and the coldest temperature recorded at the site was only -17.5°C (0°F). Between November 17, 1980, and April 30, 1981, 22 cm (8 in) of snow were reported by the Glenwood newspaper to have fallen, which appears to be about average for that time period.

The monthly averaged geothermal water temperatures and flow rates for April 1980 and the 1980-1981 winter are given in Table 2 along with the corresponding average temperature increases that were induced on the five heated surfaces. Over the three-month period from December through February, when the monthly averaged air temperatures were all near freezing, the following hierarchy in the averaged surface-temperature increases was observed: EEI 6-in [9.3°C (17°F)] > SETA 6-in [6.6°C (12°F)] ~ SETA 12-in [6.4°C (12°F)] > SETA 18-in [5.8°C (10°F)] > EEI 8-in [5.6°C (10°F)]. The monthly averaged flow rates and temperatures of the geothermal water during this period varied between 30 and 50 gal/min (114 and 189 L/min) and 24°-25°C (75°-77°F), respectively. The above hierarchy indicates that the relative performance of the various designs did not completely follow what would have been anticipated, but the severe fouling of the water pipe had a large influence on the performance of these systems. This point will be pursued later.

Table 3 delineates the performance of the heat-pipe systems in terms of various surface-freezing characteristics over the life of the experiment. This table indicates that the heated surfaces were frozen between 1 and 15 percent as long as the unheated control, which was at or below freezing 22 percent of the recorded time. A measure of the severity of the freezes is given by the area (degree days) enclosed between the freeze line and surface temperatures below freezing on a plot of temperature versus time. This freezing factor was reduced between 90 and 99 percent by the various heat-pipe modules, whereas the corresponding number of freeze-thaw cycles was decreased from 66 to 95 percent. The photographic record shows that the unheated control section was covered with snow or ice for approximately 545 h and partly covered with snow for an additional 115 h during the 1980-1981 winter. The heat-pipe modules reduced the duration of the snow and ice cover by at least 96 percent. Figure 3 depicts one of these events where the control section was iced over, as was the adjacent section of Interstate 70, while the ice on the heated surfaces on either side of the control section had melted. The SETA 12-in module can be seen on the left-hand side of the frozen control section in Figure 3, whereas the EEI 6-in module is on the right-hand side.

The SETA 6-in and EEI 8-in evaporator sections were disassembled on June 24, 1980, for examination. Figure 4 shows the 0.6-cm (0.25-in) thick fouling layer that had formed inside the water pipe through the SETA 6-in module. This layer consisted of a sludge deposited on top of a dense corrosion scale that was strongly bonded to the pipe wall. A fouling layer of this magnitude represented a 30 percent reduction in the flow cross-sectional area and would obviously have a significant effect on the system's thermal performance. An attempt was made to clean this heat exchanger with a 3-in (7.62-cm) rotary wire brush on March 19, 1981, but it appears that only the sludge layer was removed. The sludge layer pictured in Figure 4 was therefore deposited in only three months, but it was reported that the sludge layers in the other two modules had essentially the same thicknesses when they were disassembled at a later date.

The corresponding fouling that accumulated inside the water pipe of the EEI 8-in module over the total

test period is pictured in Figure 5. It indicates that the fouling deposits had in essence isolated the enclosed heat-pipe evaporator bundle from the geothermal water flow, which would account for the relatively small amount of surface heating that was observed (see Table 2) near the experiment's conclusion. For some unknown reason, the performance of the EEI 8-in module was always below par, whereas Table 2 shows that the EEI 6-in module generally produced the largest surface-temperature increases.

In order to be able to predict the performance of these heat exchangers with various water temperatures, a coefficient of performance θ was defined as the ratio between the observed temperature increase of the heated surface ($T_s - T_c$) and the maximum possible temperature increase, that is, the temperature difference between the geothermal water (T_w) and the unheated control (T_c). This coefficient of performance θ is a function both of the combined convective and radiative heat-transfer coefficient between the deck surface and the environment and of the system's overall specific heat-transfer conductance u (in watts per square meter per degree centigrade) between the water and the heated surface. The variation in a system's conductance (u) during this experiment was mainly due to the fouling and it was only slightly affected by the varying water-flow rates.

The weekly average coefficient of performance for the SETA experimental modules is plotted versus time in Figure 6. θ for the SETA 6-in module is shown to have decreased from a value near 0.4 at the beginning of the experiment down to a value around 0.29 over the coldest midwinter months and then finished with a value of 0.23 after one year. The effect that fouling had on this pipe is clearly indicated by the 20 percent drop in its θ from March through April after it had been partly cleaned on March 19, 1981, whereas the θ values of the other SETA manifolds remained essentially constant or increased during this same period.

θ for the SETA 12-in manifold decreased from 0.43 to 0.21, and its midwinter average was 0.23. The θ variation for the SETA 18-in module was from 0.29 to 0.13 with a 0.25 midwinter mean. A detailed heat-transfer analysis of these data with the corresponding environmental data indicated that the fouling had reduced the experimental observed conductance of the SETA modules by at least 55 percent. The major effect of fouling on these units appears to have been fairly early in the experiment in that they maintained a reasonably constant conductance over the latter part of the experiment. Figure 6 indicates that the relative effects of the fouling on the SETA modules were such that there was very little difference in their performance after February 1981.

The coefficient of performance for the EEI modules is compared with that for the SETA 6-in module in Figure 7. θ for the EEI 6-in manifold decreased from 0.44 to 0.27 with a midwinter mean of 0.39, whereas the EEI 8-in unit's θ decreased from 0.28 to 0.15 with a midwinter mean of 0.24. The heat-transfer analysis indicated that the conductances of the EEI modules had decreased by approximately 60 percent over the lifetime of the experiment. This analysis also implied that fouling was still causing the two EEI modules to continue to degrade at the conclusion of the experiment, whereas the conductances of the three SETA modules appear to have reached steady-state values.

Table 1. Monthly averaged environmental parameters for Glenwood Springs.

Climatological Record (1931-1960)			Experimental-Site Data (winter 1980-1981)			
Month	Air Temperature (°C)	Precipitation (cm)	Air Temperature (°C)	Precipitation[a] (cm)	Wind Speed (m/s)	Percentage of Month Recorded
Sept.	16.4	3.6	13.2	–	0.9	37
Oct.	10.6	3.6	10.8	–	0.8	95
Nov.	2.4	3.1	–	–	–	0
Dec.	–2.6	3.7	1.4	4.6	1.0	71
Jan.	–4.0	4.6	0.2	0.5[b]	1.0	93
Feb.	–1.3	4.5	–0.6	2.2	1.2	83
March	3.3	3.9	6.3	8.3	2.1	38
April	8.7	4.8	9.1	6.2	2.1	98

Note: $t°C = (t°F - 32)/1.8$; 1 cm = 0.39 in; 1 m/s = 2.2 mph.
[a]Monthly values as reported in Glenwood Springs newspaper.
[b]Major snowstorm not recorded.

Table 2. Monthly averaged water temperatures and flow rates and corresponding temperature increases of heated surfaces.

Month and Year	Water		Air Temperature (°C)	Heated-Surface Temperature Increase (°C)				
	Temperature (°C)	Flow (gal/min)		SETA 6-in	SETA 12-in	SETA 18-in	EEI 6-in	EEI 8-in
April 1980	26	138	3.4	7.6	6.4	4.8	8.4	4.7
Sept.	29	–	13.2	4.5	3.3	3.1	4.8	2.4
Oct.	28	33	10.8	4.8	3.8	3.3	5.8	3.2
Dec.	25	32	1.4	6.4	6.3	5.5	9.1	5.5
Jan. 1981	24	52	0.2	6.0	6.3	5.3	8.9	5.4
Feb.	24	50	–0.6	7.3	6.7	6.5	9.6	6.0
March	26	98	6.3	5.6	3.7	3.6	4.6	2.4
April	27	92	9.1	4.0	3.3	3.2	4.0	1.9

Note: $t°C = (t°F - 32)/1.8$; 1 gal/min = 3.8 L/min; 1 in = 25 mm.

IMPLEMENTATION AND CONCLUSIONS

Even though the fouling of the experimental heat exchangers proved to be fairly extreme, all the modules reduced their respective snow-cover time by at least 96 percent relative to the unheated control. The corrosion and deposition must in any case be curtailed if this heat-pipe system is to be feasible. There is a good possibility that this problem can be solved with the use of a protective and durable coating or liner since the sludge deposit in the polyvinylchloride supply lines was minimal. A study to investigate and test various alternatives to control the fouling without significantly decreasing the system's thermal conductance is currently being initiated.

A total surface area of 59 m^2 (640 ft^2) was heated by the heat-pipe modules, but this resulted in an insignificant drop in the water temperature even at flow rates as low as 35 gal/min (133 L/min). A much larger series of heating units could have been installed with very little degradation in the performance of the last units. This is demonstrated in Figure 8, which plots the coefficient of performance of the nth SETA 18-in heat exchanger, θ_n, versus the number of modules. This plot implies that the coefficient of performance for the

Table 3. Percentage of reduction in various freezing characteristics of heated sections.

Heated Section	Time Frozen (h)	Time Below Freezing (degree-days)	Freeze-Thaw Cycles	Snow-Cover Duration (h)
SETA 6-in	94	95	73	99
SETA 12-in	91	95	74	99
SETA 18-in	85	90	66	96
EEI 6-in	99	99	95	100
EEI 8-in	89	93	66	97

Note: 1 in = 25 mm.

Figure 3. Typical melting event with ice-covered unheated control and wet heated surfaces.

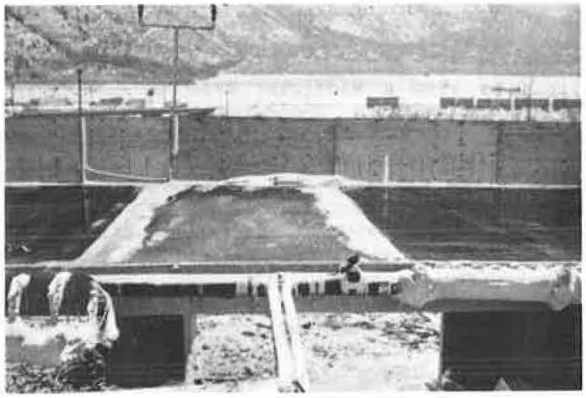

Figure 4. Sludge deposits from geothermal water in SETA 6-in evaporator.

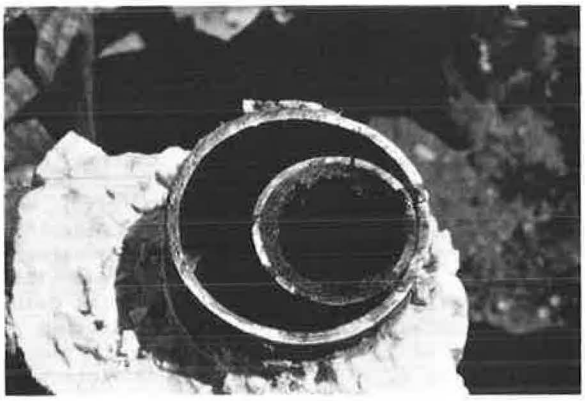

200th unfouled heat exchanger, θ_{200}, would have only dropped 21 percent from the θ_1 value for a 100-gal/min (380-L/min) flow rate and a large combined convective-radiative surface-film coefficient of 15 W/(m^2 · °C). For example, if the control surface is frozen but dry and the water temperature is 38°C (100°F), the surface temperature of the first unfouled module should be around 12°C (54°F), whereas the heated surface 498 m (1600 ft) down the road would be estimated to be around 8°C (46°F). For the same case but with fouling, Figure 8 indicates that the temperature of the first surface should be 7.4°C (45°F), whereas the 200th surface would be at 6°C (42°F). It therefore appears that a large length of highway could be easily handled with

Figure 5. Cross section of EEI 8-in evaporator section showing deposits from geothermal water.

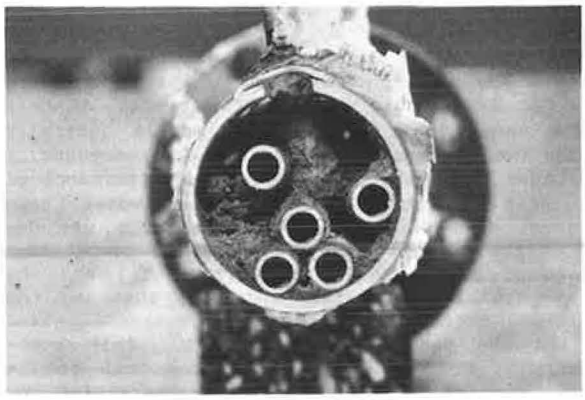

Figure 6. Coefficient of performance θ versus time for SETA heat-pipe modules.

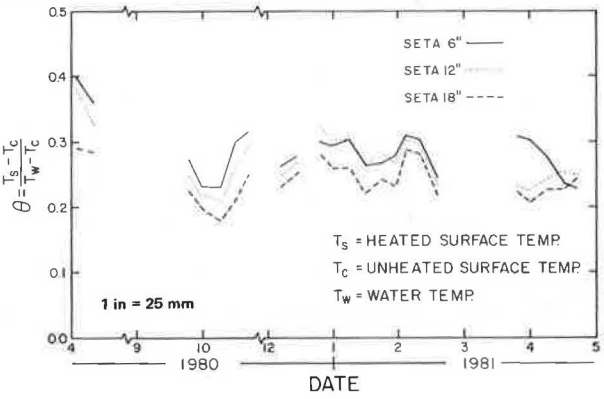

Figure 7. Coefficient of performance θ versus time for EEI heat-pipe modules and SETA 6-in module.

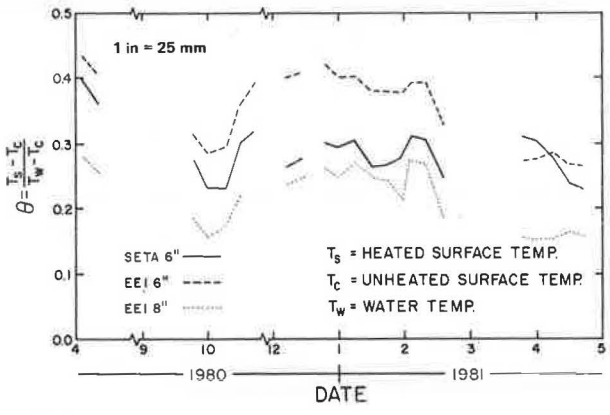

the hot springs located in the canyon. One spring, for instance, has a reported flow rate of 3000 gal/min (11 400 L/min) at 43°C and another has one of 2000 gal/min (7600 L/min) at 24°C.

It should be noted that source temperatures much lower than the ones used in this experiment can still be effective. For instance, long heat pipes have been successfully used to prevent preferential

Figure 8. Variation of θ_n with number of unfouled and fouled SETA 18-in heat-pipe modules in series.

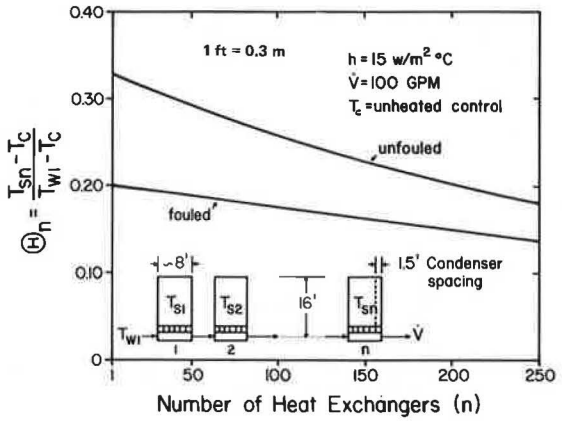

freezing and to significantly reduce the duration of snow cover on road (4,7) and bridge (5) surfaces by transferring thermal energy from the ground itself. The undisturbed winter ground temperatures 3 m (10 ft) or more below the surface were only of the order of 6°-10°C at these sites. The performance of a Glenwood-type heating system at these sites with the water temperature matching the local undisturbed ground temperature would have been superior to these ground heat-pipe systems due to the cooling of the earth around the ground heat pipes. Wells, municipal water lines, and waste water such as sewerage may therefore prove to be feasible energy sources for roadway heating systems.

In summary, all Glenwood heat-pipe modules were very effective as snow-melting systems, even when they were severely fouled. This was accomplished essentially with 25°C water at flow rates around 35 gal/min. Even at this low flow rate, the system could have supported a fairly large number of these modules in series without a large degradation in the performance of the last units. In situations requiring just the elimination of preferential icing or only requiring a limited snow-melting capability, this heating system could effectively use water with temperatures as low as 10°C.

REFERENCES

1. M. Sekioka, K. Yuhara, and M. Sato. Thermal Considerations on Snow Melting with Thermal Water at Jozanksi Spa, Sapporo, Japan. Journal of the Japan Geothermal Energy Association, Vol. 16, No. 2, 1979, p. 43.
2. H.N. Swanson. Evaluation of Geothermal Energy for Heating Highway Structures. Colorado Department of Highways, Denver, Rept. CDOH-DTP-R-80-6, 1980.
3. J. Nydahl, K. Pell, and others. Data Collection and Analysis for Geothermal Research. Colorado Department of Highways, Denver, Rept. CDOH-UW-R-81-11, 1981.
4. D.C. Long and J.S. Baldwin. Snow and Ice Removal from Pavement Using Stored Earth Energy. FHWA, Rept. FHWA-TS-80-227, 1980.
5. C.H. Wilson and others. A Demonstration Project for Deicing of Bridge Decks. TRB, Transportation Research Record 664, 1978, pp. 189-197.
6. K. Pell, J.E. Nydahl, and V. Cundy. Geothermal Heating of Bridge Decks. In TRB, Snow Removal and Ice Control Research, Special Rept. 185, 1978, p. 169.
7. O. Tanaka, H. Yamakage, T. Ogushi, M. Murakami, and Y. Tanaka. Snow Melting Using Heat Pipes. Presented at Fourth International Heat-Pipe Conference, London, 1981.
8. Water Information Center, Inc. Climates of the States: Volume 2--Western States. National Oceanic and Atmospheric Administration, U.S. Department of Commerce, Port Washington, NY, 1974.

Publication of this paper sponsored by Committee on Winter Maintenance.

Construction and Benefits of Rubber-Modified Asphalt Pavements

DAVID C. ESCH

A paving system was developed in Sweden in the 1960s in which relatively large rubber particles were incorporated into asphalt-concrete pavements. The original purpose was to increase skid resistance and durability. This system, distributed under the trade names Skega Asphalt or Rubit in Scandinavia and PlusRide in the United States, was also found to provide a new form of winter ice control because of the increased flexibility and the action of protruding rubber particles. The Alaska Department of Transportation and Public Facilities installed five experimental pavement sections by using the PlusRide system between 1979 and 1981. Major modifications to normal asphalt pavement aggregate gradations, asphalt contents, and mix design procedures are considered essential to achieve durable nonravelling rubber-asphalt pavements. Laboratory tests of PlusRide paving mixes also indicate a potential for greatly increased pavement fatigue life as a result of the elasticity of this material. The attainment of low voids in the pavement is the primary design and construction objective, and mix design and construction activities are discussed. Observations of the skid-reduction benefits under icy road conditions have been made with a British pendulum tester and a vehicle equipped with a Tapley brake meter. Tests indicate that significant reductions in icy-road stopping distances nearly always resulted from the use of the PlusRide paving system. For 19 testing dates over two winters, stopping distances were reduced by an average of 25 percent; reductions on specific dates ranged from 3 to 50 percent.

In the late 1960s, experimentation was done in Sweden on the effects of mixing rubber particles in asphaltic pavements. A system incorporating 3-4 percent by weight of relatively large (1/16 in to 1/4 in) rubber particles into an asphalt pavement was developed to increase skid resistance and durability and was found to provide a new form of winter ice control as well as a reduced noise level. The ice-control mechanism apparently results from the flexing of the protruding rubber particles and the

greater flexibility of the mix under traffic action, which cause a breakdown of surface ice deposits.

Roadway surface-ice deposits become a major problem in urbanized areas with high traffic volumes and stop-and-go traffic movements. Costs of maintaining ice-free pavements by using deicing chemicals or improving traction by using sand applications are very high and would justify considerably increased expenditures on pavement construction if ice-free pavements could be obtained.

An unrelated problem, but one of considerable magnitude, has been the disposal of the hundreds of millions of used tires discarded each year. The possibility of using this form of refuse to the benefit of the public must be seriously considered.

Encouraged by the successes of rubber-asphalt paving mixes in Scandinavia, the Alaska Department of Transportation and Public Facilities installed five experimental pavement sections in Fairbanks and Anchorage between 1979 and 1981 by using different pavement mixtures. Periodic measurements of surface friction have been made during icy winter conditions in 1980 and 1981 to analyze the benefits of the rubber in increasing traction and reducing stopping distances. Laboratory tests for resilient modulus and durability have also been performed on samples of these mixes; they indicate that major increases in fatigue life and crack-reflection control are anticipated due to the increased flexibility.

BACKGROUND

Asphalt and Rubber Mixtures

The original development work in the area of coarse rubber-asphalt paving mixtures was performed by the Swedish companies Skega AB and AB Vaegfoerbaettringar (ABV). The material application was patented under the trade name Rubit. In America, the trademark PlusRide asphalt is now used to designate this material.

It should be noted that considerable experimental work and field trials have been performed in the United States, particularly in Arizona, California, and Colorado, on rubberized asphalt seal coats (1,2). These installations have used finely ground (-No. 16 to +No. 25) crumb rubber reacted with asphalt at elevated temperatures to form a thick elastomeric material, which is then diluted with 5 percent kerosene to aid in application. It was learned from studies by the Arizona Department of Transportation that these small rubber particles swell to two to three times their original size when reacted with asphalt at temperatures of 350-400°F for periods of 30 min or more (3). As such, these installations differ substantially from the materials discussed here. Little or no use of the concept of incorporating larger rubber particles in pavement surfacing layers is indicated in North America. The potential savings in ice-control costs may justify the increased cost of rubberized surfacings. Use of such surfacings on bridge decks and on insulated roadway sections should offset the icing occurrences commonly noted on bridges and sometimes found over insulated sections of roadway.

Ice-Control Considerations

The use of sands for ice control provides only temporary skid resistance, and sand must be reapplied often. Stopping distances on sanded ice are also much greater than on dry pavement. In addition, sand must be removed from gutters and inlets in urban areas following spring thawing to avoid blockage of drainage systems.

Some recent analyses of the costs and benefits of using salt to remove roadway ice have indicated that the ultimate costs to the road user may be more than 10 times as high as the sum of the benefits (4, p. 969). The major cost item, premature vehicle destruction through corrosion, greatly outweighed the benefits of reduced maintenance and accident costs. Salts also present the possibility of contamination of ground and surface waters from roadway runoff. Benefits of salt use that are difficult to quantify, however, are the savings in travel time and reduced accident levels that result when roadways are free of ice.

PAVING MIX CONSIDERATION

Aggregate and Rubber Proportions

From experience in Sweden, three different aggregate (sand and gravel) gradations are currently recommended to serve different traffic levels, as shown by Table 1.

The rubber particles used in these mixes are produced in roughly cubical form from grinding waste tires, which have first had the steel wires in the tire-bead area removed. The rubber may include some tire cord and steel fibers from the tire belts and is required to meet the gradation specifications in Table 2. Product experience by the parent company, ABV, has indicated that some durability benefits result from the use of a modified rubber gradation, replacing 20 percent of the originally used coarse rubber with a finely ground (No. 10-40) rubber size. This change corresponds with use of a similar rubber grading in the construction of the rubberized asphalt seal coats previously mentioned and was the basis of Alaska's modified rubber gradings used in 1981.

To those knowledgeable in the area of design of asphalt paving mixtures, a review of these specifications will reveal some critical differences between modified and normal pavements. The most important difference is indicated by the shape of the aggregate gradation curve (Figure 1). To provide space for the rubber particles, it is necessary to create a gap in the gradation curve for the aggregates, primarily in the 1/8-in to 1/4-in size range. In effect, the rubber particles replace the rock particles that normally occupy this size range. Unless this gradation-curve gap is present, the rubber particles will resist compaction of the mix during the rolling operation, and the resultant pavement will have excessively high voids and no durability.

Asphalt Content Determination

The asphalt content recommended in Table 1 will generally be found to be 1-2 percent higher than that in conventional mixes. This higher asphalt level is an important factor in the durability of rubber-asphalt pavements. Laboratory mixes should be prepared at several different asphalt contents. Compaction and testing are performed by using the Marshall procedure, in which samples are placed in greased open-ended steel ring molds and compacted with 50 blows of a drop hammer on each end. Samples are then weighed both in air and immersed in water, and the percentage of voids is determined by calculation. As the asphalt content is increased, the voids will decrease as shown in Figure 2. It has been found critical to achieve low voids and thereby prevent the intrusion of water. The minimum asphalt content permitted should be that at which 3 percent voids is achieved. Marshall stability criteria cannot normally be met with PlusRide paving mixes. Stabilities as low as 350 lb were recorded for the

paving mixes used in the 1979 Fairbanks installations, yet these pavements have resisted bleeding in the two years since construction, in spite of air temperatures as high as 90°F.

Table 1. Recommended specifications for rubber-asphalt (PlusRide) paving mixtures for different levels of traffic.

Characteristic	Mix		
	PlusRide 8	PlusRide 12	PlusRide 16
Average daily traffic	2500	2500-10 000	10 000
Minimum thickness (in)	0.75	1.5	1.75
Aggregate (% passing) sieve size			
3/4 in	-	-	100
5/8 in	-	100	-
1/2 in	-	-	65-80
3/8 in	100	60-80	50-60
1/4 in	60-80	30-42	30-42
No. 10	23-38	19-32	19-32
No. 30	15-27	13-25	12-23
No. 200	7-11	8-12	6-10
Preliminary mix design			
Rubber (% of total mix)			
By weight	3.0	3.0	3.0
By volume (approx.)	6.7	6.7	6.7
Asphalt (% of total mix)			
By weight	7.5	7.5	7.5
By volume (approx.)	20.2	20.2	20.2
Maximum voids (%)	2	3	4

Table 2. Particle size specifications for rubber.

Sieve Size	Percent Passing			
	Alaska 1979-1980	Alaska 1981	ABV Combined Coarse and Fine	PlusRide 1981
1/4 in	-	-	100	-
No. 4	100	100	76-92	100
No. 10	15-35	15-36	28-36	28-40
No. 20	-	10-25	10-24	-
No. 40	0-6	-	-	0-6
No. 200	0-2	-	-	-

The differences in mix properties that can occur within the aggregate size specification limits used for the Fairbanks rubber-modified pavements in 1981 were studied by performing four mix designs by using a single aggregate source, AC-2.5 asphalt, and a rubber content of 3 percent. Gradings used in this study are shown in Figure 3 and represent the coarse and fine gradation limits (Mixes A and B), the middle of the specification band (Mix C), and the straightest-line grading possible with this specification band (Mix D). Results of this testing at asphalt contents from 6 percent to 9 percent by weight of the dry aggregate are shown in Figures 4-6 and demonstrate the low stability and high flow-test results typically obtained on these mixes as well as the sensitivity of the void levels and other mix properties to aggregate gradation changes. It should be noted that these specification limits (Figure 3) are wider than those recommended for the similar PlusRide 12 mix in Table 1, and this specification band was used by the Alaska Department of Transportation to provide more contractor flexibility in choice of a final mix gradation. It is obvious from this study that a good laboratory mix design is critical to obtaining a proper mix with low voids and adequate stability. The minimum required value for stability of these mixes has not yet been determined.

FATIGUE-LIFE ASPECTS

A series of laboratory fatigue tests have been performed on PlusRide paving mixes at Oregon State University to analyze the resistance of these mixes to failure in tension under the diametral split-tension test mode. In this work, samples were loaded to failure at selected tensile strain levels. Results as shown in Figure 7 indicate that the fatigue life of PlusRide pavements may be more than 10 times greater than that of normal mixes. This testing program provides hope that the PlusRide paving system might prove of benefit in roadways over weak foundations where fatigue cracking is the dominant failure mode.

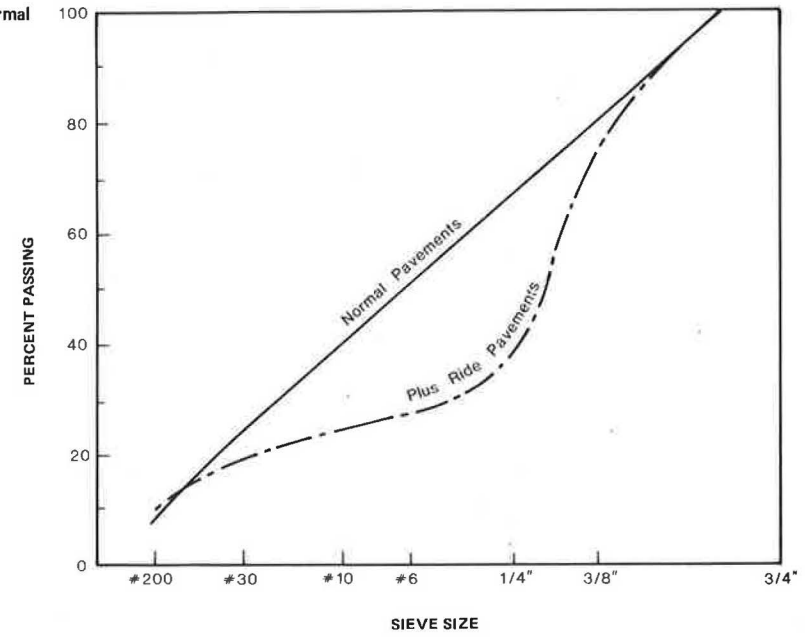

Figure 1. Comparative aggregate gradation curves for normal and PlusRide asphalt-rubber pavements.

Figure 2. Asphalt content determination on basis of voids in mix.

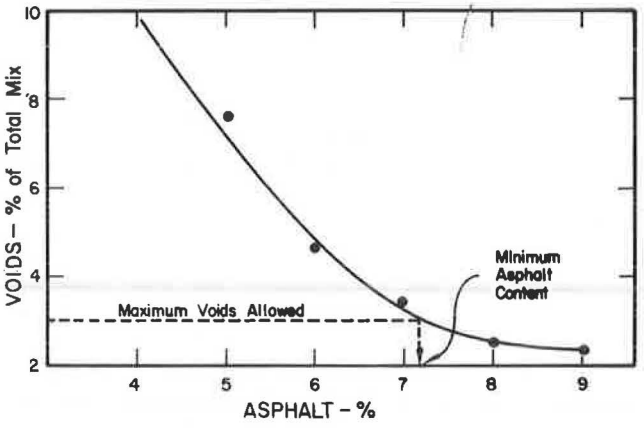

Figure 3. Aggregate gradations used to test for variations in mix properties due to gradation variations within specification band.

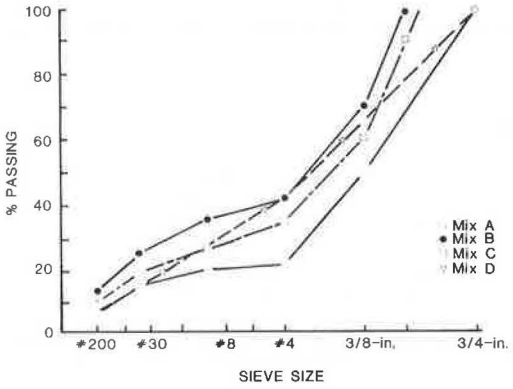

Figure 4. Differences in void content for different aggregate gradations within single specification band.

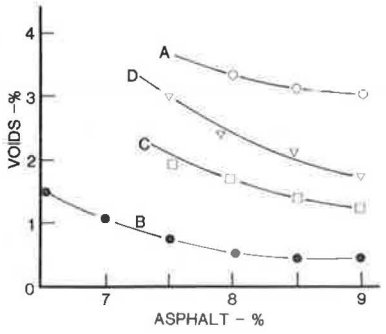

Figure 5. Differences in Marshall stability for different aggregate gradations within single specification band.

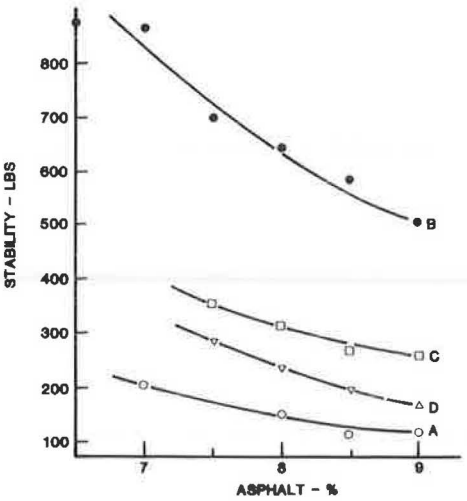

Figure 6. Differences in Marshall flow for different aggregate gradations within single specification band.

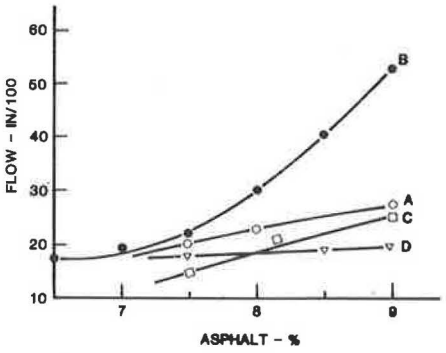

SPECIAL CONSTRUCTION CONSIDERATIONS

Mixing

In the preparation of rubber-asphalt paving mixes, use of a batch mixing plant is preferred because the required quantities of rubber, asphalt, and aggregates can be measured exactly and added separately to the pug mill or mixing chamber. In this type of plant, preweighed sack rubber can be used to advantage, with quantity control by bag count. However, both continuous-mix and drum-dryer mix asphalt paving plants have been used without difficulty. In these plants, in which the mixing operation goes on continuously rather than in batches, the rubber must be added continuously from a separate bin with a belt feed to maintain uniformity. Very close control of the rubber content is critical to assure proper field performance. Mixing temperatures and asphalt grades used are similar to those for normal paving mixes, with some indications that mixes may benefit from blending at temperatures as high as +350°F.

Placement and Compaction

Placement of the hot paving mix should be performed by paving machines equipped with full-width vibratory screeds. Rolling should commence as soon as possible after placement without the mix sticking to the roller and should continue until the mix temperature cools below 140°F. Rubber mixes are very resilient and rebound noticeably behind the roller. Rollers may be either steel-wheel static or vibratory types. Rubber-tire rollers were not to be used, according to original recommendations. However, recent experiences with rubber-asphalt pavements placed in Vancouver, B.C., and Anchorage, Alaska, in 1981 indicate that significant surface tightening might be achieved by use of a rubber-tire roller after the mix has cooled below 140°F.

Compaction to the highest possible density with minimal voids is essential to good pavement performance. When core samples are taken from the finished pavement and tested, the average void content should be less than 5 percent. Rubber-asphalt paving mixes will appear excessively high in asphalt content to personnel familiar with normal mixes, but

Figure 7. Comparisons of fatigue life for asphalt mix samples without and with rubber particles in PlusRide system.

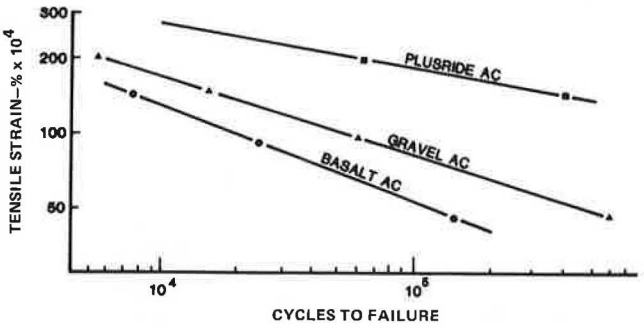

the presence of the rubber has been reported to prevent the possibility of the bleeding of excess asphalt from the mix since the rubber and asphalt combine to form a more elastic binder.

Costs

Factors that increase the cost of a rubber-asphalt paving mixture over that of a normal mix include the purchase, shipping, and handling of the 60 lb of rubber added to each ton of mix; the plant modifications needed for the rubber addition; and possibly some additional rolling costs. At the current time, the closest rubber production to Alaska is in the Seattle area, and the shipping costs are a major factor in the delivered Fairbanks rubber price of approximately 30 cents/lb. The addition of 3 percent rubber in the Fairbanks area including royality fees paid to the patent holder, All Seasons Surfacings Corporation, will increase the in-place pavement cost by roughly 50 percent, for a total cost increase of $15 000 to $30 000/mile depending on width and thickness.

FIELD TRIALS, FAIRBANKS AREA, 1979

Site Selection

Two sites were selected in the Fairbanks area for the first U.S. trial installations of PlusRide rubber-modified pavement mixtures. The first site, on a frontage road curve, is referred to as the Carnation site after the adjacent Carnation Dairy warehouse. The second site covers the northern half of a roadway insulation test section on the Fairhill Subdivision access road. The Carnation site was selected because of the frequent occurrence of skidding accidents due to the very sharp curvature of the roadway. The existing pavement was constructed in 1967 and was in good condition. Fairhill was selected because the presence of the insulation layer resulted in significant differential surface icing during the 1978-1979 winter, where the roadway was ice-covered above the insulation but not over adjacent noninsulated areas. In this area the original pavement was placed in 1978 and was 24 ft wide.

Pavement Construction

The first Fairbanks-area rubber-asphalt paving mix was prepared on September 4, 1979, by Associated Asphalt Company from Chena River gravels. The rubber was supplied by the All Seasons Surfacings Corporation. Because the asphalt plant to be used was the continuous-mix single-entry drum-dryer type, it was necessary to use the existing stockpile aggregate gradations. As a consequence, the final gradation was slightly lower (4-5 percent) than desirable (6-11 percent) in the dust or fines size range. The rubber was fed from one of the plant's four aggregate-feed bins (Figure 8) after the belt speed had been calibrated to provide a 3 percent rubber content. No problems were encountered in the mixing operation, which appeared to thoroughly distribute the rubber particles through the mix.

At the Carnation site, the mix was placed at an initial temperature of 240°F with a tracked paver in a thickness averaging nearly 2 in. Compaction commenced immediately behind the paver except for an inital delay caused by concern over roller pickup of the mix. Compaction continued until the pavement had cooled below 120°F; minor rebound was still apparent at that temperature. At this site, the final void content ranged from 2.3 to 7 percent and averaged 4.6 percent, slightly higher than the desired average of 3.5 percent.

At the Fairhill site, the mix was truck end-dumped after the application of an RC-800 asphalt tack coat. Placement was performed with a road grader rather than a paver to evaluate the ease of placing this mix with minimal equipment. Unfortunately, the mix proved too sticky for good laydown by this method. The resultant manipulations and delays in final leveling of the mix caused the mix to cool too much for good compaction. Field voids at this site therefore averaged 9 percent, much too high for good durability.

FIELD TRIALS, ANCHORAGE AREA, 1980

Three trial sections of rubber-asphalt pavement were included in the contract for the 1980 Old Seward Highway repaving project. To investigate the effects of a range of rubber contents on performance, provisions were made to place 1.25-in-thick pavement overlays that have rubber contents of 3, 3.5, and 4 percent. Traffic volumes on this road are much higher than those on the Fairbanks sections; the average is 9500 vehicles per day. Preliminary mix designs were prepared for each rubber content and indicated that the original project gradation needed modification to reduce total voids to acceptable levels and still retain some stability. Based on this testing, an increase in the dust content of the mixes to 8 percent was recommended, which reduced the recommended asphalt content to 6.6 percent for all rubber contents.

The rubber-asphalt paving mixes were prepared on June 14, 1980, in a Standard Steel batch plant; the rubber was added by manually breaking the 52-lb bags into a hopper at ground level and feeding the rubber into the mixing chamber by conveyor (Figure 9).

All three different rubber-content mixes were placed with a tracked Barber-Green paving machine and compacted with a minimum of two passes of a vibratory roller followed by two passes of a 12-ton steel-wheel roller. Temperatures of the 3 and 3.5 percent mixes varied from 240 to 280°F at the time of laydown. However, due to equipment and traffic problems, placement of the 4 percent rubber mix was delayed for several hours, and the mix had cooled excessively prior to placement.

Pavement cores taken shortly after placement showed the 4 percent rubber section to have field voids of around 12 percent compared with a desirable average of 3.5 percent, and ravelling and potholing began to occur several days after placement. On the 3 percent and 3.5 percent rubber mixes, field voids averaged 7.5 percent, still much too high for good long-term durability. Analysis of the construction operations indicated the high voids to be the result of aggregates that were out of specification on some sieves and lower than desirable in fines, in com-

bination with a specified asphalt content that was too low and the use of nonvibrated paver screed extensions. This experience is related to make potential users aware that close conformance to specifications and adequate compaction are critical to good performance. Specifications used for the various PlusRide paving mixes placed in 1979 through 1981 are summarized in Table 3.

FIELD TRIALS, 1981

Fairbanks: Peger Road

A total of 280 tons of rubber-modified paving mix was placed in late July at the intersection of Peger and VanHorn Roads. This intersection was chosen because it required a 90° turn on a major truck route.

The mix was produced with a Barber-Green Batchomatic plant in 3000-lb batches. Mixing started at 8 percent asphalt mixed at 310°F. After it had been noted that no laydown problems were found, the asphalt content was increased to 8.2 percent at 330°F and finally to 8.5 percent at 345°F. At the final asphalt content, some asphalt bleeding was noted in the trucks and the pavement was moderately tender but still placed satisfactorily.

Rolling commenced at a temperature of about 295°F with 10-15 passes of a 10-ton steel-wheel roller and continued until the temperature was below 140°F. Due to tenderness, traffic was kept off until evening cooling had lowered the pavement temperature to 60°F. No subsequent problems were noted, although air temperatures did not exceed 75°F after the date of placement. Subsequent pavement coring indicated voids that ranged from 1.3 to 7.1 percent and averaged 4.2 percent.

Anchorage: Upper Huffman Road

The 1981 Anchorage site, Upper Huffman Road, was chosen because the very steep grades on this road, as high as 14 percent, created a severe traffickability problem during icy winter conditions. A total of 1.01 miles of road was first reconstructed, then paved with a 1.5-in asphalt-concrete binder course, and finally capped with a rubber-modified asphalt pavement 0.75 in thick. The rubber mix was produced with approximately 9.5 percent asphalt in a commercial batch plant at 360°F. Due to the thinness of the lift, cooling was accelerated and field voids were indicated to be approximately 10 percent. However, due to the thin lift and the resultant flexibility of the cores, the laboratory void determinations may not be extremely accurate. The pavement durability to date has been excellent.

Figure 8. Rubber feeding from aggregate bin for dryer-drum mix plant.

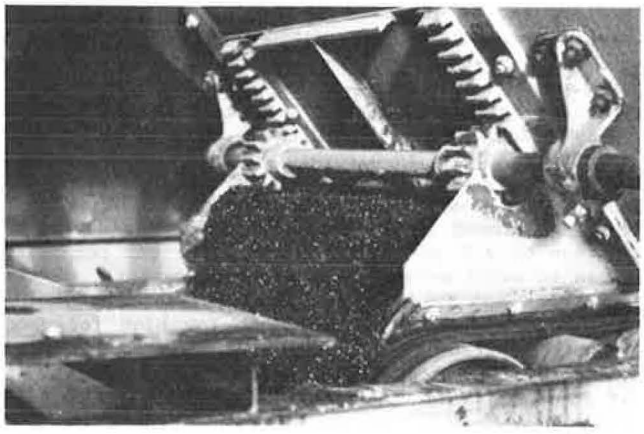

Figure 9. Conveyor loading rubber into pug mill for batch-mix plant.

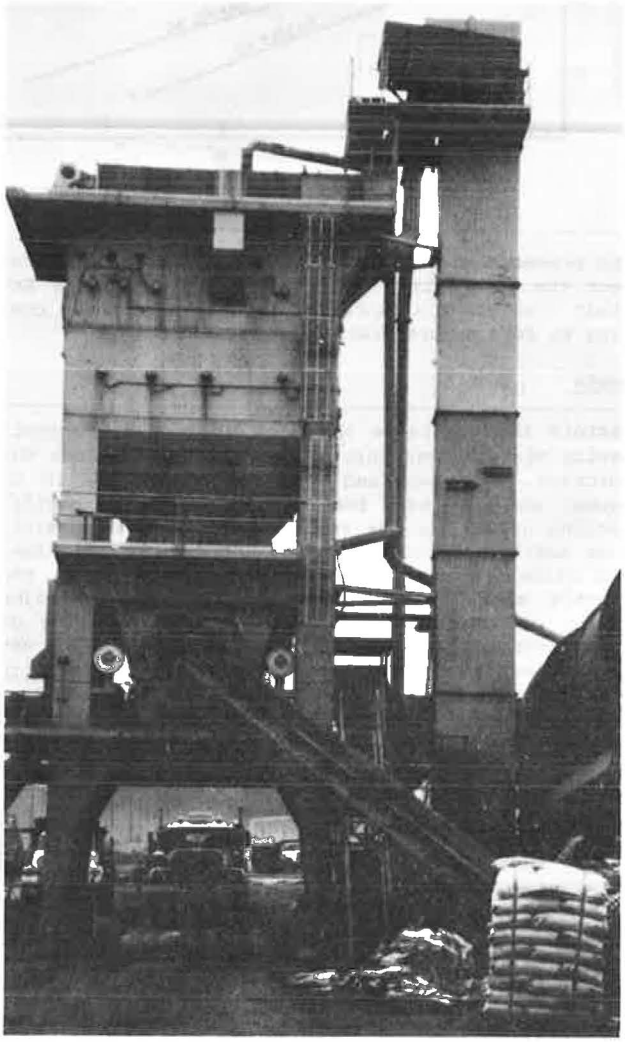

Table 3. Aggregate and mix specifications used for field control of Alaska's rubber-modified asphalt pavements.

Characteristic	Project			
	Carnation, 1979	Old Seward Highway, 1980	Peger Road, 1981	Upper Huffman Road, 1981
Sieve size (% passing)				
3/4 in	100	100	100	-
1/2 in	-	78-94	-	-
3/8 in	60-77	43-57	53-67	100
No. 4	45-59	29-43	28-42	47-60
No. 10	29-41	22-34	20-32	30-42
No. 40	12-20	15-23	14-22	15-24
No. 200	4-10	5-11	5-11	5-11
Asphalt (% dry aggregate)	7-8	6.1-7.1	8.0-9.0	9.0-10.0
Rubber (%)	3-3.5	3.0-3.5, 4.0	3.0	3.0
Asphalt type	AC-5	AC-5	AC-2.5	AC-5
Avg thickness (in)	2.25	1.5	1.7	0.75
Base	2-in AC	3-in AC	Gravel	1.5-in AC
Length of paving (ft)	212	6792	649	5330

PERFORMANCE OBSERVATIONS

Fairbanks (1979-1980)

Visual surface ice observations were made during the winter of 1979-1980 in an attempt to determine the percentage of time in which the rubber would be of benefit to motorists. A British portable friction tester was used for occasional verifications of observed friction levels under test method ASTM-E303. It became apparent from the field testing that the rubber sections did not have to be totally snow-free or ice-free to show increased friction levels. Results of four icy-road field tests indicated an average increase in the British pendulum number from 42 for the normal pavement to 70 for the pavement with rubber particles.

Public reaction to the rubber sections was favorable. In summary, the 1979-1980 winter performance at the Carnation site was as follows:

1. No skidding incidents where vehicles left the roadway were noticed on this corner after the end of the first snowfall. Skidding off the roadway had commonly been noted at this point in prior years.
2. Improved traction was often noticeable over the rubber area during the early portion of the winter.
3. During much of the winter, thick ice deposits resulting from November rains totally covered the roadway and no benefit of the rubber could again be noted until mid-February. This weather condition was abnormal, and the ice was controlled by frequent sanding.
4. Comments of area drivers indicated that the improved traction was detected by those not aware of the rubber-asphalt test.

Anchorage (1980-1981)

The durability of the high-void rubber-asphalt pavement placed on the Old Seward Highway in June 1980 was very low, particularly for those sections that had rubber contents above 3 percent. Ravelling commenced soon after placement, and it was necessary to patch and eventually repave over the 4 percent rubber area. The center two-thirds of the roadway width over the 3.5 percent rubber area also required repaving during September 1980. Observations for surface ice differences were made occasionally during the 1980-1981 winter on the 3 percent and outer-wheelpath areas of the 3.5 percent rubber areas. However, this winter was exceptionally warm and surface ice was rarely noted on any area pavements.

Fairbanks (1980-1982)

A mu-meter trailer for measuring surface friction was obtained and used for early winter testing to determine the differences in friction between pavements with and without rubber particles at the Carnation and Fairhill sites. However, it rapidly became apparent that this device was unsuitable for measuring friction on icy roads, sanded roads, or PlusRide sections. Test runs on sanded roads demonstrated that the mu-meter, apparently because of its design, could not distinguish friction differences even between glare ice and sanded ice. To provide better data, a Tapley decelerometer was installed in a sedan and used for subsequent measurements of friction levels for PlusRide pavements. This device has the advantage of directly measuring the maximum vehicle braking g forces and gives estimated stopping distances from a speed of 25 mph. It has proved to be much superior to the mu-meter and British pendulum tester for measuring the merits of different roadway treatments under icy conditions. The same vehicle was used for all 1981 and 1982 tests.

Testing procedures for stopping-distance comparisons between PlusRide rubber-asphalt and normal asphalt-concrete pavements involved making a series of stops on each surface type. On an icy road surface not in a normal stopping zone, repeated test stops were found to polish the surface and increase subsequent stopping distances, as shown in Figure 10. On the date of this test series, a thin ice cover was present on all sections, but the protruding rubber particles of the PlusRide pavement still resulted in a 50 percent reduction in stopping distances compared with that of adjacent normal pavements.

Results of all stopping-distance tests made on the Fairbanks areas PlusRide sections during the 1980-1981 and 1981-1982 winters are shown in Table 4. Tests results represent the average of two to six stops on each pavement type. For this test series, performed under icy-road conditions with some roadway sand occasionally present, an average reduction of 25 percent in stopping distance was achieved from the use of rubber in the paving mix. No salting for ice control had been done on these pavements. By comparison, tests of bare pavements at these air temperatures indicated minimum stopping distances of 25-30 ft. The use of coarse sands for ice control in similar areas would normally result in reduced stopping distances for only a short period of time, since the sand blows off under traffic action. Results of Tapley-meter stopping tests for sands (1 lb sand/ft^2) on road ice adjacent to the Carnation test site (Figure 11) show that stopping distances at a temperature of -6°F were not significantly reduced from a normal icy-road value of 140 ft by sanding, except for the first two to four stops.

From these comparative tests, it can be seen that stopping-distance reductions achieved with the PlusRide pavements were lasting and quite significant in magnitude, whereas roadway sanding was of only temporary and minor benefit. A few tests of sand applications over PlusRide pavements indicated that significantly greater reductions in stopping distances were obtained from the use of sand than was obtained on normal pavements. The use of rubber in the pavements tested did not provide the same degree of reduction in stopping distances that would have been achieved by salting but did significantly increase the safety aspect at the locations where it was applied. The benefit of the rubber particle (Figure 12) was most notable in higher-speed and higher-traffic areas, where traffic action serves to whisk away the snow and ice particles from the pavement. Applications that meet this criterion and occasionally present icy-surface hazards include bridge decks and insulated roadway sections.

SUMMARY

Between 1979 and 1981, seven experimental rubber-modified pavement sections, which totaled 2.5 miles in length, were constructed by the Alaska Department of Transportation. In these projects 3 to 4 percent of coarse rubber particles were incorporated into hot mixed asphalt pavements by using a system developed in Sweden under the trade name Rubit and now patented in the United States under the name PlusRide. The paving mixes have been successfully prepared in both batch and drum-dryer plants and placed with conventional pavers and rollers. Mix design experience by the Marshall method has demonstrated that the rubber greatly changes the

Figure 10. Tapley-meter test comparisons of stopping distances for rubber-asphalt versus regular asphalt pavement by repeated stops in same wheelpath.

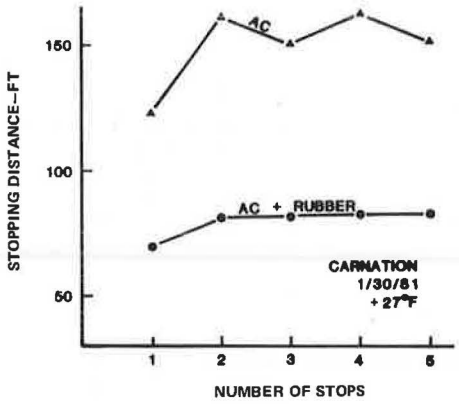

Figure 11. Effects of different sands on stopping distance for repeated stops on smooth road ice.

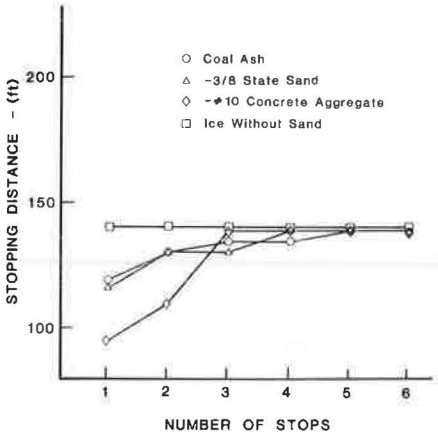

Table 4. Comparative tests of PlusRide and normal AC pavements under icy road conditions at 25 mph.

Date	Pavement Temperature (°F)	Site	Stopping Distance (ft)		Percent Reduction with Rubber
			PlusRide	Normal	
01/22/81	-13	Carnation	91	114	20
01/22/81	-13	Fairhill	64	129	50
01/30/81	+27	Fairhill	75	113	34
02/02/81	+27	Carnation	98	101	3
02/05/81	+27	Carnation	53	91	42
02/06/81	+21	Carnation	52	64	19
12/10/81	+13	Peger Road	61	66	7
12/11/81	+6	Peger Road	43	49	12
12/16/81	+6	Peger Road	58	90	36
12/18/81	+18	Peger Road	63	77	18
01/11/82	-9	Peger Road	82	97	15
01/14/82	-11	Peger Road	82	100	18
01/29/82	0	Peger Road	55	109	50
02/02/82	10	Peger Road	80	93	14
02/03/82	17	Peger Road	48	55	13
02/04/82	25	Peger Road	65	80	19
02/09/82	21	Peger Road	70	87	20
02/10/82	14	Peger Road	94	123	24
02/11/82	6	Peger Road	62	124	50
Avg value			68	93	25

Figure 12. Demonstration of ice-free benefits of rubber-modified asphalt pavement (foreground) versus ice-covered normal pavement (background), Feb. 1980.

mix properties, and from 1 to 2 percent more asphalt is normally required for the attainment of a 3 percent or lower void content, the primary factor used in selection of a suitable mix design. The attainment of a field void level of less than 8 percent, through high asphalt content and compactive effort, has been shown by field experience to be critical to pavement resistance to ravelling. Field voids of less than 5 percent are highly desirable. In spite of the high asphalt contents and soft asphalt grades used in these mixes, no asphalt bleeding has occurred.

Benefits of rubber-modified paving mixes include the ability to shed an ice cover more quickly than conventional pavements, the development of a more flexible and fatigue-resistant pavement, a significant reduction in tire noise, and the beneficial use of what is normally a troublesome waste product, used tires. Under Alaskan conditions of icy non-salted roadways, stopping distances were consistently reduced by the use of rubber-modified asphalt pavements; stopping distances averaged 25 percent less than on normal pavements. Further field and laboratory studies are needed to optimize these benefits and determine the most satisfactory material specifications.

ACKNOWLEDGMENT

This research work was accomplished in cooperation with the Federal Highway Administration under the Highway Planning and Research funding program. Appreciation is extended to Nyla Ford, Emory Richardson, and Gary Hicks for information used herein and to Construction and Materials Section personnel of the Alaska Department of Transportation and Public Facilities for design and construction analyses and reporting. The field studies of friction benefits by R. Gaffi were particularly appreciated.

The contents of this paper reflect my views and I am responsible for the facts and accuracy of the data presented. The contents do not necessarily reflect the official views or policies of the Alaska Department of Transportation and Public Facilities or the Federal Highway Administration. This paper does not constitute a standard, specification, or regulation.

REFERENCES

1. C.H. McDonald. A New Patching Material for Pavement Failures. HRB, Highway Research Record 146, 1966, pp. 1-16.
2. C.H. McDonald. An Elastomer Solution for "Alligator" Pattern on Fatigue Cracking in Asphalt Pavements. Presented at International Symposium on Use of Rubber in Asphalt Pavements, Salt Lake City, UT, 1971.

3. E.L. Green and W.J. Tolonen. The Chemical and Physical Properties of Asphalt-Rubber Mixtures. Arizona Department of Transportation, Phoenix, 1977.
4. D.C. Murray and U.F. Ernst. An Economic Analysis of the Environmental Impact of Highway Deicing. Office of Research and Development, U.S. Environmental Protection Agency, EPA 600/2-76-105, May 1976.

Publication of this paper sponsored by Committee on Winter Maintenance.

Benefits and Costs of Snow Fences on Wyoming Interstate 80

RONALD D. TABLER AND RICHARD P. FURNISH

Snow-fence protection along a 100-km section of Wyoming Interstate 80 has gradually been increased from none to 50 percent since 1970. This presents a unique opportunity to identify effects of the snow fences on snow-removal expenditures, accident frequency, and road closure. This information is needed for economic analyses to determine the feasibility of future snow-control projects. The study indicated that snow-removal costs were reduced by more than one-third as a result of the effective elimination of snowdrifts. Accidents during blowing snow conditions decreased in proportion to the length of highway protected, with a 70 percent reduction at the current level of fencing. There is some indication of a comparable reduction in wind-related accidents. These effects reflect the improved visibility and road-surface conditions observed in the areas protected by snow fences. The fences have had no significant effect on the length of time the highway is closed to traffic, and it is hypothesized that protection might have to approach 100 percent before such an effect could be expected. Fence construction costs can be amortized within 10 years through reduced winter maintenance costs and property damage. Effectiveness of the snow fences is attributed primarily to adequate snow-storage capacity and the use of tall (3.78-m) fences.

On October 3, 1970, a 124-km section of Interstate 80 (I-80) between Laramie and Walcott Junction, Wyoming, was opened to traffic. This new road was in a different location from US-30, which it replaced; by following the old Overland Trail along the foot of the Medicine Bow Mountains, the new route was about 27 km shorter. Because the new highway was in a sparsely populated region up to 30 km from US-30, there was little beforehand knowledge of weather conditions, and highway engineers thought it necessary to gain a winter's experience before building snow fences.

The first winter, large drifts formed on the highway and snow-removal expenditures were excessive in comparison with those on US-30. Frequent ground blizzards caused poor visibility that required the highway to be closed to traffic for a total of 8.4 days. Several factors contributed to more severe snow problems on the new route than had been experienced on US-30. About two-thirds of the old route was immediately downwind of the Union Pacific Railroad, which was well protected with snow fences that also provided protection for US-30, although this was not generally appreciated at the time. The new route is also much closer to the Medicine Bow Mountains, which resulted in more snowfall and stronger winds.

As a result of the first winter's experience, highway engineers gave high priority to construction of snow fences to reduce drifts forming in the road cuts. The first snow-fence construction began in the summer of 1971 and continued into the summer of 1972. By the end of the second winter, it was apparent that fences would alleviate drift formation on the road, but, in addition, dramatic improvements in visibility and road-surface conditions were also evident (1). As a result, additional snow fences have been constructed over subsequent years; the last ones were completed in the summer of 1979. The gradual addition of snow fences along this highway provides a unique opportunity to evaluate their effectiveness in relation to accidents, snow-removal expenditures, and days of road closure. Although there are many published references to the effectiveness of snow fences in qualitative terms, we are not aware of any quantitative evaluation comparable to that provided by this 11-year study.

PHYSICAL AND CLIMATIC CHARACTERISTICS

The section of this highway with the greatest winter weather problems is that between Miles 235 and 295, where the road is closest to the mountains, and this 96.6-km segment comprises the study section. General road orientation is southeast-northwest, and mean elevation over the study section is about 2250 m (Figure 1).

Typically, the first snow falls after mid-September and the last in mid-May. During the study, only 0.8 percent of the ground blizzard accidents were in September and May combined, which led us to choose October 1 to April 30 as the period for the accident analyses. More than 95 percent of the precipitation over this period is snow.

Mean monthly precipitation, wind speed, and air temperature for the study period (1970-1981) are shown in Table 1. Mean water-equivalent precipitation from October 1 to April 30 is 31.1 cm. Snowfall in October and April usually melts within a few days. Most drifting is between November 1 and March 31; precipitation averages 19.8 cm for this period.

Westerly winds are dominant and strongest. Maximum wind gusts up to 45 m/s were recorded in three years of the study. Although major snowstorms are often associated with easterly winds, these are of relatively short duration and are not so strong as the prevailing westerlies. More than 95 percent of the annual snow transport is from the west, and all the snow fences are on the west side of the highway. Because of the strong, persistent winds and long periods of below-freezing temperatures, most of the snowfall is relocated by the wind.

The highway passes through uncultivated rangeland vegetated with low-growing grass and sagebrush 10-45 cm in height; there are only a few isolated groves of trees and taller shrubs. The upwind "fetch"

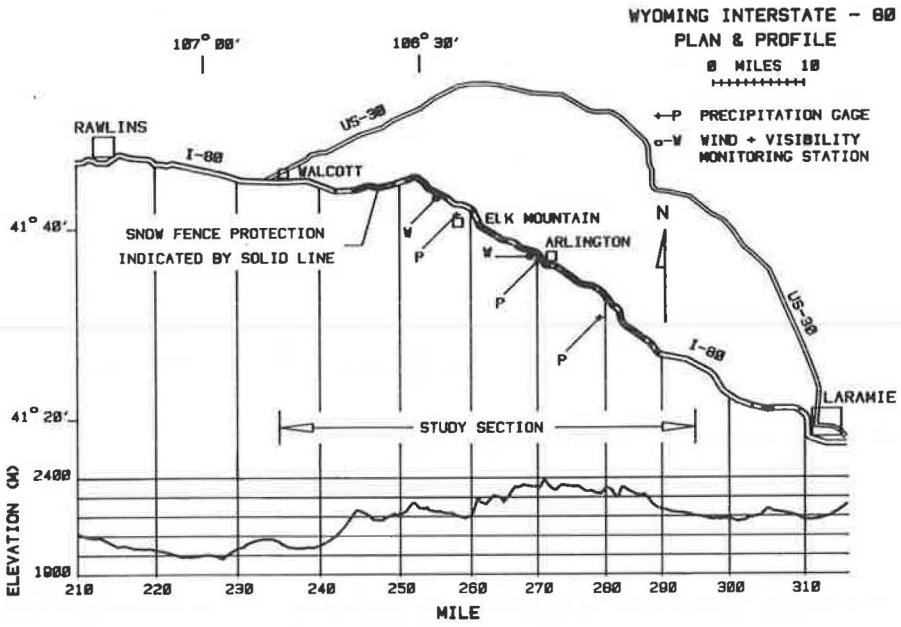

Figure 1. Location map and profile of I-80 between Laramie and Walcott, Wyoming.

Table 1. Climatological characteristics of I-80 study section.

Characteristic	Oct.	Nov.	Dec.	Jan.	Feb.	March	April	Total
Wind speed (m/s)								
Mile 255[a]	4.9	7.0	9.3	7.9	8.3	6.6	5.4	
Mile 270[b]	6.0	8.2	10.0	9.5	9.4	8.0	6.7	
Air temperature (°C)[c]	6.7	–0.6	–3.4	–5.9	–3.4	–0.9	3.3	
Precipitation (cm)[d]								
Mile 261	3.5	3.1	3.0	3.0	2.4	3.6	5.2	23.7
Mile 270	5.9	4.4	4.9	4.9	3.5	5.8	8.1	37.6
Mile 282	4.3	4.2	4.2	4.0	2.7	5.6	6.8	32.0
Mean	4.6	3.9	4.0	4.0	2.9	5.0	6.7	31.1

[a]Location, Mile 255; elevation, 2225 m. Means are for January 1975 to April 1981; 7.3 m measurement height [from Martner (2)].
[b]Location, Mile 270; elevation, 2400 m. Means are for February 1974 to April 1981; 8.2 m measurement height [from Martner (2)].
[c]Location, Mile 261; elevation, 2217 m. Means for 1971 to 1981 from Elk Mountain station (Climatological Data for Wyoming from National Oceanic and Atmospheric Administration).
[d]Means for 1971 to 1981 from gages operated by the Rocky Mountain Forest and Range Experiment Station, Forest Service, U.S. Department of Agriculture. Elevations are as follows :Mile 261, 2210 m; Mile 270, 2364 m; Mile 282, 2358 m.

distance contributing blowing snow to the highway ranges from 200 m to 7000 m; a typical value is 3000 m. Total annual snow transport, as measured in the snow-fence drifts, has ranged from a maximum of 195 water-equivalent m^3/m of width transverse to the wind over the 1978-1979 winter to a low of 22 m^3/m for the 1980-1981 winter.

SNOW-FENCE SYSTEM

The snow fences between Laramie and Walcott were built in five stages, starting in 1971 (Table 2). Of the 53 km of snow fence in the total system, 70 percent is 3.78 m in height, 5 percent is 3.17 m, 24 percent is 2.44 m, and 1 percent is 1.83 m. About 98 percent of the snow fences are within the study section, providing protection for 49 km, or 51 percent, of this section of highway. Total construction cost, including that outside the study section, has been $1 910 000, or about $38 200/km of protected highway.

Fences built in the first contract protected road cuts where large drifts formed on the roadway during the first winter. Half of the second contract was to improve visibility in a 4-km section of the highway; the other half was to eliminate smaller drifts not severe enough to have been included in the first contract as well as drifts at interchanges and grade separations. Subsequent contracts have concentrated on locations with unusually high accident frequency and locations where drifts encroach on the traffic lanes only during the heaviest snowfall years.

The snow fences are of a standard design adopted by the Wyoming State Highway Department in 1971 and have been described in a previous publication (3). The structures consist of horizontal boards 15 cm wide separated by 15-cm spaces, a bottom gap of approximately one-tenth of the fence height, and a 15° inclination downwind (Figure 2). Net porosity (open area) of the structure, excluding the bottom gap, is about 48 percent.

Studies of the geometry of the snowdrifts formed by these fences indicate that their storage capacity equals or exceeds that of other designs (4). Combined cross-sectional area of the windward and leeward equilibrium drifts is $21.9H^2$, and water-equivalent capacity in cubic meters per meter is about $7.8H^{2.18}$, where H is total vertical fence height in meters. Maximum length of the lee drift when the fence is full is about 30H.

Placement criteria for the fences have been revised from those reported previously (3) as more information has become available concerning the drift geometry. Current specifications include a minimum distance of 30H from the right-of-way, a

Table 2. Snow-fence contracts between Miles 235 and 295, Wyoming I-80.

Contract	Construction Date	Location (Mile)	Fence Height (m) 1.83 Length (m)	1.83 Price ($/m)	2.44 Length (m)	2.44 Price ($/m)	3.17 Length (m)	3.17 Price ($/m)	3.78 Length (m)	3.78 Price ($/m)	Road Protection (m)
1	1971-1972	246-280	419	17.23	2 589	20.51	2643	24.61	12 728	26.84	12 746
2	1973	246-285	0	–	2 165	22.97	0	–	12 504	29.53	14 489
3	1974-1975	244-256	0	–	1 741	33.63	0	–	2 507	55.61	5 757
4	1977-1978	242-279	0	–	3 706	29.20	0	–	5 413	46.75	9 494
5[a]	1979	281-289	0	–	1 589	31.17	0	–	3 852	50.86	6 708
Total			419		11 790		2643		37 004		49 194

[a]Values for fifth contract do not include 927 m of 2.44-m fence built outside study section.

Figure 2. Standard 3.78-m snow fence used on I-80 (Mile 254.2, Feb. 18, 1972).

35-40H spacing between tandem rows, a minimum length of 30H to minimize "end effect," orientation perpendicular to the prevailing wind, a 10H extension of fences beyond the length of road to be protected, and placement of fences on hills or at the upwind edge of depressions to increase storage capacity.

Fence systems at each site are designed to have sufficient capacity to store all the anticipated snow transport over an average winter by using the method described by Tabler (5). At most locations, one row of 3.78-m fence is adequate. Because the storage capacity of the new fence design was uncertain when the first contract was engineered, those fence systems were overdesigned to such an extent that they have not filled completely over the 10 years they have been in place.

DATA AND ANALYSES

Accident Data

Accident data were compiled by computer by the Highway Safety Branch of the Wyoming State Highway Department from standard reports filed by the Wyoming Highway Patrol and motorists. The Wyoming state standard categories of weather conditions used for this analysis were as follows:

1. Snow: snowfall without appreciable blowing snow;
2. Ground blizzard: conditions with blowing and drifting snow sufficient to reduce visibility (the term "ground blizzard" is not strictly correct because there may or may not be concurrent precipitation; under conditions of moderate to severe blowing snow, it is difficult to tell whether or not it is snowing);
3. Wind: wind speed averaging about 10 m/s or more without precipitation or appreciable blowing snow; and
4. Other: a category that includes rain, fog, dust, and clear-weather conditions.

These categories include all road-surface conditions and are not necessarily related to the cause of the accidents.

Number of vehicles traveling the study section was measured by a permanent traffic counter, allowing accidents to be expressed per million vehicle kilometers.

Weather Data

To account for annual variations in snowfall, accidents and duration of road closure were normalized with respect to precipitation. A National Oceanic and Atmospheric Administration (NOAA) cooperative observer weather station is located in the town of Elk Mountain, but this station alone is not representative of the entire study section. The usefulness of the NOAA gage is also limited because the location has been moved several times during the study period, none of the sites has been sufficiently protected from the wind, no wind shield has been used, and there are periods of missing data. Unfortunately, the gage was not in operation during the 1970-1971 winter when the highway was first opened to traffic.

For these reasons, recording precipitation gages have been maintained at three locations along the highway since September 1971 (Figure 1). These gages are equipped with wind shields and are also located in small openings in groves of trees to reduce undermeasurement caused by wind. We believe that these sites furnish exceptionally accurate precipitation measurements and provide a reasonable estimate for precipitation along the study section.

A linear regression was used to estimate precipitation for the 1970-1971 winter by using the mean values from these gages with the mean of NOAA weather stations at Leo, Rawlins, and Laramie for the winters of 1971-1972 through 1980-1981. This analysis provided an estimate having a 0.95 confidence interval of ±11 percent of the estimated mean.

In addition to the precipitation-gage network, the Wyoming State Highway Department also operates weather-condition monitoring stations (Figure 1) by using instrumentation developed by Schmidt (6). Wind-speed and visual-range data are transmitted

from these locations to the district maintenance office in Laramie, where they are recorded on strip charts and analyzed by an on-line computer (7). These stations are the source of the wind data in Table 1 and are also used for the traffic operations decisions discussed later in this paper.

Snow- and Ice-Removal Expenditures

Maintenance for the highway in the study section is provided by several crews, which makes precise calculations impossible. Crews at Laramie provide winter maintenance from Mile 280.5 to 295, and it is not possible to isolate those expenditures on the study section. Consequently, snow- and ice-removal data used in this report are for Miles 235-280.5, which is served by maintenance crews stationed at Arlington and Elk Mountain; the length of highway protected by fencing for the analysis of snow- and ice-removal costs is different from that used for the accident analysis.

Snow- and ice-removal expenditures were difficult to retrieve and suffer from several deficiencies. Although the maintenance station at Elk Mountain was in operation by September 1970, the Arlington station was not built until July 1971. Much of the snow-removal work the first winter was done by crews stationed at Laramie and Rawlins, which makes it difficult to separate expenses incurred on the study section. Charges for special heavy equipment to clear the larger drifts were identifiable, however, and constitute most of the expenditures for the study section during calendar year 1971. Maintenance crews from Laramie and Rawlins have continued to help the Arlington and Elk Mountain crews on special occasions, and these expenses cannot be identified from accounting records.

Calendar-year accounting was used until June 1973, which makes it impossible to separate expenses by the winter in which they were incurred. Fiscal-year accounting was instituted in 1973, and records were computerized by fiscal year 1977. The 1975-1976 winter was the only one for which maintenance costs could not be retrieved for this study.

To account for the effects of inflation over the analysis period, snow-removal expenditures for the Arlington-Elk Mountain maintenance sections were expressed in relation to expenditures for the remainder of Wyoming I-80 (about 550 km). This ratio is essentially independent of inflation and should partly adjust for annual variations in snowfall.

Snow-Fence Protection

Snow-fence protection was measured on aerial photographs as the road length between lines parallel to the prevailing winter wind direction drawn from the ends of the fences. Wind directions are known for all fence locations from preconstruction studies that measured orientation of snowdrifts shown on aerial photographs. No adjustment was made for the poorer efficiency near the ends of the snow fences (3,4).

RESULTS

Snow- and Ice-Removal Expenditures

Snow- and ice-removal expenditures and snow-fence protection are shown in Table 3 and Figure 3. For the reasons discussed previously, costs for the study section in the first half of the 1970-1971 winter are unknown, and the calendar-year accounting combines the last half of 1970-1971 with the first half of the 1971-1972 winter, by which time more than half of the first contract had been installed. Despite this complication and the fact that an appreciable portion of the costs on the study section are not included, snow- and ice-removal costs in calendar year 1971 were about 50 percent higher than the average over succeeding years. For calendar year 1972 through fiscal year 1981, the ratio of expenditures on the study section to those on the rest of I-80 was 0.31 ± 0.10, with a 0.999 confidence interval. There is little doubt that the decrease from the calendar year 1971 value of 0.48 was caused by the snow fences built under the first contract, which comprised 35 percent of the total system.

There is no significant further decrease in costs as additional fences were built, but this is to be expected because the first contract protected all sites where snowdrifts formed in traffic lanes the first winter; subsequent contracts have been primarily to improve visibility and protect structures.

The data suggest that the fences reduced snow- and ice-removal costs by at least a third and, considering the conservative nature of the 1971 data, the actual reduction was probably closer to 50 percent. Visual observations over the study period, as documented by photographs such as Figures 4-6, support the conclusion that the fence systems have eliminated drifts on the traffic lanes, even in years of record precipitation.

Road Closures

The most common reason for closing the highway to traffic is poor visibility caused by blowing snow. Occasionally, however, closure is necessitated by intense snowfall that accumulates faster than plows can remove it or because of an excessive number of accidents.

Road-closure data for 1970-1981 are included in Table 4. As shown in Figure 7, the fences had no apparent effect on the amount of time the highway had to be closed to traffic. The variability in closure time suggests that normalizing this variable with respect to total precipitation does not account for all the yearly differences in weather conditions, but, in addition, closure decisions are often largely subjective, which in itself contributes to the year-to-year variability.

A reasonable explanation for the apparent failure of the fences to reduce closure time is that poor visibility in even a short section of unfenced highway could necessitate closure of the road, which suggests that fence protection might have to approach 100 percent before a reduction in closure time could be expected.

Accidents

Accidents by categories, snow-fence protection, and supporting data for 1970-1981 are shown in Table 4. As shown in Figure 8, snow accidents were independent of the degree of fence protection, and this was also true for "other" accidents. This is to be expected, by definition of these weather-condition categories. In Figure 6, accident frequency for the first two categories is expressed per centimeter of precipitation from October 1 to April 30.

Ground blizzard accidents, however, have been reduced significantly (Figure 8). Although there is some suggestion of a convex curvilinear relationship, the residual variance is reduced very little by any transcendental transformation, and it is difficult to justify a particular model on theoretical grounds. The curve might be expected to level out at some accident frequency greater than zero as 100 percent protection was approached, but there is no indication that such a plateau has been reached

Table 3. Expenditures for snow and ice removal, Miles 235-280.5, Wyoming I-80.

Period	Snow-Fence Protection (%)	Expenditure ($)		
		Mile 235-Mile 280.5	Remainder of I-80	Ratio
Jan. 1-Dec. 30, 1970	0	–	–	–
Jan. 1-Dec. 30, 1971	4.54	235 800	489 485	0.482
Jan. 1-Dec. 30, 1972	12.82	104 147	393 177	0.265
Jan. 1-June 30, 1973	16.55	137 055	360 613	0.380
1973-1974 winter	32.34	175 442	604 979	0.290
1974-1975 winter (to Feb. 1)	36.71	53 710	219 634	0.245
1975-1976 winter	40.20	–	–	–
1976-1977 winter	40.20	118 729	294 597	0.403
1977-1978 winter	44.04	227 184	623 397	0.364
1978-1979 winter	53.17	297 777	856 804	0.348
1979-1980 winter	53.17	345 580	1 141 134	0.303
1980-1981 winter	53.17	137 240	574 315	0.239

Figure 3. Expenditures for snow and ice removal (Miles 235-280.5 to remainder of I-80) versus snow-fence protection.

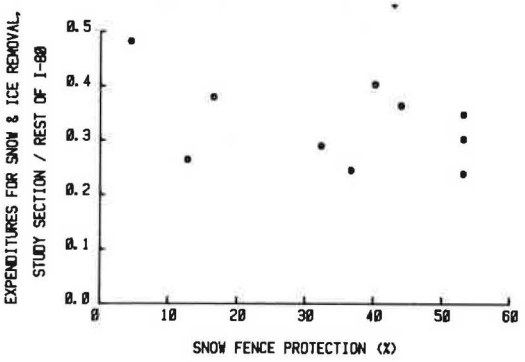

Figure 4. Snow accumulation at Mile 269.5 on Feb. 19, 1971, before installation of snow fences.

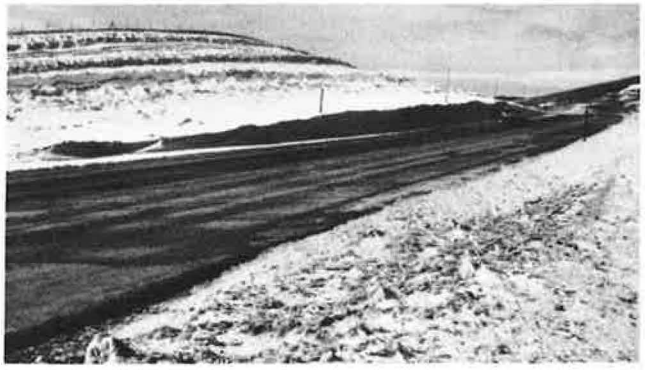

Figure 5. Snow accumulation at Mile 269.5 on Feb. 1, 1972, after installation of snow fences.

Figure 6. Aerial view of system protecting cut at Mile 269.5 on Feb. 11, 1972.

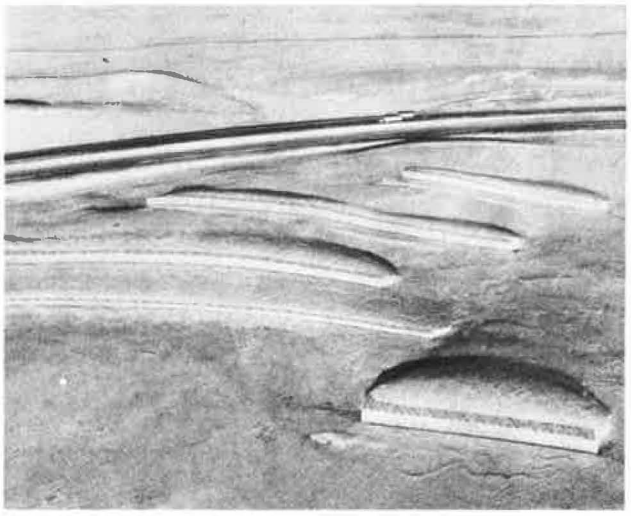

with the current level of fence protection. The data provide little justification for choosing a curvilinear model, which leads us to fit the following linear regression:

$$G/P = 0.0281 - 0.000\,39X, X \leq 51 \quad (R^2 = 0.62; SE = 0.001\,65) \quad (1)$$

where

- G = number of ground blizzard accidents per million vehicle kilometers,
- P = precipitation from October 1 to April 30 (cm), and
- X = fence protection in percentage of total study section length.

This regression indicates that ground blizzard accidents have been reduced about 70 percent with the current level (51 percent) of fence protection. Expressing the accident frequency in terms of precipitation improves the correlation, but the regression between X and G alone also shows a significant decrease in ground blizzard accidents.

Another test that does not require normalization with respect to precipitation is the ratio of ground

Table 4. Road-closure data, Oct. 1 to April 30, 1970-1981, Wyoming I-80, Miles 235-295.

Winter	Snow-Fence Protection (%)	Total Vehicles	Precipitation (cm)	Time Closed (days)	Accidents[a]					Valuation per Accident ($)
					Total	Snow	Ground Blizzard	Wind	Other	
1970-1971	0	683 020	32.3 ± 3.6	8.4	148 (110)	32 (18)	55 (48)	27 (20)	34 (24)	1301
1971-1972	7.54	662 655	28.4	6.2	128 (57)	12 (4)	41 (27)	54 (21)	21 (5)	1683
1972-1973	13.20	527 043	45.9	14.8	187 (101)	28 (18)	62 (36)	40 (19)	57 (28)	1180
1973-1974	28.21	554 560	32.8	7.8	132 (70)	17 (9)	36 (25)	52 (24)	27 (12)	1639
1974-1975	31.52	666 669	28.4	5.3	94 (52)	20 (25)	25 (3)	28 (12)	21 (12)	1763
1975-1976	34.17	708 192	30.6	4.4	140 (66)	20 (10)	52 (28)	38 (12)	30 (16)	1236
1976-1977	34.17	818 456	22.6	1.5	84 (59)	20 (20)	13 (11)	7 (7)	44 (21)	1711
1977-1978	37.08	857 638	25.4	4.8	133 (82)	23 (10)	27 (14)	36 (22)	47 (36)	1846
1978-1979	44.00	941 716	35.0	9.4	145 (85)	24 (10)	49 (32)	30 (19)	42 (24)	2930
1979-1980	50.95	779 443	41.4	15.6	163 (88)	33 (16)	29 (26)	43 (15)	58 (31)	2994
1980-1981	50.95	920 676	18.8	0.7	61 (53)	20 (16)	2 (4)	7 (5)	32 (28)	3041

[a]Injuries plus fatalities are shown in parentheses.

Figure 7. Days of road closure per centimeter of precipitation Oct. 1 to April 30 versus percentage of highway protected by snow fence.

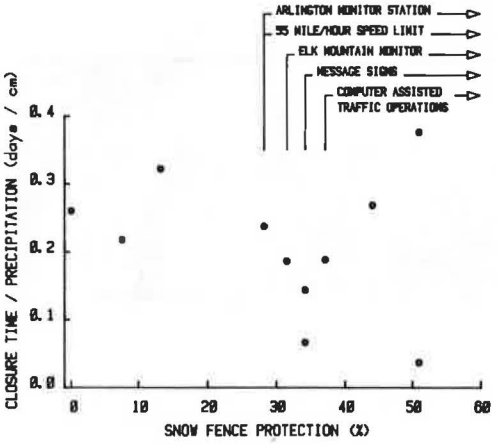

Figure 8. Snow, ground blizzard, and wind accidents in relation to percentage of highway protected by snow fence.

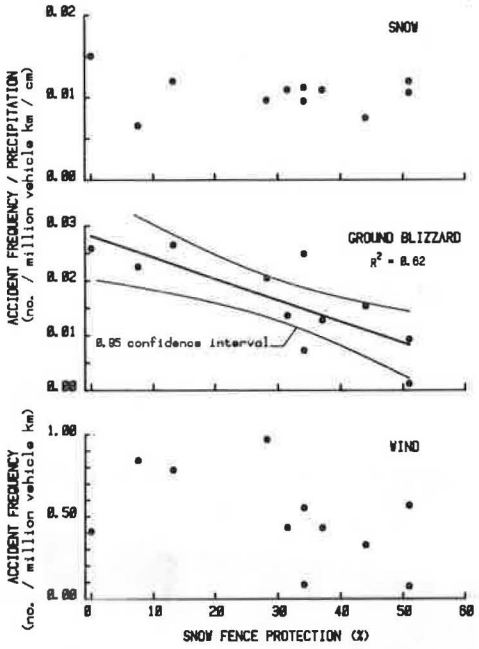

blizzard accidents to "other" (O) accidents. A linear regression fitted to these data is given as follows:

$$G/O = 1.8134 - 0.0254X, X \leq 51 \ (R^2 = 0.49) \quad (2)$$

This relationship also suggests a 70 percent reduction in ground blizzard accidents with the current level of fence protection.

The reduction in this category of accidents is to be expected, considering the dramatic improvement in visibility observed in the areas protected by snow fences (Figures 9-11). There is also a general improvement in road-surface conditions downwind of the fences (Figure 12) caused by a reduction in snow transport across the road, which reduces heat loss and slush accumulation during periods of sunshine with air temperature above -5°C. A dark road surface provides much better delineation than a snow- or ice-covered surface under conditions of reduced visibility. All these effects contribute to the reduction in ground blizzard accidents.

It should be noted that precipitation over the 1972-1973 winter (13 percent protection) was the highest since records were begun in 1906 at Elk Mountain, and the 1978-1979 winter was the fifth highest on record.

Were it not for the anomalous value for the 1970-1971 winter, there would also be a significant reduction in the frequency of wind accidents over the study period. The relatively low number of accidents in this category over the first winter may be due to the fact that before the first fences were installed there was reduced opportunity for wind accidents because of the prevalence of blowing snow. If it were reasonable to exclude the 1970-1971 data for this reason, the linear regression relating the frequency of wind accidents (W) to fence protection would be as follows:

$$W = 0.9656 - 0.0137X, 0 < X \leq 51 \ (R^2 = 0.43) \quad (3)$$

If this effect were real, it could reflect the improvement in road-surface conditions that contribute to wind accidents. There is also some evidence that wind speeds on the roadway are significantly reduced downwind of the snow fences. In March 1979, Tabler measured wind profiles (in the first 10 m above the ground) upwind and downwind of a 3.78-m snow fence nearly filled to capacity with snow. On the highway at 190 m (50H) downwind of the fence, mean horizontal wind speed up to the 3.4-m height averaged about 14 percent less than that of the wind measured simultaneously at 134 m upwind of the fence (ambient 10-m wind averaged 20 m/s). This would

Figure 9. Aerial view of two rows of 3.78-m snow fence showing effect of fences on visibility (Mile 263, Feb. 11, 1972).

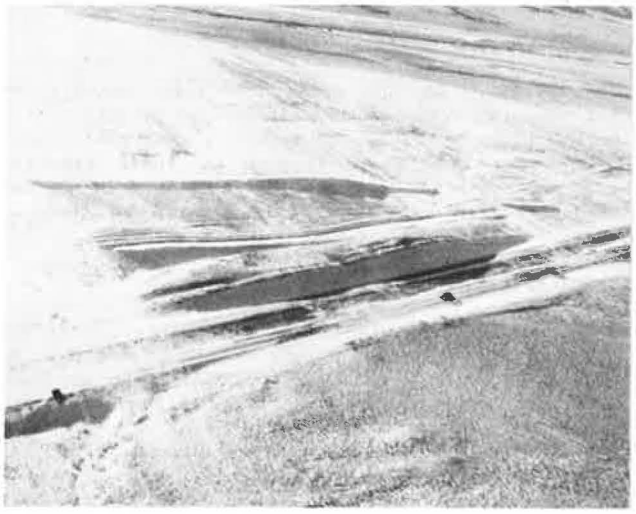

Figure 10. Visibility 70 m outside area protected by two rows of 3.78-m snow fence (Mile 262, Feb. 15, 1972).

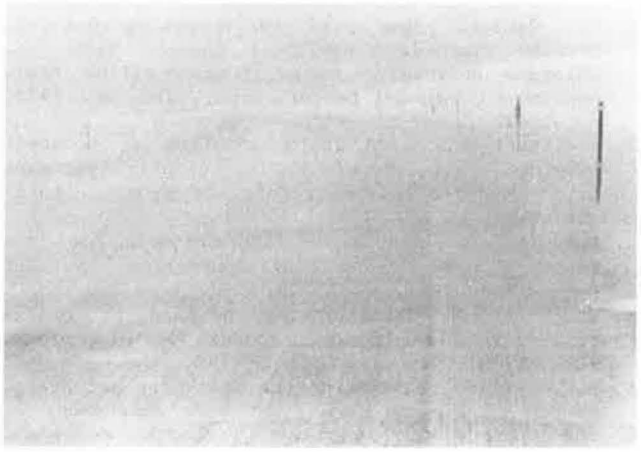

Figure 11. Visibility of same area as in Figure 10 inside area protected by two rows of 3.78-m snow fence.

Figure 12. Effect of single row of 3.78-m snow fence on road-surface conditions; end corner of fence extending left near center; most of fence hidden behind lee drift (Mile 247.6, March 22, 1973).

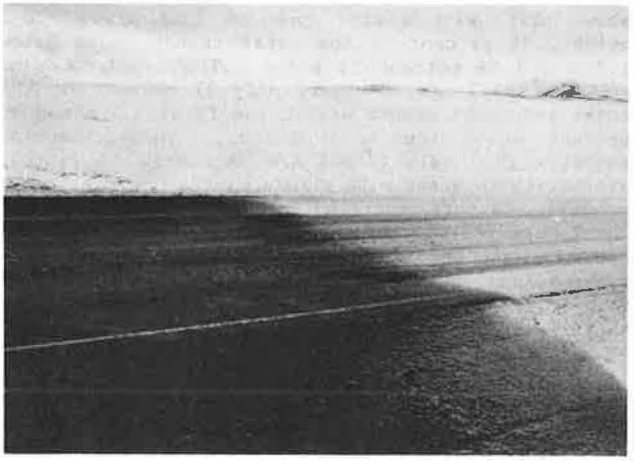

imply a reduction of about 25 percent in wind load on a standard tractor-trailer combination. The reduction in wind speed may be even greater before a fence fills with snow, but these data are not yet available.

DISCUSSION AND CONCLUSIONS

Representativeness of Study Period

Average winter precipitation from 1970 to 1981 at our Elk Mountain gage (23.7 cm) was comparable with that from 1906 to 1969 published for the NOAA station at Elk Mountain (21.5 cm). Precipitation over the 1972-1973 winter (39.8 cm) exceeded the previous maximum (36.3 cm) recorded over the winter of 1916-1917. Precipitation in 1979-1980 was the fifth highest on record. We conclude that the study period included winters as severe as any in the last 75 years and was representative of long-term precipitation to be expected over the study section.

Effect of Other Safety Measures

The snow fences have not been the only step taken to improve highway safety on this section of I-80. The first weather-monitoring station (as described previously) was installed in January 1974, and a second was in operation by January 1975. Since the on-line computer for analysis of these data was installed during the 1977-1978 winter, standardized criteria have been available to the maintenance foremen who make decisions relative to road closure.

In March 1976, overhead variable-message signs were installed at Laramie and Walcott, where traffic can be stopped or rerouted as conditions require. Optional automatic computer control of these signs was available for the 1978-1979 winter. A motorist information low-power radio system was also in operation from 1976 to 1978.

All these measures could contribute to the reduction in accidents, but two pieces of evidence suggest that the effect was due largely to the snow fences. First, the efficacy of these other measures should be reflected in the frequency of snow accidents, which was shown to be independent of fence protection. The absence of any significant decrease in snow-accident frequency over the 1970-1981 period suggests that the snow fences were primarily responsible for the reduction in the ground blizzard and wind accidents. Second, the downward trend in

ground blizzard accidents was evident prior to the institution of these other measures, although the other safety aids may contribute to the more marked reduction evident in the last five years.

The 55-mile/h (89-km/h) speed limit went into effect on March 4, 1974. This would not be expected to influence the snow or ground blizzard categories but could have some effect on the frequency of wind and other accidents when road-surface conditions were conducive to high-speed driving.

Factors Contributing to Fence Effectiveness

Improved visibility and more favorable road-surface conditions in areas protected by snow fences are considered to be the primary reasons for accident reduction on the study section. In turn, these favorable effects are only possible because of the adequate design of the fence systems. A primary requirement for these effects to be realized is that the fence systems have sufficient capacity to store all snow transported over a winter with average precipitation.

Although most of the snow transport is within the first meter above the ground, a significant portion is carried at greater heights; the vertical distribution of blowing snow becomes more uniform as wind speed increases. Our analysis of Antarctic data (8) shows that, with a wind speed of 11.6 m/s at 10-m height, 95 percent of the total transport is below 1.2 m and 99 percent is below 3.7 m. With a wind speed of 22.3 m/s, however, only 77 percent of the total transport occurs within the first 1.2 m and 95 percent below the 3.7-m height. This reasoning suggests that tall fences are necessary to improve visibility in areas with strong winds.

Other factors contributing to effectiveness of the fences include the structural design itself, the use of long fences without holes or gaps in the systems, and optimum fence placement.

Amortization of Fence Construction Costs

If snow- and ice-removal costs are assumed to be reduced by one-third, the total savings in the last five years (when costs are most accurately known) is $563 000. This suggests that the cost of fence construction is easily amortized over their anticipated physical life (≥25 years) by the savings in expenditures for winter maintenance.

For a winter with average precipitation and current traffic levels, 23 ground blizzard accidents are expected with the current level of fence protection (51 percent) compared with 77 without fencing (Equation 1). The average property-damage valuation per accident has been about $3000 over the last three years. If the entire fence system were rebuilt at 1979 contract prices, then construction cost could be amortized in about 15 years by the reduced accident damage alone. The average number of injuries plus fatalities per ground blizzard accident has been 0.65, which implies that over the average winter, 35 injuries are also prevented. This represents a further economic benefit as well as a humanitarian one. Inclusion of the possible reduction in wind accidents would further shorten the repayment period.

CONCLUSION

The experience on this section of I-80 demonstrates that properly designed snow fences can significantly improve highway safety and reduce winter maintenance costs. For conditions similar to those reported here, it appears that construction costs of an extensive system can be amortized in less than 10 years.

ACKNOWLEDGMENT

We gratefully acknowledge the invaluable assistance provided by the Highway Safety Branch of the Wyoming State Highway Department in compiling the accident records. This study would not have been possible without the support and commitment of the many highway department personnel involved with the snow-fence construction program.

This paper is dedicated to the maintenance personnel and patrolmen on the Arlington-Elk Mountain section, who have served the public with unexcelled dedication and self-sacrifice.

REFERENCES

1. R.D. Tabler. New Snow Fence Design Controls Drifts, Improves Visibility, Reduces Road Ice. Colorado University Annual Transportation Engineering Conference, Denver, Proc., Vol. 46, 1973, pp. 16-27.
2. B.E. Martner. Wind Characteristics in Southern Wyoming: Part I--Surface Climatology. Department of Atmospheric Sciences, Univ. of Wyoming, Laramie, Rept. AS 127, 1981, 117 p.
3. R.D. Tabler. New Engineering Criteria for Snow Fence Systems. TRB, Transportation Research Record 506, 1974, pp. 65-78.
4. R.D. Tabler. Geometry and Density of Drifts Formed by Snow Fences. Journal of Glaciology, Vol. 26, No. 94, 1980, pp. 405-419.
5. R.D. Tabler. Estimating the Transport and Evaporation of Blowing Snow. In Snow Management on the Great Plains Symposium, Bismarck, ND, Great Plains Agricultural Council Publ. 73, 1975, pp. 85-104.
6. R.A. Schmidt, Jr. Measuring Visibility in Blowing Snow. In Snow Removal and Ice Control Research, TRB, Special Rept. 185, 1979, pp. 200-207.
7. R.D. Tabler. Visibility in Blowing Snow and Applications in Traffic Operations. In Snow Removal and Ice Control Research, TRB, Special Rept. 185, 1979, pp. 208-214.
8. W.F. Budd, W.R.J. Dingle, and U. Radok. The Byrd Snowdrift Project: Outline and Basic Results. In Studies in Antarctic Meteorology, American Geophysical Union, Washington, DC, 1966, Antarctic Research Ser. Vol. 9, pp. 71-134.

Publication of this paper sponsored by Committee on Winter Maintenance.

Icing Conditions on Different Pavement Structures

KENT GUSTAFSON

In 1976, Test Field Linköping 1976 was constructed at the National Swedish Road and Traffic Research Institute at Linköping. The object of the investigations at the test field was to make a general study of the interaction between climate and road construction that results in slippery conditions in cold weather and to make a particular study of the icing risk potential of different road constructions. The investigations included road constructions representing both conventional uninsulated road pavements and constructions insulated with plastic foam, sulfur foam, expanded clay, and pelletized slag. The field was provided with instrumentation that automatically recorded, inter alia, the temperatures on and in the various road sections and in the air, the humidity, and the radiation balance. Investigations at Test Field Linköping 1976 were carried out over the winter seasons 1976-1977 to 1979-1980. A comprehensive review of the results is given. The climatic and road conditions in conjunction with ice formation are described, as well as examples of the variation in friction, surfacing temperature, etc., on the different road pavements in the winter. On the basis of these results, the relative icing risk potential of different road pavements has been determined.

Slippery conditions on roads in cold weather occur due to the interaction of climate and road construction. Climatic parameters such as air temperature, humidity, radiation balance, and amount of precipitation are significant for the formation of ice and snow. At temperatures below 0°C and when humidity is high, there is a risk, for instance, of hoar frost, which can give rise to slippery road conditions. Under other weather conditions, ice or snow may reduce skid resistance on the road surface, thus causing problems for road users.

The construction of the road and its surfacing plays an essential role in the formation of ice. Transfer of heat at the surface of the road is affected by the construction of the road and the road materials used. A certain section of a road may, for instance, become slippery more often than others because of differences in the construction of the road. Bridge decks, which have a lesser heat-storage capacity, cool down more rapidly than adjacent conventional sections of road. Similar conditions occur on roads with thermal insulation. The insulation layer retards the flow of heat upward, which gives rise, primarily in the autumn and winter, to more rapid cooling and ice formation. Investigations of skid resistance have been carried out by the National Swedish Road and Traffic Research Institute (VTI) on insulated roads and other roads (1), and the results showed that in many cases the road construction exerts a great influence on the occurrence of slippery conditions. Different types of conventional road construction exhibit differences in icing risk potential because of the differences in materials, such as sand, gravel, and ungraded crushed rock, that are used.

In the summer of 1976, a field, referred to as Test Field Linköping 1976, was constructed at the VTI at Linköping, Sweden. The object of the investigations at the test field was to make (a) a general study of the interaction between climate and road construction that results in slippery conditions in cold weather and (b) a particular comparative study of the icing risk potential of different road constructions. The investigation included both uninsulated and insulated types of road.

Investigations of road icing on different pavements were carried out at the test field over the period 1976-1980. The results from this four-year study have been published in VTI Report 216A (2).

ASPECTS OF THERMAL PROPERTIES OF ROAD-CONSTRUCTION MATERIALS

It is the energy balance and primarily the radiation balance that govern the variation of surface temperature on a road. The temperature of the road surface is affected both by climatic action on the surface such as radiation and precipitation and by heat exchange with the underlying soil strata. Chiefly by conduction, movement of heat takes place in the road structure to or from the road surface. The temperatures prevailing in the road structure depend, among other things, on road construction and the road materials used. The thermal conductivities and heat capacities of the materials have great significance for the variation of temperature on and in a road. For mineral materials the thermal conductivity largely depends on the density and water content but also on the conductivities of the constituent minerals. Materials of low density have lower conductivity owing to the fact that there are few points of contact where thermal conduction can take place. Increase in water content results in an increase in conductivity. Ungraded crushed rock of low density contains very little water and therefore has a lower thermal conductivity than, for instance, gravel or sand.

The effect on surface temperature of materials of relatively low thermal conductivity that are placed near the road surface varies somewhat depending on whether the energy balance is positive or negative. When the road is receiving energy, primarily from radiation, a low conductivity results in a smaller heat flow down into the construction, and the surface layer therefore warms up more and its surface temperature gets higher. On the other hand, when the road is emitting energy, the construction is cooled down more at the surface, owing to the fact that the upward heat flow, to compensate for the radiated energy, is retarded.

From the point of view of icing, the situation in conjunction with a negative radiation balance is of interest. For the same climatic stresses, a road pavement made up of, for instance, ungraded crushed rock will cool down more due to its lower thermal conductivity than will a pavement with gravel. A greater degree of cooling and the consequently lower surface temperature increase the risk of icing. The extreme example of the above reasoning is provided by materials of very low thermal conductivities, i.e., thermal insulation materials. Plastic foam is used for frost insulation of road pavements (3,4). Owing to the extremely low thermal conductivity of the material, $\lambda \sim 0.03$ W/mK, it cannot be placed too near the surface because of the cooling effect, which is schematically illustrated in Figure 1 (5). In winter when the energy balance is normally negative, the heat flow is directed upward. In an insulated road this flow is reduced, resulting in lower surface temperature conditions. The surface temperature also depends on the heat capacities of the pavement materials. When radiation is outward, the magnitude of cooling is dependent on the rate at which heat can be conducted up to the surface to compensate for the energy loss. The degree of cooling also depends on how much heat there is available, i.e., on the heat capacity. The available quantity of energy is mostly obtained from cooling of the material and from freezing of the

water present in the material. A moist and relatively fine-grained material, such as sand, has therefore a greater heat capacity than a coarser-grained material of lower water content, for instance, ungraded crushed rock and gravel.

For insulated road pavements, the material above the insulation layer is of the greatest significance. The greater risk of icing, generally entailed by the presence of an insulation layer, may be further accentuated if a coarse-grained and dry material such as ungraded crushed rock is placed above the insulation. A material of high heat capacity may, on the other hand, reduce the drop in temperature in cooling situations, which is beneficial from the point of view of icing.

Figure 1. Heat-flow conditions in conventional road and insulated road in winter.

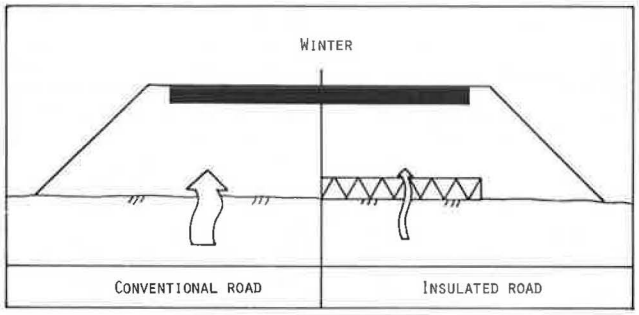

STRUCTURE AND INSTRUMENTATION OF TEST FIELD

The test field was constructed in 1976 and consisted originally of 38 different road constructions. In 1978, four more sections were added to make a total of 42 sections. Each section has a surfacing area measuring 1.5x1.5 m^2, and the depth is 70-90 cm, depending on the construction. In order to prevent transfer of heat between the different sections, each section was insulated with 5-cm plastic foam at the sides. A conventional asphalt-concrete surfacing was laid over the test field. Figure 2 shows schematically the different road pavements. The following types of pavement were represented: (a) uninsulated conventional, (b) insulated with plastic foam at varying depths, (c) insulated with plastic foam of varying thicknesses, (d) insulated with plastic foam and including different materials in the courses above the insulation, (e) with surface dressing, (f) with rubber asphalt (Rubit), (g) insulated with sulfur foam, (h) insulated with pelletized slag, and (i) insulated with expanded clay.

The instrumentation at Test Field Linköping 1976

Figure 2. Pavement types at Test Field Linköping 1976.

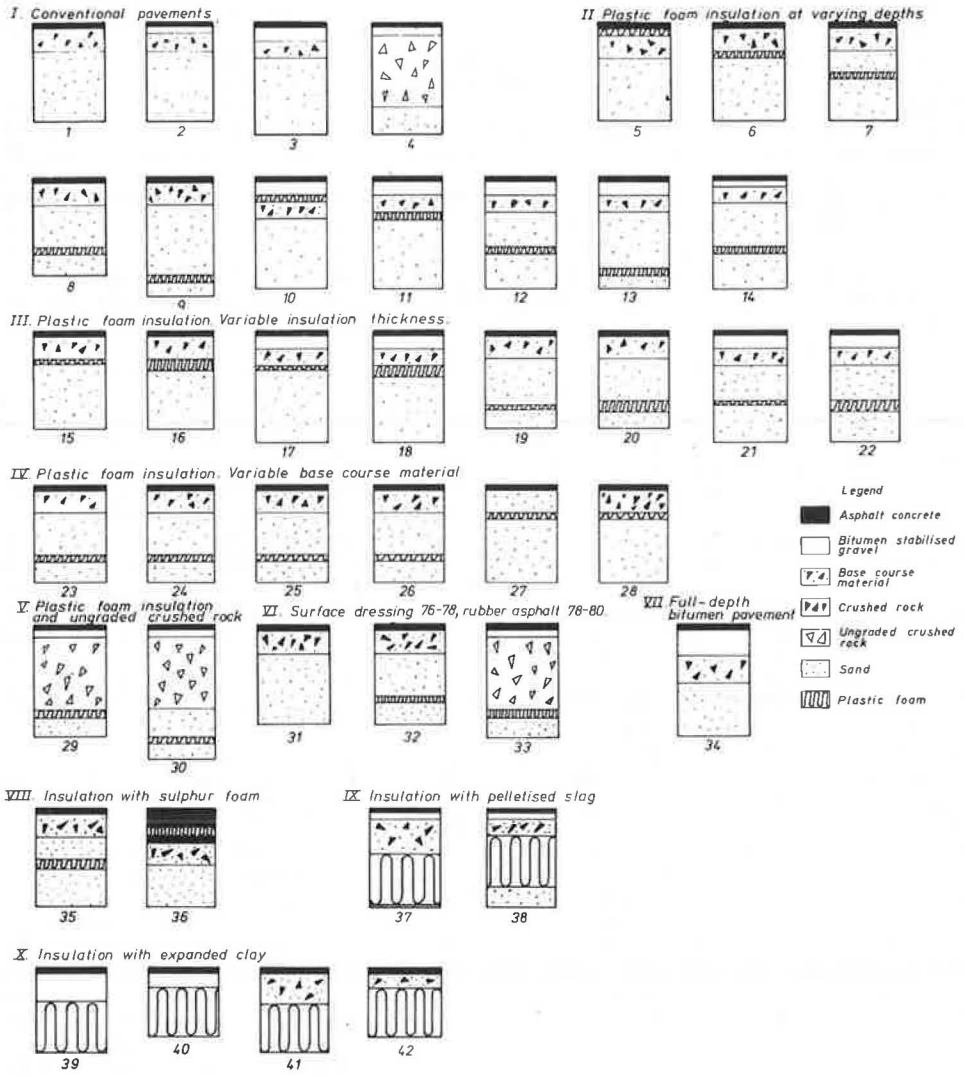

Figure 3. Instrumentation at test field.

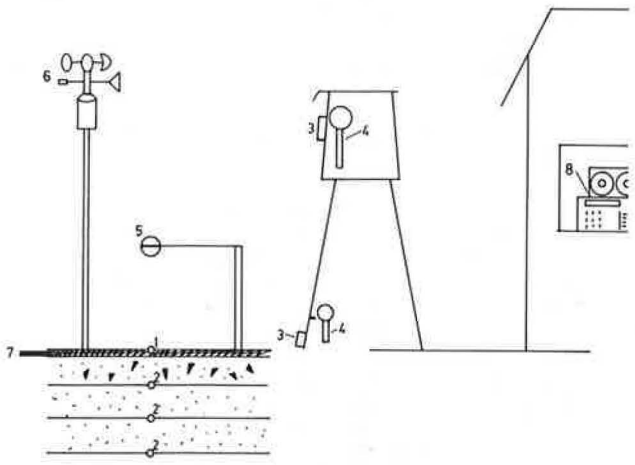

includes sensors for the determination of temperature conditions on and in a road structure and climatic stresses on a road. The instrumentation is shown schematically in Figure 3.

The surface temperature (1, Figure 3) was measured on all sections with resistance temperature detectors of the PT100 type. The same type of temperature sensor was used for measuring the temperature at different levels in the road pavement and in the air (2 and 3, Figure 3). The air-temperature sensors were placed at two levels, 2.0 m and 0.1 m, above the surfacing and the relative humidity (4, Figure 3) was measured at the same two levels. It was therefore possible to determine the temperature and humidity gradients immediately above the surface.

The radiation balance or the net radiation (5, Figure 3) was measured with a radiation balance meter placed about 1 m above the field in order to minimize the background radiation, i.e., the thermal radiation from surfaces and objects outside the field. During parts of the four-year study, measurements of wind speed (6, Figure 3) and heat flow (7, Figure 3) in the pavement surface were also carried out. Temperatures and other measurements were recorded automatically every hour by a data-acquisition system (8, Figure 3).

During the measuring seasons the test field was kept under observation, especially when there was a risk of slippery conditions. The regional weather forecasts were used to assess this risk. On the occasions when the surface was slippery, the coefficient of friction was measured. Friction was measured during the winter seasons of 1976-1977, 1977-1978, and 1978-1979 with a portable skid-resistance tester. During the winter season of 1979-1980, however, a hand-drawn friction trolley developed at the VTI was used. In conjunction with measurements of friction, the road conditions for each section and weather conditions were recorded in a journal. During the winter any snow on the test field was removed as far as possible so that conditions would be similar to normal road conditions. No salt or other deicing chemicals were used.

ICING SITUATIONS

Slippery conditions at Test Field Linköping 1976 occurred on several occasions during the four winter seasons (1976-1980) during which the investigations were carried out. The degree of icing was usually very different among the sections of the field. The cause of this differential icing is of course the presence of the many different road pavements of variable thermal properties that are represented in the field. In certain weather situations, there is a difference in the degree of cooling of the different sections, and the surface temperatures are consequently different. It is these differences in surface temperatures that govern whether hoar frost or glaze will form or whether the road surface will remain dry. Some road pavement sections in the test field were found to be extremely prone to icing (for instance, Section 5, which has the insulation at the top), and these sections became slippery at times when roads are not usually expected to be slippery. On these sections, the surface became slippery much earlier in the autumn and was slippery more frequently during the winter season than is the case on more conventional road pavements. In Figure 4 an example of a typical cooling situation is illustrated. The net radiation, together with air, surface, and dew-point temperatures, has been plotted for November 17-18, 1977. The morning of November 18 had been preceded by clear cold weather that caused the test field to undergo considerable cooling due to radiation; i.e., there was a radiation-loss situation. Net radiation was practically constant during the night at about -90 W/m^2, which is near the maximum radiation loss that can occur in the autumn-winter period. As will be seen, there is a pronounced drop in surface temperature during the night, in some cases to below the dew point owing to the very high humidity at the time, which indicates that there is a risk of slippery conditions.

It is evident from Figure 4 that the differences in surface temperature have become very large between sections. In a radiation-loss situation of this type, the road pavement exerts a very great influence on the cooling process and thus on the surface temperatures. Different road pavements are cooled to different extents, and differential icing occurs. For instance, road conditions were different over sections 1, 5, and 28, the surface temperatures of which are plotted in Figure 4. It can be seen that the temperature of Section 5, with insulation at the top, and Section 28, with insulation near the surface and crushed rock above this layer, was below the dew point, whereas this was not the case in the uninsulated Section 1. Hoar frost is formed by direct transition, or sublimation, of water vapor in the air into ice crystals on the road surface, which has a surface temperature below 0°C and at the same time below the dew-point temperature. Hoar frost had consequently formed on Sections 5 and 28, whereas Section 1 was dry on the morning of November 18.

Another example of a situation in which the road pavement exerts a critical influence on the temperature on the surface and thus on the formation of hoar frost and ice is shown in Figure 5. The photograph shows the appearance of the test field on the morning of December 10, 1979. The radiation balance was insignificantly negative during the night prior to this icing situation, indicating that there was considerable cloud cover. During the night and morning the air temperature increased more than the surface temperature because of somewhat warmer and more moist air that came in over the area. The surface temperature was therefore in many cases lower than the dew point, and hoar frost covered several sections, as may be seen in Figure 5. In this case the construction of the road pavement had a decisive influence on the surface temperature and the formation of hoar frost. The greatest amount of hoar frost formed where cooling had been most intense. On some sections the surface temperatures were insignificantly lower or higher than the dew point, and very little or no hoar frost formed here

(judging from friction measurements and visual examination). This indicates that there is a risk of slippery conditions due to hoar frost when the surface temperature is lower than the dew point but that hoar frost is formed only when the difference between the surface temperature and the dew point is sufficiently great. The differential icing on the morning of December 10 may also be seen in Figure 6, in which the results of friction measurements are shown. (For section drawings, see Figure 2.)

Low friction was measured mainly on sections with the insulation placed high up, for instance, Sections 5, 6, 7, 10, and 11, and on sections that have coarse material near the surface, for instance, Sections 4, 29, and 30. However, the uninsulated Sections 1, 2, 3, and 34 have high values of friction, but this is also the case on the sections insulated according to Swedish specifications, namely, Sections 8, 9, 24, and 25.

It is evident from the above description and Figure 5 that the reason for the low friction on most sections is the thick deposits of hoar frost that had formed because of the low surface temperatures and the high humidity. It is also evident from the above that there is a very clear relationship between low surface temperatures and the development of slippery conditions. Road pavements that are very likely to have low temperatures in the winter--for instance, road sections containing coarse materials such as ungraded crushed rock near the surfacing or insulated road pavements in which the insulation is placed high in the structure--therefore also have the greatest icing risk potential.

EFFECT OF ROAD CONSTRUCTION ON SURFACE TEMPERATURE AND ICING RISK POTENTIAL

The surface temperatures and thus the icing risk potential of road constructions vary depending on differences in the structure of the road and the materials used. It has been shown that the surface temperature is of critical significance for the formation of ice, and, apart from the pavement construction, this is affected by the local climate, the color of the road surface, etc. Owing to the fact that the local climate and the other factors are the same for all the road sections at the test field, it has been possible to make a very thorough study of temperature variation in the different road constructions.

Uninsulated Road Constructions

In roads without insulation, it is the materials used in the road structure that govern the variation

Figure 4. Icing situation: surface, air, and dew-point temperatures and net radiation, November 17-18, 1977.

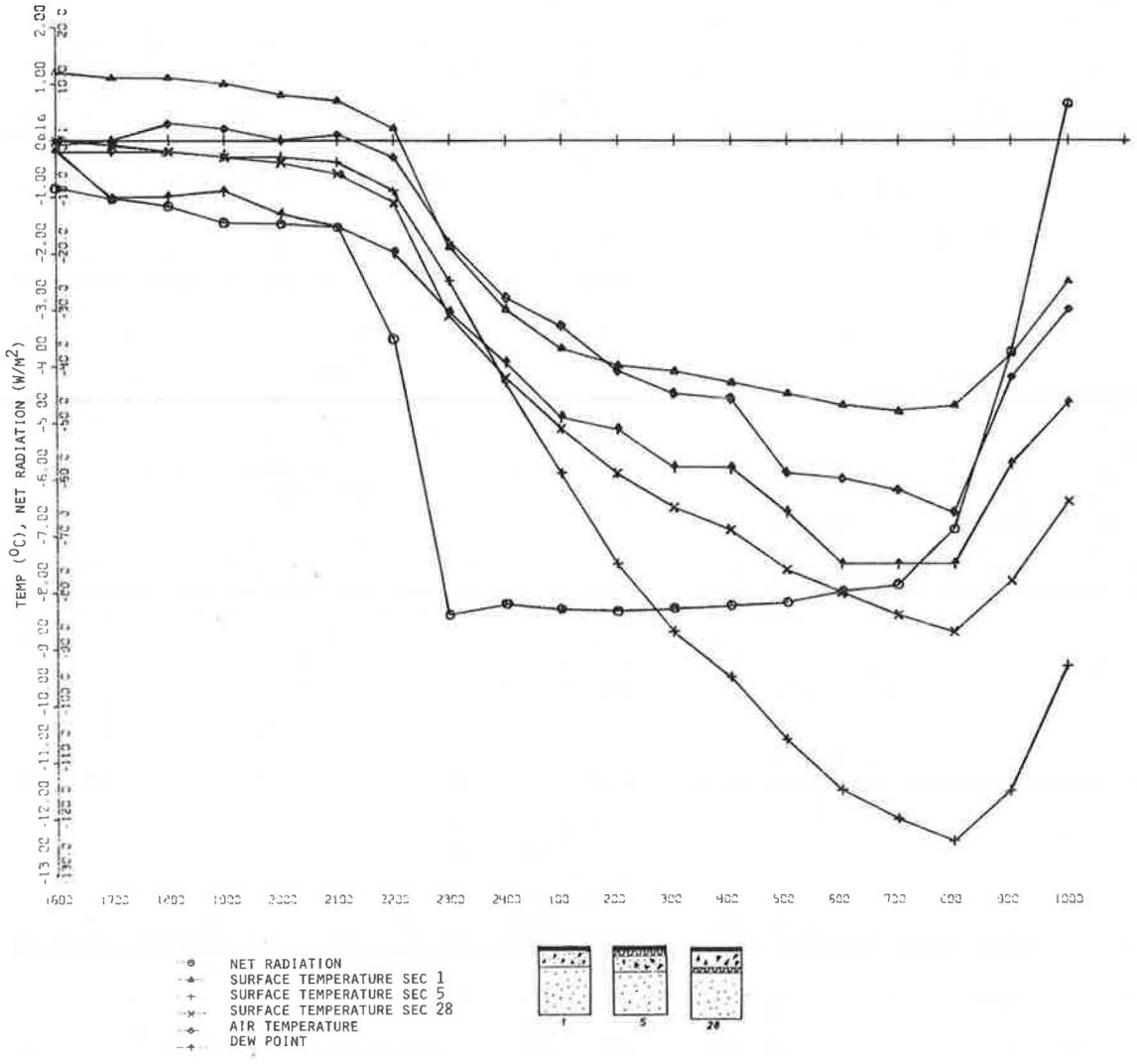

Figure 5. Test field, December 10, 1979, 10:00 a.m.

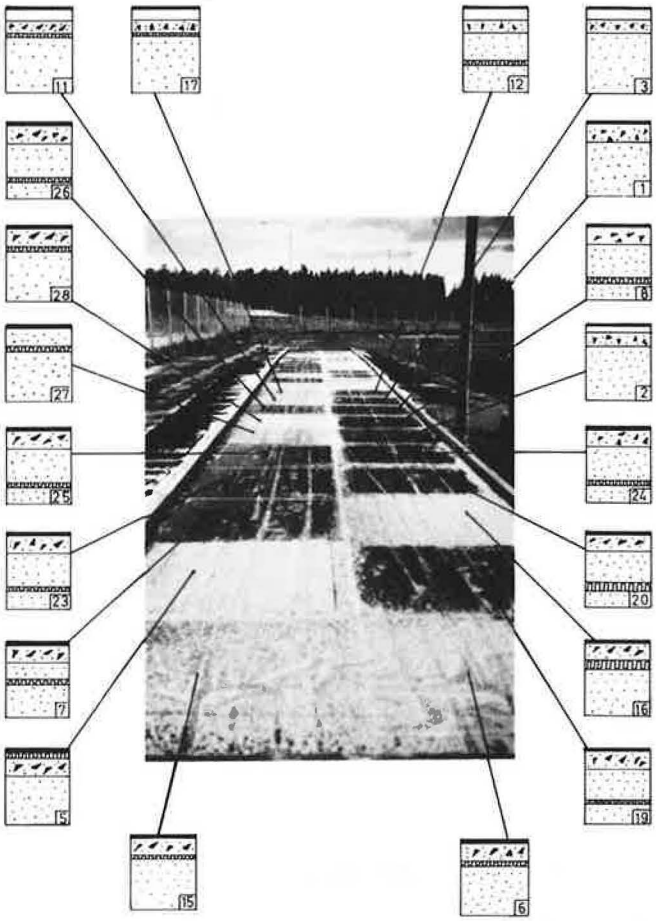

Figure 6. Friction at test field on December 10, 1979.

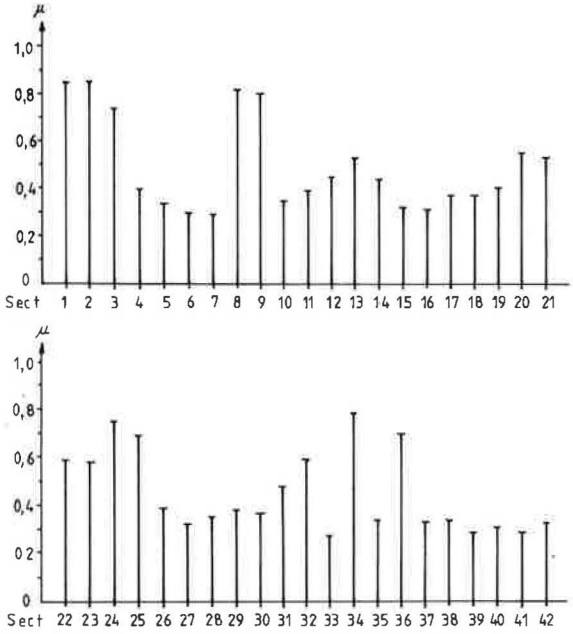

in temperature on and in the road and primarily in the courses nearest the surface. The thermal properties, thermal conductivities, and heat capacities of the materials are of great significance, and these properties in turn depend on factors such as density, water content, and mineral composition.

Figure 7 shows the variation in surface temperature on some uninsulated sections at the test field over the period November 17-18, 1977. The differences in surface temperature that can occur due to differences in the construction of the road can be seen extremely well. The differences between the sections are clearly marked, and agreement with the theoretical views is good.

Cooling was most intense in Section 4, which had an ungraded crushed-rock construction, as a result of which the minimum temperature during the night was much lower than that in the other sections. The cause of this greater cooling is the relatively low thermal conductivity and heat capacity of the ungraded crushed rock. In a cooling situation, the result of a low thermal conductivity is that upward flow of heat from the material courses located lower down in the pavement is retarded. The energy lost by radiation is compensated for only partially, and a temperature drop at the surface is the consequence. The low heat capacity of the ungraded crushed rock, which is due, inter alia, to its low water content, also contributes to the more extensive cooling, since, when the heat capacity is low, there is little energy available in the material to compensate for losses in energy, and this also contributes to the lower surface temperature.

When a pavement with a base course of only gravel (Section 1) is compared with one in which the base course includes bitumen-stabilized gravel (BG), it is seen that the surface temperature of the latter is a little lower overnight. Owing to the somewhat lower thermal conductivity and heat capacity of BG, the surface temperatures of Sections 2 and 34 are a little lower than that of Section 1. When the BG course is thicker, cooling is greater and the surface temperature lower. The highest temperature overnight was measured in Section 1 of gravel construction, which is due, inter alia, to the higher water content of gravel in comparison with that of ungraded crushed rock or BG.

Insulated Road Constructions

The presence of a layer of thermal insulation affects both upward and downward flow of heat in the road structure. Surface-temperature conditions in an insulated road are therefore affected by a number of factors, such as the depth at which the insulation is laid, the thickness of the insulation layer, and the material or materials in the course or courses above the insulation. The thermal conductivity λ varies for different insulating materials, and the type of material is therefore also significant with regard to temperature oscillations in the road structure.

Depth of Insulation Layer

The depth at which the insulation is placed has been shown to have a critical influence on surface temperature and therefore also on the icing risk potential. The results of the icing investigations at the test field clearly show that the icing risk potential decreases as the distance between the top of the insulation and the top of the surfacing increases. When the layer of plastic foam is laid deeper in the road pavement, the heat-storage capacity of the courses above the insulation increases, and the effect of the insulation thus decreases.

The distributions of surface temperature in some uninsulated (Sections 1 and 4) and some insulated (Sections 5, 7, and 8) road pavements during the

Figure 7. Surface temperature on uninsulated Sections 1, 2, 4, and 34, November 17-18, 1977.

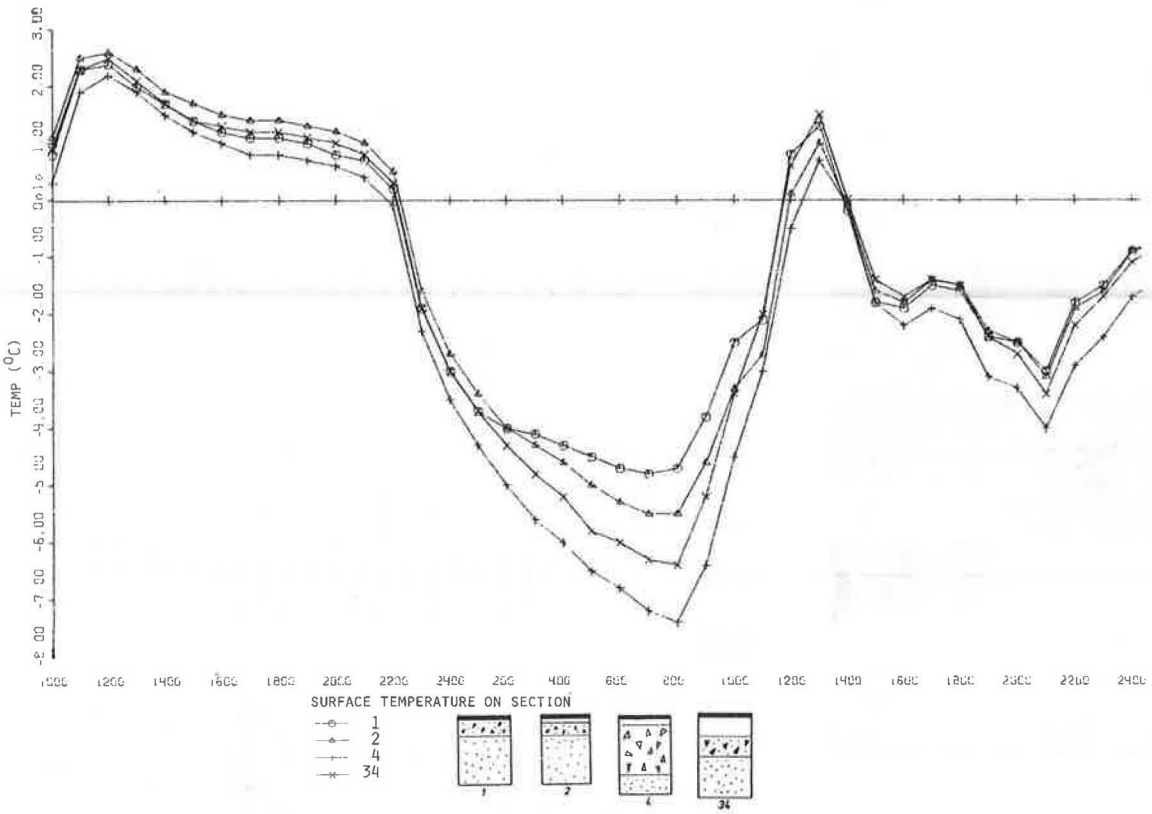

winter seasons of 1977-1980 have been compared and are given in Figure 8. Sections 5, 7, and 8 are insulated with 5 cm of plastic foam at a depth of 4 cm (Section 5), 35 cm (Section 7), and 50 cm (Section 8). The left-hand bar for each section indicates the number of hours during these three winter seasons when the surface temperature was lower than -10°C. The middle bar indicates the number of hours when the temperature was lower than -5°C and the right-hand bar, when it was lower than -2°C. The distribution in Section 1 has been taken as the reference, and the amount of increase in the other sections has been shaded and indicated as a percentage. When Sections 5, 7, and 8 are compared, it is seen that the proportion of low surface temperatures drops when the insulation layer is placed lower down in the pavement structure. Extremely low surface temperatures have been measured in Section 5, where the insulation is placed at the top. Compared with the uninsulated Section 1, which has a gravel pavement, surface temperatures are lower in insulated sections, whereas Section 4, which is constructed with ungraded crushed rock, has a surface temperature distribution that is practically the same as that of Section 7, in which the insulation is placed 35 cm below the surface.

In other words, the results of surface-temperature measurements show that it is not generally true that the icing risk on insulated roads is greater than that on uninsulated roads. In comparison with uninsulated gravel pavements of the Section-1 type, insulated roads generally have a higher icing risk potential. The degree of this increase is naturally dependent on factors such as depth of insulation, insulation thickness, and base-course material. On the other hand, an uninsulated ungraded crushed-rock pavement of the Section-4 type has an icing risk that is greater than that of several insulated road pavements.

Thickness of Insulation Layer

The thickness of the insulation layer has some influence on the temperature at the top of the surfacing, and this influence is greatest when the insulation is placed high up in the pavement. In sections with thicker insulation, cooling is more rapid, and the lowest minimum temperatures overnight occur in these.

At a lower depth the effect due to thickness of insulation is less. The temperature differences between the different sections are small, and the rates of cooling are very similar. The courses above the insulation damp the temperature oscillations, and the effect of the insulation material is less pronounced.

It has been found in the course of investigation at the test field that in sections with a gravel base course in which the insulation is placed high up in the pavement, an increase in the thickness of the insulation gives rise to a slightly higher icing risk potential. The temperature distribution during the winter showed that a thicker insulation caused a slight drop in surface temperature and thus also gave rise to a greater number of hours of slippery conditions. If, for instance, an examination is made of the number of hours when the surface temperature was lower than -2°C during the winter seasons 1977-1978 to 1979-1980, it is seen that Section 16 (with 8-cm insulation at a depth of 20 cm) had about 10 percent more hours of slippery conditions than Section 6 (5 cm) and about 11 percent more than Section 15 (3 cm).

Different Materials Above Insulation Layer

It has been found that the materials nearest the surfacing have a great significance for icing risk potential in uninsulated roads but perhaps an even

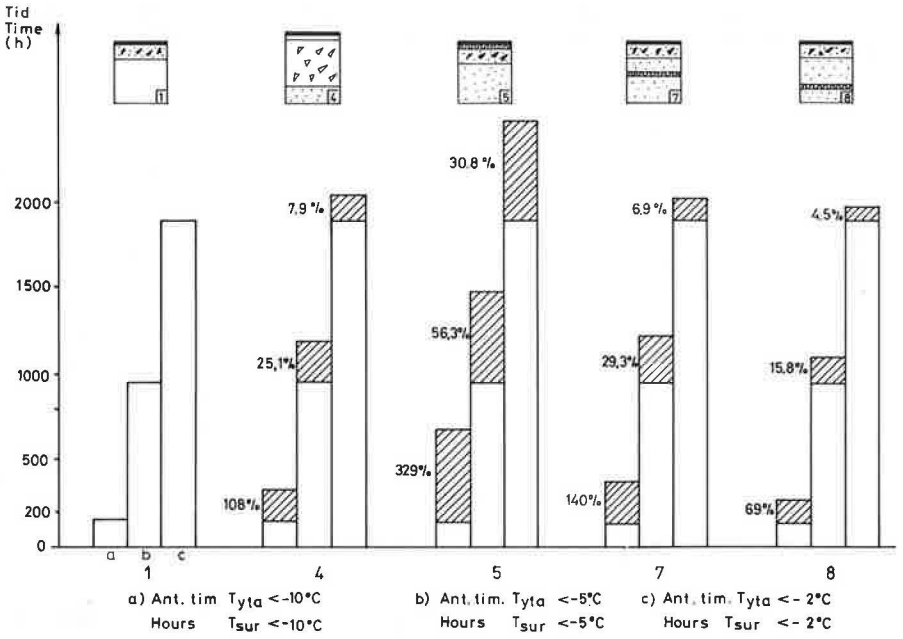

Figure 8. Surface-temperature distributions for Sections 1, 4, 5, 7, and 8 during winter seasons 1977-1978 to 1979-1980.

greater significance in insulated roads. The unfavorable effect that an insulation layer has on icing risk potential may be reduced or further accentuated depending on the choice of material in the courses above the insulation. At the test field, the effect of materials could be investigated by placing materials of such different properties as sand, gravel, and ungraded crushed rock above the insulation.

Sections 8 and 23-26 are all insulated with 5-cm plastic foam at a depth of 50 cm, but they have different base-course materials. Sections 23 and 24 have a fine-grained base-course material and Sections 25 and 26 have a coarse-grained material, whereas Section 8 could be said to have a normal base-course gravel, i.e., between the fine and coarse-grained materials.

The distributions of surface temperature during the winters 1977-1978 to 1979-1980 have been calculated for the sections at the test field, and Figure 9 gives the results for Sections 23 (fine-grained base course), 8 (normal), and 26 (coarse-grained). The explanation of the different bars is the same as that for Figure 8. In Figure 9, the increase in the number of hours in relation to Section 23 has been shaded and indicated as a percentage. As will be seen from Figure 9, Section 26 has evidently had the largest proportion of low surface temperatures. Owing to the coarse-grained base course of low water content, the icing risk potential increases and is of the same magnitude as that in a section constructed with a finer-grained base course in which the insulation is placed higher up (for instance, Section 7 with 35 cm between surfacing and insulation).

The effect of an extremely coarse material, ungraded crushed rock, above the insulation layer has also been studied. Sections 29 and 30 are insulated at 60 and 80 cm, respectively, below the surface (i.e., they satisfy the Swedish construction specifications) and have a thick course of ungraded crushed rock above the insulation. During the seasons when the icing investigations proceeded, icing occurred more often and was more extensive on these sections than on all other uninsulated road types. On an insulated ungraded crushed-rock pavement the icing risk potential is reduced somewhat if the insulation is placed at a very great depth in the pavement. However, a pavement such as Section 30 in which the insulation is at a depth of 80 cm below the surface nevertheless exhibits a greater risk than Section 4, which is the uninsulated road section of the most unfavorable icing risk properties.

CONCLUSIONS

With the aid of the road-icing investigations, and particularly the measurements of surface temperatures and friction and observations of road conditions that were carried out at Test Field Linköping 1976 over the period 1976-1980, it has been possible to estimate the relative icing risk potential of different types of pavements. The icing risk potential of the different road constructions at the field has been ranked according to a five-point scale in which 1 signifies the lowest icing risk potential and 5 the highest. The relative icing risk potential is given in Figure 10, and the following summary may be made with regard to the icing risk potential of different road pavements.

Of the uninsulated road pavements, those incorporating ungraded crushed rock obviously had the greatest icing risk potential owing to the relatively low thermal conductivity and heat capacity of the crushed-rock material. The differences among the other uninsulated pavements are relatively small. However, thicker courses of bitumen-stabilized gravel produce a somewhat elevated icing risk in relation to a pavement incorporating a gravel base course.

The depth at which the insulation is laid has a critical influence on icing risk potential. Roads with the insulation placed near the surface have a very high icing risk potential. If the insulation is laid at a depth of about 35 cm, the icing risk potential is high in relation to most uninsulated road structures but is about the same as that of a pavement incorporating ungraded crushed rock below the asphalt-concrete wearing course. For roads insulated in conformity with Swedish specifications, i.e., with the insulation laid at a depth of 50 cm or more, the risk of icing is relatively small but is still somewhat higher than that of most uninsulated roads.

Figure 9. Surface-temperature distributions for Sections 23 (fine-grained base course), 8 (normal), and 26 (coarse-grained) during winter seasons 1977-1978 to 1979-1980.

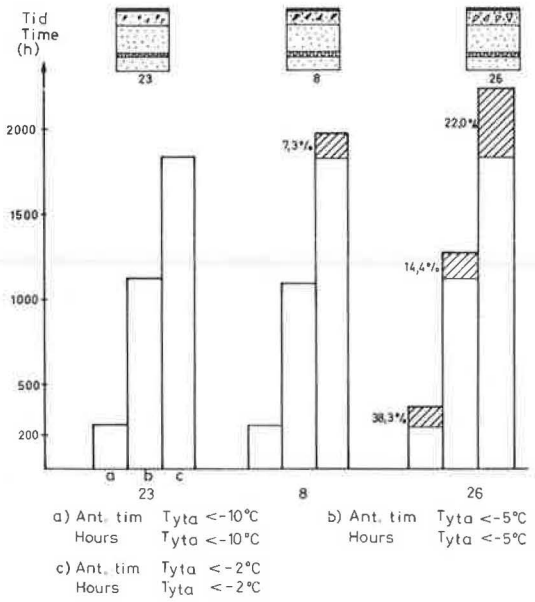

When insulation is laid high up in the road structure, the thickness of the insulation layer has a certain, but comparatively small, effect on icing risk potential, whereas the significance of the thickness is even smaller when the insulation is at a greater depth. Thicker insulation layers involve a somewhat higher risk of icing than thinner layers.

In the case of road types provided with thermal insulation, the materials in the course above the insulation have great significance with regard to the occurrence of slippery conditions. Pavements containing coarse and relatively dry materials such as ungraded crushed rock and coarse-grained base-course material have a higher icing risk potential than roads containing finer-grained materials of greater water content, such as fine-grained base-course material and sand.

REFERENCES

1. K. Gustafson. Halka på värmeisolerade vägar: II. Undersökningar vid provvägarna Lasele 1972 och Lasele 1973, utförda hösten 1977. (Road Icing on Thermally Insulated Roads: II. Investigations in the Autumn of 1977 at the Test Roads Lasele 1972 and Lasele 1973, in Swedish.) National Swedish Road and Traffic Research Institute, Linköping, VTI Meddelande 109, 1978.
2. K. Gustafson. Road Icing on Different Pavement Structures: Investigations at Test Field Linköping 1976, over the Period 1976-1980. National Swedish Road and Traffic Research Institute, Linköping, VTI Rept. 216A, 1981.
3. R. Gandahl. Road Insulation with Polystyrene Foam. National Swedish Road and Traffic Research Institute, Linköping, VTI Rept. 180, 1979.
4. R. Gandahl. Plastic Foam Insulation of Roads: Frost Resistance Capacity, Partial Insulation and Frost Heaving, Special Transitions, Icing, and Economy. National Swedish Road and Traffic Research Institute, Linköping, VTI Rept. 214A, 1981.
5. Frost i Jord, Vol. 17, 1976.

Figure 10. Icing risk potential of road pavements represented at Test Field Linköping 1976.

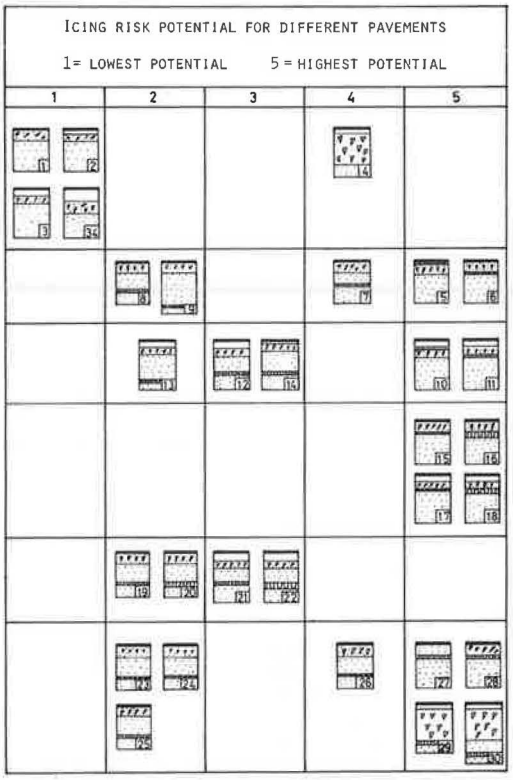

Publication of this paper sponsored by Committee on Winter Maintenance.

Effect of Moving Traffic on Fresh Concrete During Bridge-Deck Widening

HOWARD L. FURR AND FOUAD H. FOUAD

Traffic in lanes adjacent to a deck that is being widened or reconstructed causes deflections and vibrations in the fresh concrete deck. A study of the effects of these disturbances in concrete decks is reported here. Decks in service for years were inspected for signs of deterioration; deflections and vibrations were mea-

sured during concrete placement and initial curing; bridge-deck cores were analyzed for cracks and signs of bonding problems in the reinforcing steel and tested for strength and soundness. Laboratory beams were constructed and tested to simulate a transverse strip of a deck slab. Periodic deflections and vibrations were applied from time of casting to one day. No deterioration that could be attributed to traffic during construction and curing of the decks was found in existing decks. The study of the cores showed no difference in cracking in cores taken from disturbed areas of the deck from that in cores taken from undisturbed areas. There was evidence of creation of a void in the new concrete around certain rebar dowels bent at right angles in a horizontal plane on emerging from the old concrete. This situation was found only in cores taken at the joint between old and new concrete, and only one bridge of all that were studied had this bent-dowel detail. The study shows that no detrimental effects should be expected in deck concrete supported by steel and prestressed concrete beams spanning up to about 100 ft when the decks are widened or reconstructed under normal traffic.

Bridge-deck concrete that is placed adjacent to moving traffic undergoes considerable disturbance from vibrations and deflections caused by the traffic. A study made to determine the effects of that disturbance is reported here.

Concrete, in a fluid state when placed, rapidly becomes plastic and then solid within a period of 2 or 3 h after mixing. Disturbances at very early ages could cause changes in its physical character that would influence its behavior in service. Puddling of the fluid material causes segregation, which causes problems in durability and reduced strength. If the reinforcing steel moves about in the plastic concrete, it could wallow out a void, depending on the relative movement and the plasticity of the concrete. Such areas reduce or destroy bond, and they can cause durability problems if invaded by water. The early-age solid concrete (that only a few hours old) has little strength and little capacity for strain. It is easily cracked when the strain becomes great.

In both widening and deck replacement, new concrete is joined to older concrete by a construction joint. In deck widening, the curb and a short width of deck are cut back, usually to the outside beam of the original structure. The reinforcing steel at that joint, referred to here as the break line, is left to form dowels extending from the old deck into the concrete of the new portion of the deck. In replacement, construction is done in stages to permit continued use of the bridge. A portion of the old deck is removed and traffic is routed over to the other lanes until the broken-out part is replaced and cured out. Traffic is then moved over to the new part and another part is broken out and replaced. This is continued until the entire deck has been replaced. Some of the earlier work of this kind provided no tie between the older and the new concrete (1), but the current practice ties the two parts together with reinforcing bar dowels (2,3). Some of the typical joints are shown in Figure 1.

A vehicle moving over the structure causes the loaded lanes to deflect with respect to the portion being replaced. This causes bending in the new slab in a manner somewhat like that shown in Figure 2. Negative bending moment develops over the first new beam and puts the top of the deck over that beam in tension. If the curvature exceeds the capacity of the fresh concrete, the slab will crack. Another occurrence in the new concrete bay might be relative movement between reinforcing steel and the fresh concrete. If such movement does occur and if the concrete is plastic, there is a danger that a wallowed-out area will form around the steel.

Both the bending over the beam and the relative movement between steel and concrete make the inside bay of the fresh new concrete a critical area. For purposes of differentiating it from the much more stable areas beyond that bay and near supports, it is referred to as the disturbed region. The more stable areas are called undisturbed regions.

The investigation reported here consisted of a field and laboratory study to determine whether moving traffic on a deck under construction caused any of the problems discussed above or any other recognizable problem. The field study included a visual inspection, core sampling, and deflection measurements of existing bridges that had been widened or had had decks replaced under traffic. All these bridges except four had been in service at least two years when inspected. Following this inspection, nine bridges, four of which were under construction, were studied for the effects of moving traffic on the new concrete deck. In addition to the field study, model beams were studied under laboratory-controlled conditions to gather information on properties of fresh concrete and to test theories about the behavior of early-age reinforced beams. In the context used here, early age refers to ages not exceeding 24 h.

INVESTIGATION

Visual Inspection

A visual inspection of 30 bridges was made to determine the overall condition of the decks that had been widened while traffic was being carried in an adjacent lane. Bridge types consisted of simple continuous and overhanging steel beams, simple reinforced and prestressed concrete beams, and reinforced concrete simple slabs. The spans ranged from 25 ft for slab types to 110 ft for prestressed-concrete-beam types. The overall condition of the top deck surface was of concern, but greater emphasis was given to the region at the break line and the region over the new beam adjacent to that joint. In most of the bridges, the underside of the deck was also inspected. All the bridges were in service during the inspection, and in most cases no effort was made to control traffic during the inspection.

Vibration and Deflection Measurements

Recordings were made of midspan deflections of beams on five existing bridges as random trucks crossed in the lane adjacent to the break line. A 10-channel recorder was used to record the deflections measured by 10 linear potentiometers connected as shown in Figure 3. Figures 4 and 5 show a typical record of a truck crossing adjacent to the break line on a three-span continuous steel I-beam bridge. During measurements, the widened portion (the newer concrete) was closed to traffic, but no other control was imposed. Records made under normal traffic were collected only for larger trucks by using, in most cases, the lane adjacent to the break line. Transverse curvature of the deck at midspan was calculated from the deflection records, and the vibrational frequency was determined from the same traces.

Deflection and vibration measurements were made on four bridges during deck replacement in stages. In all except one, the same procedure was used as that followed for existing bridges. In that one exception, deflections were measured at selected midspan locations on reinforcing steel and concrete forms as well as on beams. The data were used to determine whether there was relative movement between the steel, the forms, and the concrete as well as in determining curvature of the new concrete. A typical record of deflections in the exception cited is shown in Figures 6 and 7.

Bridge-Deck Cores

Cores were drilled from the decks for purposes of

Figure 1. Types of construction that connect new concrete to existing bridges.

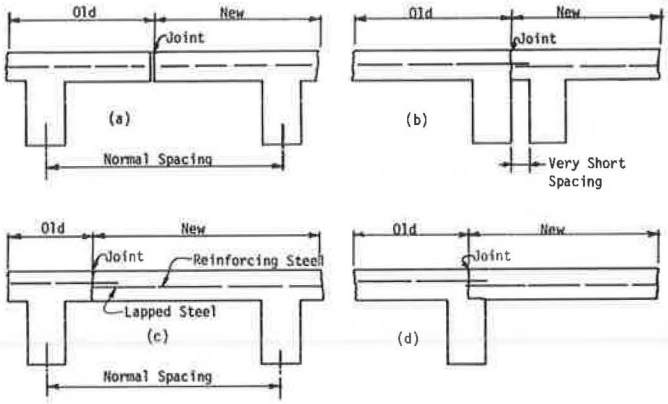

Figure 2. Relative movements between old and new concrete when traffic moves across bridge.

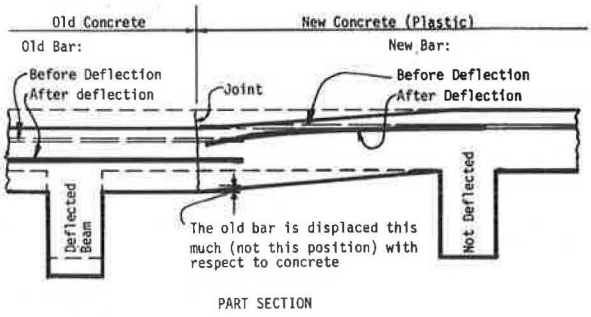

Figure 3. Detail of attachment of cable to bridge beam.

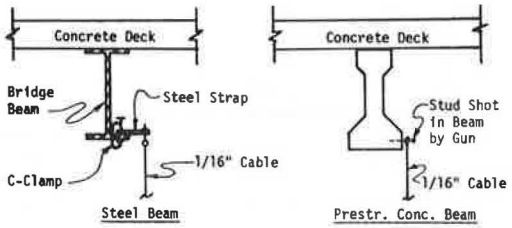

Figure 4. I-45 and FM-517, Dickenson (Houston): midspan deflections of beams due to one crossing.

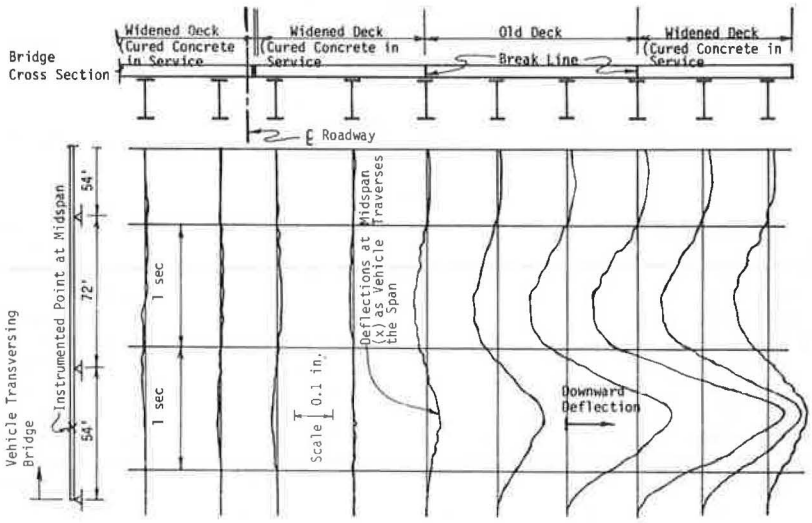

determining the condition of the concrete and to detect any differences that might be evident in the concrete from different areas of the deck. A total of 109 nominal 4-in-diameter cores was taken from nine bridges. Five of these bridges had been in service for some time when cored, but no traffic had been permitted on the new parts of the other four. More than half of the cores were taken from the midspan disturbed areas, as defined earlier, and the others were taken from the undisturbed regions at or near supports. A schedule of the cores is given in Table 1, and Figure 8 shows locations of cores removed from one deck.

Each core was carefully inspected for visual evidence of flaws. Some of them were then sawed through perpendicular to their axes, polished, and inspected through a magnifying glass. These polished surfaces were then treated with a crack-detecting substance that was fluorescent under black light; they were then studied further for crack patterns. The cracks on one of these surfaces have been inked in for emphasis in Figure 9.

Other cores were trimmed to a length of about 4 in to include the reinforcing steel from either the dowel bar crossing the break line or the reinforcing steel from the top or bottom mat. These cores were immersed in red ink and subjected to 14 psi negative pressure for about 3 h. They were then broken to reveal the steel and inspected for dye stains that might have penetrated between the steel and the con-

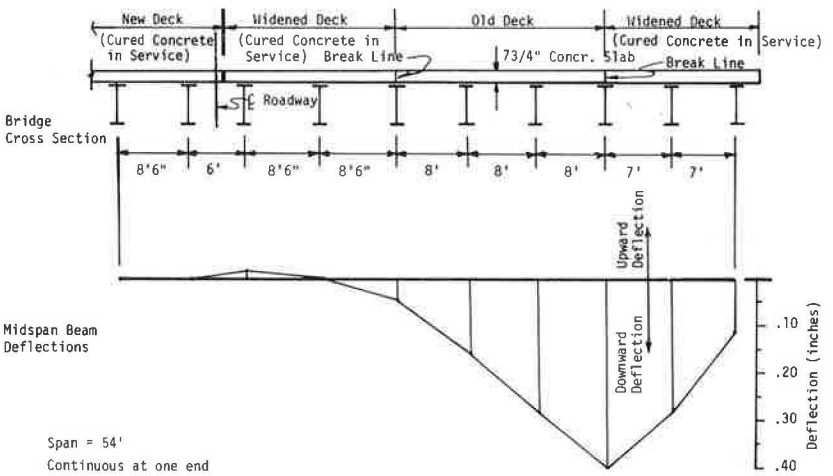

Figure 5. I-45 and FM-517, Dickenson (Houston): maximum midspan beam deflections for one crossing.

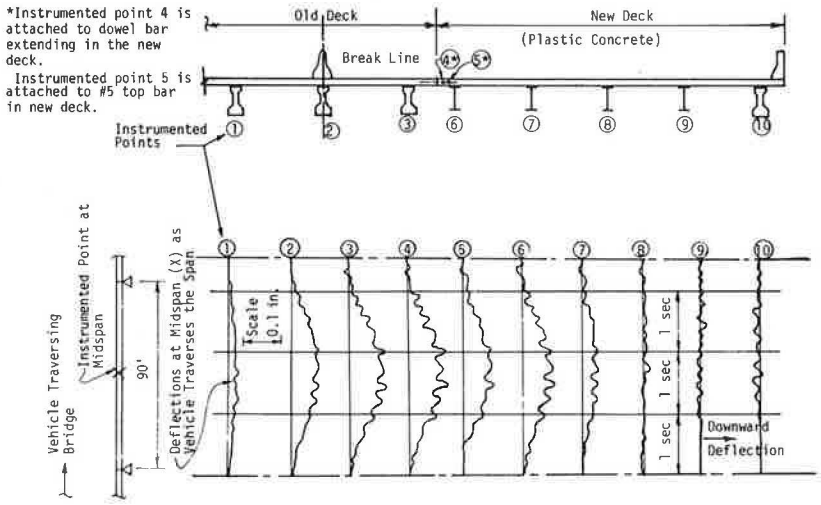

Figure 6. US-75 and White Rock Creek, Dallas, northbound (90-ft span): midspan deflections of beams and rebars due to one crossing.

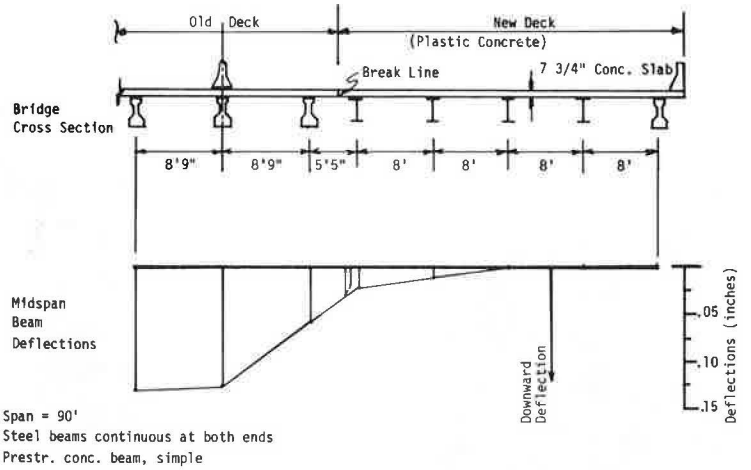

Figure 7. US-75 and White Rock Creek, Dallas, northbound (90-ft span): maximum midspan beam deflections for one crossing.

crete. Figure 10 shows a specimen being broken to reveal the steel; the grooves in the core were sawed after removal of the core from the vacuum pot.

Ultrasonic pulse-velocity soundness tests were made on 15 cores by passing a 50-kHz longitudinal pulse through polished surfaces on the ends. Some of the cores came from disturbed regions; the others were taken from undisturbed areas. Following the ultrasonics, compression-strength tests were made on these cores.

Laboratory Beams

Five laboratory beams were fabricated and tested to gather further information on conditions that were revealed in the field study. The beams, designed to represent a transverse strip of bridge-deck slab, were 7 in deep, 12 in wide, and 10 ft 8 in long. One was not reinforced, and the other four were reinforced as shown in Figure 11. The beams were cast and tested in the forms shown in Figure 11. The

Table 1. Schedule of bridge-deck cores.

Bridge Location	Number of Cores		Beam Type[a]		Core Marks
	Disturbed Area	Undisturbed Area	Old	New	
I-35 and Avenue D, Temple	7	5	C-Stl	C-Stl	ADTD1-7 ADTU1-5
I-35 and Atchison, Topeka, and Santa Fe Railroad, Temple	7	5	C-Stl	C-Stl	RRTD1-7 RRTU1-5
I-45 and FM-517, Dickenson (Houston)	7	5	C-Stl	C-Stl	F7HD1-7 F7HU1-5
I-45 and FM-519, League City (Houston)	7	5	S-PC	S-PC	F9HU1-7 F9HU1-5
I-10 and Dell Dale Avenue, Houston	8	4	S-PC	S-PC	DDHD1-8 DDHU1-4
US-75 and White Rock Creek, Dallas					
Southbound	10	3	S-PC	C-Stl	WRDD1-10 WRDU1-3
Northbound	7	3	S-PC	C-Stl	WRDLD1-7 WRDLU1-3
US-84 and Leon River, Gatesville	10	6	OH-Stl	OH-Stl	LRGD1-40′ LRGU1-56′
TX-183 and Elm Fork, Trinity River, Irving (Dallas)	10	0	C-Stl	S-PC	EFDD1-10

[a]C = continuous; S = simple; OH = overhanging; PC = prestressed concrete; Stl = steel.

Figure 8. US-75 and White Rock Creek, northbound: core locations.

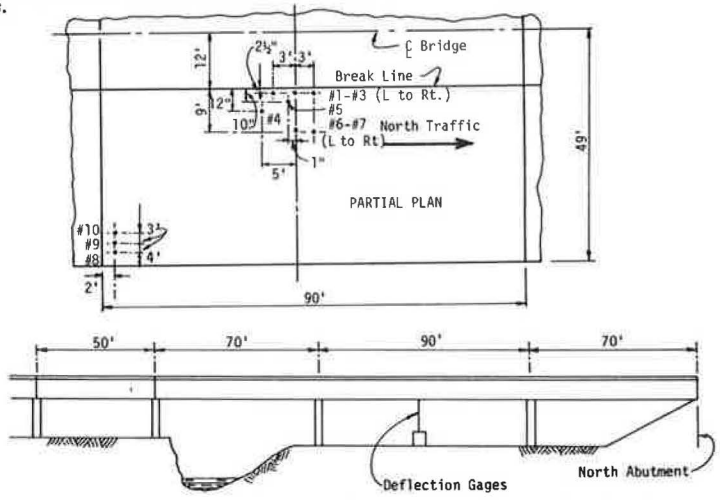

Figure 9. Trace of cracks on polished surface of 4-in-diameter concrete core.

Figure 10. Grooved core prepared for inspection of dye penetration.

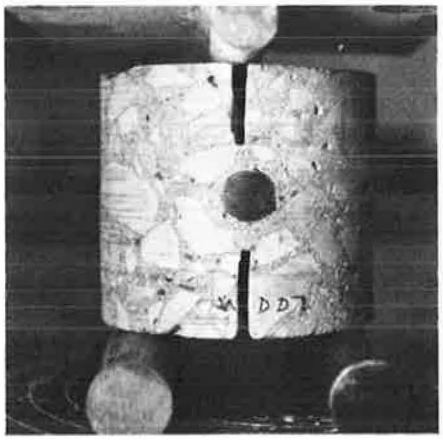

vertical sides of the forms were cut into 6-in segments to permit flexibility during testing. The forms were supported by flexible supports at one end and at midspan to simulate bridge beams. The other end was loaded by a pulsating ram to simulate the behavior of the bridge slab during the crossing of the bridge by truck traffic. Figure 12 shows some details of the test setup. Each of the beams was deflected periodically by the ram, beginning at the time of casting and lasting until the concrete was 24 h old.

The first four beams, including the one not reinforced, were deflected 0.25 in at the unsupported end at 5-min intervals to simulate heavy truck traffic. The fourth beam of this series was subjected to a 0.020-in, 6-Hz end vibration superimposed on the 5-min-interval 0.25-in deflection. The end deflection of the fifth beam was reduced to 0.15 in, and it had no superimposed vibration.

The five beams were inspected continuously during testing to detect any cracks that might develop on the top surface, which was the only exposed surface, since the beam remained in its mold during the testing. After the close of the tests, 3-in-diameter cores were taken from each of the beams, some in cracked areas and some through the dowel and reinforcing bars.

RESULTS AND DISCUSSION

Visual Inspection of Bridges

All bridges except one had dowels crossing the break line. The joint in the one exception was open due to the differential deflection of the deck on the two adjacent sides. The joints in all of the other bridges were in excellent condition. Short lengths of hairline cracking along the joints were visible in a few of the bridges, but there was no serious spalling at any of them. The general condition of the decks was good. Crack patterns were generally the same on the new portions of the decks as those on the older portions. No deterioration was found that could be attributed to construction techniques during widening.

Deflection Measurements

Although the deflections were used only for curvature calculations, it is interesting to note that the minimum span-to-deflection ratio was approximately 1600, and the maximum was approximately 8100. The former occurred in the end span of a 54-72-54-ft three-span continuous steel beam unit on an Interstate route. The latter occurred in a prestressed concrete beam bridge that had a 90-ft span. The vibrational frequencies, counted from the oscillographs, ranged from 3.5 to 10 Hz. The frequencies, along with other information, are given in Table 2.

The laboratory beam deflections were used to calculate the beam curvature, which was designed to simulate the transverse curvature of the bridge slab. The procedure used in calculating curvature assumed that an arc of a circle passed through three successive points on the deflected slab. The three points used for the bridge slab were (a) the beam at the break line, (b) the adjacent beam toward the outer edge of the bridge, and (c) the next outer beam. Corresponding points for the laboratory beams were the two flexible supports and the loaded end; however, deflections measured at closer intervals were used in calculating curvature. The curvature found in this manner was checked against a parabolic fit, and the two were almost indentical. Curvature for the bridges is shown in Table 2.

The maximum curvature in fresh bridge concrete was found to be 0.114×10^{-4}/in. It occurred in the 7.75-in deck of the TX-183 Elm Fork, Trinity River, bridge. No longitudinal cracking at the point of calculated maximum curvature was found in the concrete of that new deck. Hilsdorf and Lott (4), reporting on statically deflected 6-in-thick reinforced concrete slabs in the laboratory, found appreciable cracking at 2-4.5-h age when curvature was 5×10^{-4}/in.

Figure 11. Layout of reinforcement and formwork.

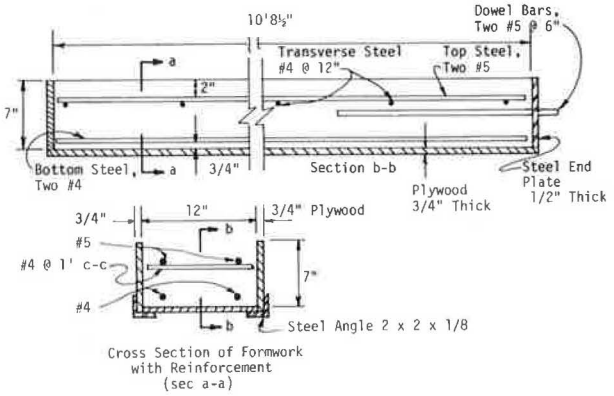

Figure 12. Side elevation of loading frame and test specimen details.

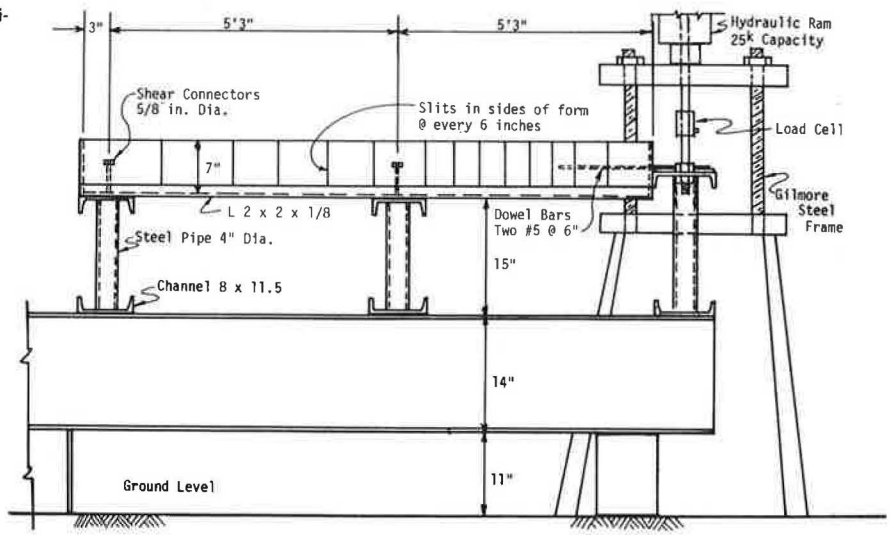

Table 2. Natural frequencies of bridges and maximum transverse bending curvature.

Bridge Location	Beam Type[a]		Span (ft)	Natural Frequency (Hz)	Maximum Differential Deflection[b] (in)	R_{min}[c] (in)	$(1/R_{min}) \div (1/10^5$ in)
	Old	New					
I-35 and Avenue D	C-Stl	C-Stl	60	5	0.032	465 333	0.215
I-35 and Atchison, Topeka, and Santa Fe Railroad	C-Stl	C-Stl	70	5	0.041	300 976	0.332
I-45 and FM-517	C-Stl	C-Stl	54	5	0.120	405 140	0.247
I-45 and FM-519	S-PC	S-PC	110	3.5	No traffic on old deck		
I-10 and Dell Dale Avenue	S-PC	S-PC	87	4	0.060	118 580	0.843
US-75 and White Rock Creek							
Southbound	S-PC	C-Stl	50	10	0.032	429 684	0.233
Northbound	S-PC	C-Stl	90	5	0.058	120 869	0.827
US-84 and Leon River	OH-Stl	OH-Stl	67.5	4.5	0.058	145 455	0.688
TX-183 and Elm Fork, Trinity River	C-Stl	S-PC	50	6	0.040	87 803	1.139

[a]C = continuous; S = simple; OH = overhanging; PC = prestressed concrete; Stl = steel.
[b]Maximum differential deflection between outside existing beam and adjacent new beam under new deck.
[c]R = radius of curvature of deck in transverse bending.

In a theoretical elastic model, concrete curvature is inversely proportional to the distance from middepth to the top of the slab, one-half the thickness. It appears reasonable then that the slab thickness would have some bearing on the curvature of fresh concrete. In order to have a fair comparison between the curvature in Hilsdorf and Lott's work and that for the bridge, the former curvature must be modified to account for the different thicknesses. Assuming that the strains were the same at cracking in the two cases, Hilsdorf and Lott's curvature must be multiplied by 0.75 for comparison of values. If that is done, their curvature is about 33 times the maximum given above for the bridges.

Data from the laboratory beams showed that a curvature of approximately 0.36×10^{-4}/in was required to crack the 7-in-thick beams. This is about three times the maximum curvature found in the bridge decks. This finding and the comparison made with Hilsdorf and Lott test information indicate that cracking of fresh concrete on a bridge deck due to passage of traffic is not likely if the bridges are similar to those of this study.

Core Study

Examination of the bridge cores revealed numerous microscopic to hairline cracks, but the patterns were random and the depths were, for the most part, shallow. The few that extended through the slabs were attributed to shrinkage or a combination of shrinkage and flexure from traffic. Twenty-one of 55 randomly cracked cores were taken from undisturbed areas, and 34 came from disturbed areas. The 21 cores make up 58 percent of all undisturbed cores, and the 34 make up 47 percent of the disturbed cores. It is concluded from this that random cracking was not caused by traffic disturbance during placement and curing of the deck concrete. There is no indication that transverse bending caused longitudinal cracking in the decks.

The laboratory beams did crack at sections of maximum negative bending moment at approximately the age of setting, but their curvatures were far in excess of those in the bridge concrete. The cracks in the reinforced laboratory beams extended no further than the top steel, and it is most unlikely that if cracks did form in the fresh concrete of the decks, they would extend deeper than the top mat of steel.

Neither the pulse velocity measurements nor the compression tests revealed any differences in soundness between disturbed and undisturbed cores.

An exceptional core from the break line of the 90-ft center span of a three-span continuous unit provided the clearest evidence found in the entire study of disturbance in the fresh concrete. The top surface was cracked in the general direction of traffic, and the interface of steel to concrete had the appearance of puddled plastic concrete. All traces of bar deformation marks were lost. It is believed that intermittent deflections from traffic caused puddling of the fresh concrete. This puddling formed a layer of uncemented particles that was flushed out by the water from the core drill. Figures 13a-13d show details of the core.

The bridge from which this core was taken had a dowel-bar detail that was different from any other in the study, and no record has been found of its use in any other bridge. This dowel was bent 90 degrees in the horizontal plane on emerging from the older concrete, and it was embedded when the new concrete was placed. In some spots either longitudinal steel or transverse steel or both were tied to or rested on the bent dowel prior to placement of the new concrete. The bent dowel can be seen in Figure 13. The dowels in all of the other bridges ran straight across the joint and were not bent. No problems were found with the straight dowels.

Four other cores from the bent-bar dowel bridges (they were twin structures) showed evidence of differential movement between the steel and the concrete. All of them were located within 12 in of the break line. Puddled areas or poor bar imprints were found at the dowel or at steel that was tied directly or indirectly to the dowel. No cores located more than 12 in from the joint showed any distress.

Under vacuum, dye penetrated around the bars of three of the four cores mentioned in the paragraph above. One of these is seen in Figure 14. In all of these, penetration along with poor bar imprints indicated poor or total absence of bond at the particular location. Some dye penetrated a fraction of an inch along the ends of all bars cut by the drill in coring, but bar imprints were good in all except those noted above.

A study by Larnach (5) in 1952 found that revibration of partially set concrete might cause some loss in bond but that vibration applied directly to the steel in fresh and partially set concrete had little effect on the bond. No discernible differences in the deflections of mat steel and fresh concrete were found in the present study, and none was shown from the study of the cores. This would indicate that there were no problems with the steel vibrating differently than the concrete, except in the situations described above. Only movement of the steel at the break line caused problems, and from Larnach's work one can say that such movement caused the problems after the concrete had partially set.

Figure 13. Core WRDD10F from southbound traffic bridge, US-75 and White Rock Creek: (a) layout, (b) side view, (c) lower section, and (d) upper section.

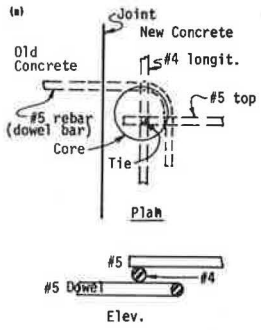

Figure 14. Core WRDD4: (top) schematic indicating location, (bottom) actual dowel bar and imprint.

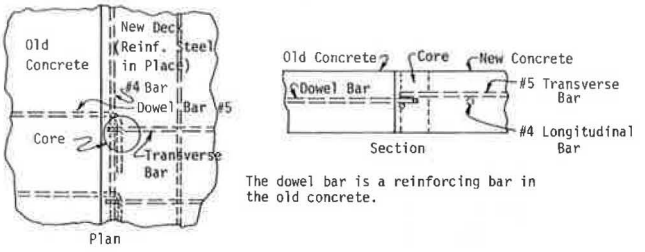

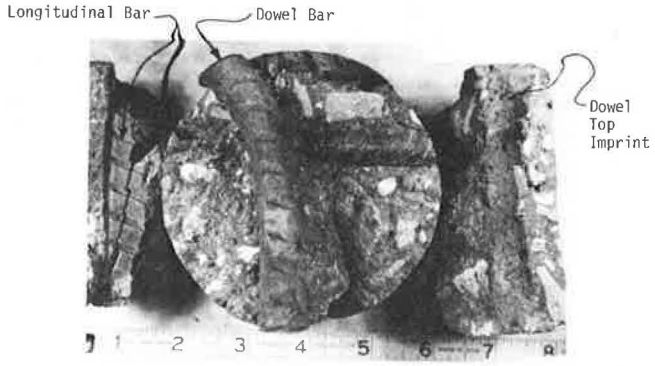

CONCLUSIONS

A study was made of bridges that were widened while normal traffic was maintained in lanes adjacent to fresh concrete used for widening or staged reconstruction. Bridges that had been in service for years and bridges that were under construction were studied. Laboratory beams designed to simulate a new deck placed and cured during normal traffic use were studied. From the results of the study, the following conclusions may be stated for bridges made of prestressed concrete and steel beams spanning up to approximately 100 ft:

1. No evidence of problems in concrete placed and cured while traffic was maintained was found in bridges that had been in service for years after the new concrete had been placed.
2. Traffic can be maintained during placement and curing without causing flexural problems in the fresh concrete.
3. Voids develop in fresh concrete around dowels bent at a right angle in a horizontal plane on emerging from the old concrete. No surface evidence was found that these voids cause problems in the performance of the deck. No such voids were found in dowels that extended into the new concrete without bends.
4. Vibrations caused by normal bridge traffic have no detrimental effect on the concrete, the reinforcing steel, or the interaction between the reinforcing steel and concrete.

RECOMMENDATIONS

Extend all dowel reinforcing bars approximately 24 bar diameters straight into the new deck area. Lap splice these dowels 20 bar diameters with the reinforcing bars that serve as transverse reinforcing for the new concrete. Tie the top-mat steel system to the dowels to prevent relative vertical movement between the dowels and the top-mat steel. This detail will provide a space between the end of the

top rebars and the break joint for a temporary filler, sometimes used in construction by stages, and sufficient lap length for transfer of flexural stress. The ties are needed to ensure that the dowels and the rebars move in harmony, thus preventing the occurrence of voids found at the bent dowels.

ACKNOWLEDGMENT

The research on which this report is based was done by the Texas Transportation Institute (TTI) for the Texas State Department of Highways and Public Transportation (TSDHPT) in cooperation with the Federal Highway Administration of the U.S. Department of Transportation. The report is based on TTI Research Report 266-1F, January 1981. J.L. Barnes, H.D. Butler, and W.R. Casbeer, all TSDHPT staff, were particularly helpful throughout the work. We were on the TTI research staff during the study and are grateful to those organizations, the personnel named, and others for their valuable support and assistance in carrying out the work.

REFERENCES

1. J.E. McMahan and J.C. Womac. Bridge Widening Problems. Division of Highways, State of California Transportation Agency, Sacramento, Rept. 951120 HPR-1(2) DO 422, April 1965, 12 pp.
2. T.V. Shaw and C.F. Stewart. Effectiveness of Attached Bridge Widenings. California Department of Transportation, Sacramento, Rept. CA-DOT-DS-4165-1-72-2, March 1972, 48 pp.
3. H.L. Furr and F.H. Fouad. Bridge Slab Concrete Placed Adjacent to Moving Live Loads. Texas Transportation Institute, Texas A&M Univ. System, College Station, Research Rept. 266-1F, Jan. 1981, 131 pp.
4. H.K. Hilsdorf and J.L. Lott. Revibration of Retarded Concrete for Continuous Bridge Decks. NCHRP, Rept. 106, 1970, 67 pp.
5. W.J. Larnach. Changes in Bond Strength Caused by Re-Vibration of Concrete and the Vibration of Reinforcement. Magazine of Concrete Research, London, No. 10, July 1952, pp. 17-21.

Publication of this paper sponsored by Committee on Structures Maintenance.

Cathodic Protection of Continuously Reinforced Concrete Pavement

GLENN R. KORFHAGE

Some sections of continuously reinforced concrete pavement (CRCP) in Minnesota are experiencing a spalling-type deterioration caused by corrosion of the reinforcing steel. In an attempt to develop a method of stopping this corrosion, a cathodic protection system was designed and installed along a 1000-ft section of Interstate CRCP just north of St. Paul. High silicone chromium iron alloy anodes energized by a constant-current output rectifier were placed at the edge of the 10-ft bituminous shoulder at 50-ft intervals. On half the project, the anodes were buried in a trench that was backfilled with coke breeze. On the other half of the project, canisters containing the anodes packed in coke breeze were placed in post holes and backfilled with additional coke breeze. It appears that both types of installation are providing at least partial cathodic protection to the pavement.

During the late 1960s, the Minnesota Department of Transportation (MnDOT) constructed considerable mileage of continuously reinforced concrete pavement (CRCP). In rural areas pavement thickness was generally 8 in and in urban areas 9 in. The steel reinforcement was 0.6-0.7 percent and was deformed wire mesh or deformed reinforcing bar.

During the past seven years, an increasing number of CRCP sections in Minnesota have begun to show a spalling-type deterioration. The frequency of this deterioration progressed from isolated and random in 1975 to widespread and concentrated on certain pavement designs by 1978. Pavements showing the most severe spalling are of the two-course construction type with a steel-to-concrete ratio of 0.60-0.65 percent. Reinforcement used was deformed wire mesh with specified clear cover of 2-4 in. In most cases the steel had been placed at the minimum specified cover of 2 in.

In 1976, a survey of a deteriorating section of CRCP on I-94 between downtown St. Paul and downtown Minneapolis was conducted. Tests performed during this survey included cover measurements, delamination detection, and half-cell potentials for corrosion detection. A visual survey was also performed. Strong evidence was found to support the theory that corrosion-induced spalling was occurring. Survey results showed that corrosion-potential measurements were generally at or well above the corrosion threshold of 350 mV relative to the copper sulfate electrode. Many measurements were in the range of 500-600 mV of active corrosion. The maximum potential noted on corrosion-damaged bridge decks in Minnesota was also about 600 mV. Delamination surveys revealed that 13 percent of the pavement tested was delaminated. Reinforcing steel cover generally measured 1.75-2.25 in.

At the time of the survey on I-94 (August 1976), nearly all noticeable spalling-type deterioration was confined to the oldest sections of CRCP in the metropolitan area. However, it was feared that eventually the problem could become very extensive.

A research study was undertaken to develop procedures for stopping or at least reducing the rate of corrosion in CRCP. One known method for preventing corrosion of steel is cathodic protection. It has been used successfully to protect buried pipelines for many years. More recently it has proved to be an effective means of arresting corrosion of rebars in concrete bridge decks (1,2). By using procedures developed in these two applications as a starting point, a design was developed to cathodically protect a section of CRCP.

The location selected for the cathodic protection installation is on I-35W a few miles north of St. Paul. Factors considered in making the selection were pavement type, traffic, state of deterioration, and convenience for monitoring. The pavement type is one that has exhibited the most frequent and

severe corrosion-related deterioration. It was approximately 10 years old and was built by using two-course construction techniques. The slab is 8 in thick and has a steel-to-concrete ratio of 0.6 percent. Reinforcing steel is deformed wire mesh. Clear cover over the reinforcement was specified at 2-4 in. Average daily traffic was 8000-9000 vehicles/day, which included about 500 trucks.

This report describes the design and installation of the cathodic protection system and discusses the preliminary indications of its effectiveness in arresting corrosion of the CRCP.

SYSTEM DESIGN

Corrosion of steel is an electrical as well as a chemical process. In its basic form it is caused by stray current discharging from one area of the steel (the anode) and returning to another (the cathode) (Figure 1). A driving potential of less than 0.5 V is able to cause the current jump.

Figure 1. Corrosion process.

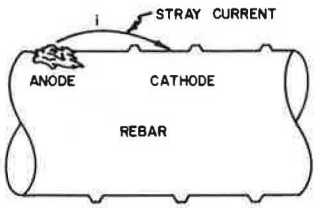

Figure 2. Pipeline cathodic protection system.

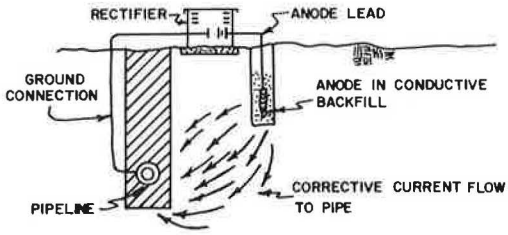

Figure 3. Schematic of bridge-deck cathodic system.

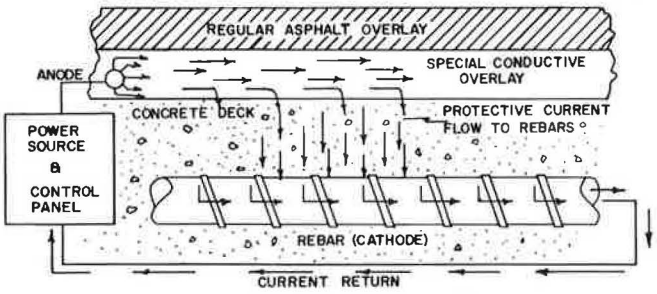

Figure 4. Cathodic protection for CRCP.

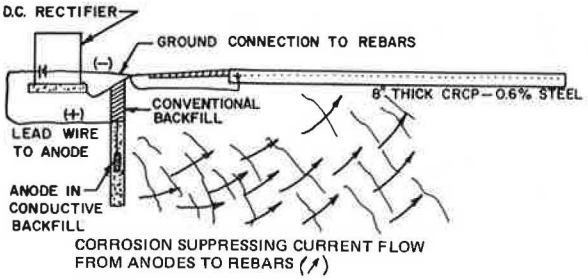

Corrosion, or oxidation, occurs at the anode only, whereas hydrogen evolution or reduction occurs at the cathode. As corrosion continues, its by-product, pack-rust, accumulates at the anode, whereas there is no harmful side effect at the current-receiving cathode. If all steel could be placed in a current-receiving mode, the discharge would be stopped and corrosion would cease.

Cathodic protection of buried pipelines is accomplished by placing anodes in a conductive backfill material, usually near the in-place pipeline (3). A ground connection is attached to the pipeline, and when the system is energized, an electrical potential field is set up between the pipe and the anode. Current flows through the field to the pipe, which is the cathode of the system. This system is illustrated in Figure 2. With the pipe in a current-receiving mode, stray current discharge cannot occur and corrosion is stopped.

Reinforcing bars in concrete bridge decks have also been protected with impressed current. Achieving this protection required a somewhat more specialized system. To conduct the current, a coke-modified asphalt overlay and special anodes were placed on the deck surface (Figure 3). In this case the special asphalt overlay created the electrical field needed to distribute current to protect the rebars.

The design of the cathodic protection system for CRCP was achieved by integrating essential elements from the pipeline and bridge-deck systems and is shown in Figure 4. The concept involved burying anodes in a trench or in post holes backfilled with conductive coke aggregate and located along the right shoulder. A ground connection was attached to the continuous reinforcing at five locations to complete the circuit. The anodes, when energized, would create a potential field between themselves and the steel within the CRCP. This field would conduct current to the reinforcing steel in a manner similar to that in which the soil conducts current to the pipeline. With pavement-reinforcing steel in a current-receiving mode, it was believed that corrosion would be stopped. With corrosion stopped, the forces necessary to generate pressure-causing cracks and eventual potholes in the pavement would be eliminated.

A prerequisite to achieving effective cathodic protection is uniform current distribution. If distribution is nonuniform, then hot spots (overprotection) will occur at some locations and cool spots (underprotection) will occur at others. Several factors influence current-distribution characteristics; some can be controlled, others cannot. These factors are as follows:

1. Resistivity in the medium separating the anode and cathode,
2. Continuity of the steel in the structure under protection,
3. Uniformity of the applied potential, and
4. Proximity of the source (anode) to the protected structure (pavement).

In addressing each of these factors, it is immediately apparent that the first factor, resistivity, is generally fixed and cannot be altered except perhaps by environmental influences of temperature and moisture.

The second factor, continuity, can be tested for and, when deficient, corrected by installing cross links over the break. This is not considered to be a major problem.

Figure 5. Trench method.

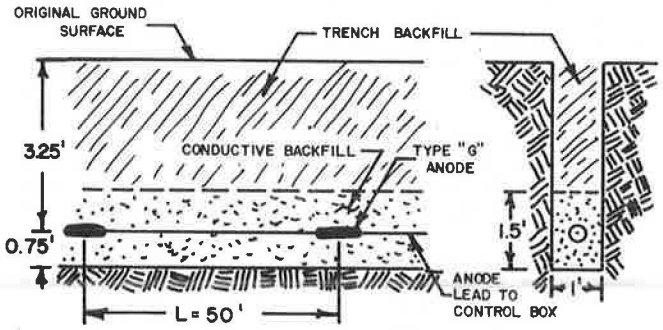

Figure 6. Post-hole method.

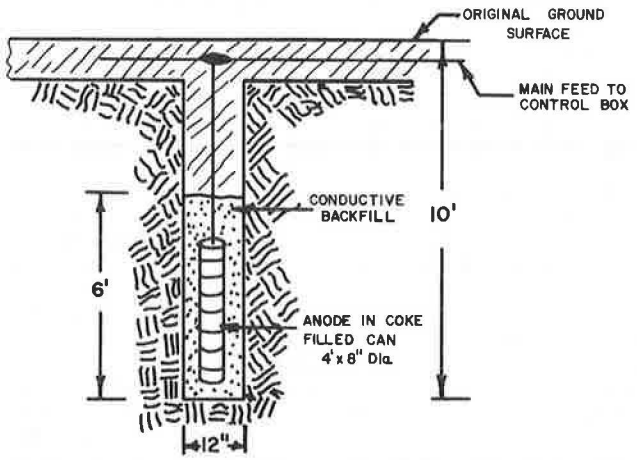

The third and fourth factors are the most significant but can be treated by proper design. The third factor, uniformity of applied potential, is controlled through use of reference cells in the protected structure (pavement). Theoretically these reference cells act as sensors. If applied potentials get too low, the power can be increased.

The two most commonly used methods for applying impressed current cathodic protection to pipelines are the distributed-anode groundbed and the remote-anode groundbed. Experience with these two methods seems to indicate that the distributed-groundbed approach offers the most uniformly applied potential and is the most responsive to control efforts.

In general, the disturbed-anode groundbed design involves placing an array of anodes along the structure requiring protection. The anodes are usually placed in a continuous trench backfilled with a conductive aggregate or in post holes as prepackaged assemblies; each assembly contains an anode surrounded by conductive aggregate. The purpose of the conductive aggregate is to make the anode bigger, thus distributing the current more uniformly. In both cases the anode leads are connected to a main line from the controller. It is common practice to provide separate circuits of staggered anode wiring arrangements so that if part of the system goes out, the domino effect is avoided and protection can be maintained. When the review of all available information was completed and consideration given to all options, a decision was reached to use the distributed-anode groundbed concept for this trial system. It was felt that this approach would provide the most uniformly applied potential and current density. It was also decided that a constant-current output rectifier would be used rather than a constant-voltage rectifier.

The two schemes for anode installation, continuous-trench and post-hole approach, were used in this study. The test area was divided into two major sections, each 500 ft long. The first 500-ft section would be protected with a continuous-trench anode scheme (Figure 5) and the second 500-ft section with the post-hole method (Figure 6). Each test area was further subdivided into five zones, and each zone would be independently controlled at the rectifier.

For this section of pavement, it was determined that the steel surface area was 0.55 ft^2/ft^2 of pavement. A running foot of pavement 24 ft wide would therefore have approximately 13 ft^2 of steel. Since a 1000-ft experimental test section was planned, protection of 13 000 ft^2 of steel would be required. Based on the maximum current output criterion of 1 mA/ft^2 of steel, the system should have the capability of supplying a total of 13 A. The anode selected for both trench and post-hole type cathodic systems was the high silicone chromium iron alloy cylinder. The cylinder is 9 in long and 2 in in diameter. It has a maximum current output of 0.8-1.0 A. Based on current requirements, each anode is capable of protecting 50 lineal ft of pavement with some allowance for increasing output to a given zone if necessary. In order to monitor the potential applied to the steel, reference cells were placed in each lane at 100-ft intervals. The reference cells were zinc encapsulated in zinc sulfate and gypsum.

INSTALLATION OF SYSTEM

Installation of the system took place in mid-November 1978. This operation was a combined effort of personnel from District 9 Maintenance, the Electrical Services Unit, and the Physical Research Section.

Excavation for the 500-ft-long trench system began at the south end of the installation by using a small trenching machine. The trench was 4 ft deep and 8 in wide.

The excavated material was generally granular, ranging from coarse to fine sand with little or no silt. Trenching proceeded at a speed of 2-3 ft/min with minor delays when rocks were encountered.

Conductive coke breeze and anodes were placed after a sufficient length of trench had been dug. A 1-ft layer of coke breeze (uncompacted) was placed in the trench as shown in Figure 7. Discharge of the coke breeze into the trench was accomplished by using a sanding truck with an auger-fed distribution chute. The rotary sand-spreader device had been removed and a 3-ft metal chute fabricated and installed. Anodes were placed on top of the first layer of coke at specified locations. Wires from all five separate anode strings were placed in the trench on top of the first layer of coke. Each anode string consisted of two anodes connected by 50 ft of cable. Once the anodes had been positioned, a second 1-ft layer of coke was placed. After this layer had been placed, leveled, and tamped, considerable consolidation was evident. The amount of settlement of the two layers was observed to be of the order of 2-4 in. This left the consolidated depth of coke at approximately 20-22 in.

Personnel from MnDOT's Electrical Services Unit performed various tests for continuity and resistance of the anode strings to ensure that they were functioning properly prior to burial. When the first layer of coke was in place, they positioned the anodes at their proper locations in the trench and ran the lead wires to a temporary junction box located where the permanent controller would be installed.

Figure 7. Placement of coke breeze.

Figure 8. Canister anode assembly.

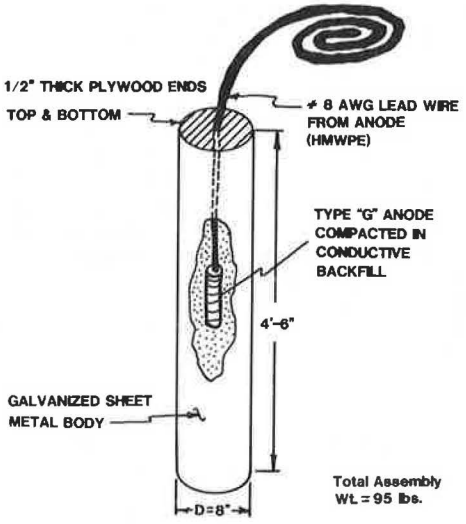

After the second layer of coke had been placed and compacted, the trench was backfilled with the excavated material. Final consolidation and leveling were achieved with a motor grader.

Installation of the post-hole system began the day following completion of the trench-type system. Initially a light-duty auger was tried, but problems occurred when the holes caved in. After a larger, more rigid drilling device was brought in, these problems were substantially eliminated. However, the bottom portions of the larger auger holes did cave in, and it was necessary to drill to a depth of about 15 ft in order to obtain an open hole to a depth of 10 ft after the auger was removed. As soon as the auger had cleared the hole, the canister containing the anode was lowered by using ropes. Eye bolts had been attached to the top of each assembly for this purpose. Once the anode was in place, a measurement was made to determine the depth to the top of the canister. The hole was then backfilled with 2-3 ft of coke aggregate. Backfill was completed by using the excavated material. A 10-ft No. 6 AWG lead was coiled at the top of each anode for eventual connection to a main feed line from the rectifier.

The canister anodes used were 4.5 ft long and 8 in in diameter. It was necessary to use prepackaged anode assemblies to eliminate problems associated with coke placement in the unstable soil. Canister assemblies are quite simple, as may be seen in Figure 8.

Two anode leads were spliced to each of the five feeder cables that were buried in a trench 4 in wide by 18 in deep in the road shoulder. The feeder cables terminated at the temporary junction box. Split bolt connectors were used to connect the leads to the feeders. An epoxy-type splice kit was used to seal the connection against the elements.

The reference cells were placed under contract in the fall of 1979. The concrete was removed to the depth of the steel by using saws and jackhammers. The reference cells were then placed and connected as shown in Figure 9, and the lead wires were run to the junction box. A reference cell was placed in the center of each traffic lane and midway between the two anodes comprising each anode pair.

METHOD OF EVALUATION AND RESULTS

The system was energized in March 1980. Field evaluation consists of both internal and external monitoring. Internal monitoring consists of measuring applied potentials and current output to each of the anode circuits or zones. Each circuit consists of two anodes and two reference cells cast into the pavement slab. Readout data are obtained by means of a Fluke Model 2240B data logger (Figure 10). When the system was initially energized, readings were taken at 15-min intervals. As the system stabilized (which took about two weeks), the interval was increased and now is 12 h.

Initially the current output from each of the 10 zones in the system was approximately 1.3 A. The voltage being applied varied somewhat from zone to zone. Mean values measured in mid-June 1981 were 7.1 V for the trench system and 13.4 V for the post-hole system. On July 16, 1981, the current was increased to 1.8 A. Mean voltage values measured one week later were 9.0 and 15.1 V for the trench and post-hole systems, respectively.

The accuracy of the zinc reference cells is questionable. Testing was done in late June 1981 (under the guidance of Ken Clear of the Federal Highway Administration) to determine whether the reference cells were functioning properly. It was determined that only about half of them were reliable. Because of the marginal reliability of the reference cells, it is difficult to determine how effective the cathodic protection installation is. However, there are indications that the system is providing at least partial protection.

Two criteria used for evaluating cathodic protection of underground structures were applied (4). These criteria were as follows:

1. A negative voltage of at least 0.85 V as measured between the structure surface and a saturated copper-copper sulfate half-cell contacting the electrolyte, and
2. A negative voltage shift of at least 300 mV in criterion 1.

When the system was first turned on, about one-third of the reference cells indicated a voltage more negative than -0.85 V. In late October 1980, 12 of 19 reference cells met this criterion; by late December, 14 of 19 were more negative than -0.85 V. In late October, 5 of 19 reference cells indicated a negative voltage shift of more than 300 mV. In late December, 9 reference cells showed a shift more negative than 300 mV, but 16 showed a shift greater than 200 mV. Results in 1981 were not so good as those in 1980. Possibly the change in values was caused by an increase in moisture content of the subgrade, base, and/or concrete.

Figure 9. In-place reference cell.

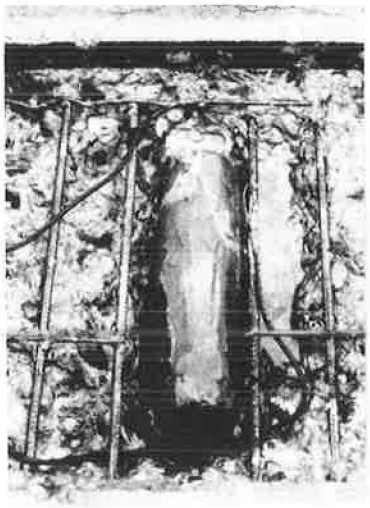

Figure 10. Fluke Model 2240B data logger.

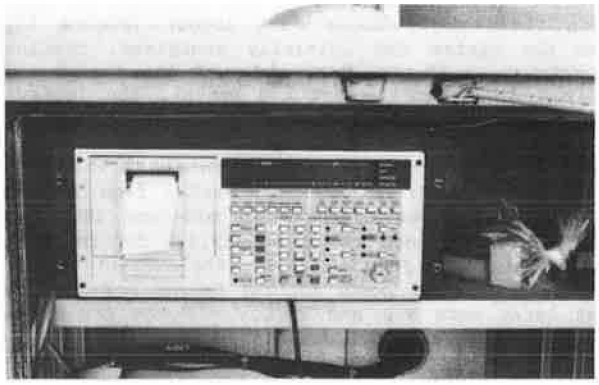

Copper-copper sulfate half-cell tests were conducted several times. Mean values were -516 mV in 1979, -432 mV in June 1981, and -375 mV in September 1981. Thus, the cathodic protection system was effective in reducing electrical potential values. It would be desirable to have the half-cell values reduced to below -350 mV.

Neither internal nor external monitoring has indicated any significant difference in effectiveness between the trench system and the post-hole system. However, the passing lane seems to be protected better than the driving lane even though the anodes are closer to the latter. A possible reason for this is that the mortar used to backfill around the reference cells in the passing lane was intentionally contaminated with calcium chloride. Unfortunately, the calcium chloride was inadvertently omitted in the mortar used in the driving lane.

FINDINGS AND CONCLUSIONS

Experience with this project to date indicates that it is feasible to use cathodic protection as a means of arresting corrosion in CRCP by modifying technology previously developed for protecting buried pipelines and bridge decks. Further work is needed to determine such particulars as amount of current and spacing and location of anodes. At present the trench system is recommended over the post-hole system because, while the effectiveness of the two systems is similar, the former uses less electricity.

ACKNOWLEDGMENT

The contribution of Robert Tracy, former MnDOT research project engineer, to this study is acknowledged. He developed the concept and design of the system described in this paper following discussions with experts on cathodic protection of bridge decks and buried pipelines. The many contributions of Andrew Halverson, research project engineer, and Mark Hagen, research assistant, are also gratefully acknowledged. Special thanks go to Ken Clear, Office of Research, Federal Highway Administration, for his assistance in evaluating the effectiveness of the cathodic protection system.

This research was partly funded by the Federal Highway Administration as part of the Highway Planning and Research Program.

REFERENCES

1. R.F. Stratfall. Experimental Cathodic Protection of a Bridge Deck. California Department of Transportation, Sacramento, Jan. 1974.
2. H.J. Fromm. Cathodic Protection of Bridge Decks in Ontario. Presented at Annual Meeting, National Association of Corrosion Engineers, March 1976.
3. M.E. Parker. Pipeline Corrosion and Cathodic Protection. Gulf Publishing Co., Houston, TX, 1962, 2d ed.
4. B. Husock. Pipe-to-Soil Potential Measurements and Cathodic Protection of Underground Structures. Harco Corp., Medina, OH, 1971.

Publication of this paper sponsored by Committee on Corrosion.

Evaluation of Platinized Niobium Wire Anodes for Cathodic Protection of Bridge Support Structures

H.J. FROMM AND F. PIANCA

An investigation was conducted to determine whether platinized niobium wire could be used as anode material to provide cathodic protection without necessitating the use of a conductive surface mix, as has been done previously. Experiments were carried out both in the field and in the laboratory. In the

field, various anode spacings were used to determine optimum spacing for corrosion protection. These experiments indicated that the platinized niobium anodes could not spread the voltage evenly across the bridge deck to establish proper cathodic protection. Because of the higher voltages required to overcome concrete resistance, some acid formed at the anodes and attacked the concrete.

The problem of corrosion of rebars in concrete bridge decks has been recognized for years (1); the problem is no longer confined only to the decks. It has been observed that corrosion-induced deterioration is occurring in reinforced concrete bridge substructures (2). This is becoming a growing concern to transportation agencies.

The principle of cathodic protection has been employed for years to stop corrosion on buried pipelines, concrete water tanks, and the hulls of ships. Since 1977, cathodic protection has been a standard method adopted by the Ministry of Transportation and Communications (MTC) to protect the reinforcing steel in bridge decks from corrosion (1). The current method of cathodic protection does not lend itself easily to installation on bridge substructures, since it is difficult to apply a conducting layer to a vertical surface. Platinized niobium anode wires have been used in an attempt to impress direct current into a bridge deck without the use of a conductive mix (3). If this system proves feasible on a bridge deck, it could easily be applied to the support systems of bridge decks. The anode wire could be set and cemented in grooves cut into the length of bridge columns or bents. The spacing of the anodes, to produce an even distribution of current, would depend on the conductivity of the concrete and would have to be determined by a field project. It was decided to do this test on a bridge deck, since it would be easier to set out a series of different anode spacings and the results would be applicable to both support systems and decks.

A bridge in Toronto was selected for this purpose. This was Bridge No. 9, located in the Highway 401-Don Valley interchange. It is a voided, post-tensioned structure 113 m (370 ft) long by 9.6 m (31.5 ft) wide, and it was built in 1966. This deck had some minor cracking, but corrosion was not a serious problem. Since the deck was in good condition, there was no need for repairs to spalls and delaminations. This made Bridge No. 9 an ideal choice for the experiment; also, it received the same salting treatments in winter as did the busy highway associated with it.

ANODE DESCRIPTION

The term "platinized anode" refers to an anode that is made by applying a thin coating of platinum over a substrate of niobium, which is passive under anodic conditions (4). The purpose of the substrate is to reduce the overall cost of the anode since a solid platinum anode would be extremely expensive. The use of a passivating material has the effect of confining the current discharge to the platinum surface (4).

In addition to the passive substrate of niobium, an inner core of copper was used for increased conductivity. This was necessary in long, thin anodes due to the higher resistivity of niobium (4). Also, an outer layer of copper was provided to protect the platinum layer from scratches during handling.

TEST INSTALLATION

One end of the bridge was chosen for the test installation. The entire deck was not treated. The reinforcing steel (rebars) in this deck was about 50 mm (2 in) below the deck surface. The rebars were No. 5 deformed bars, and both the longitudinal and the transverse bars were set on 300-mm (1-ft) centers.

The installation was designed to test the following anode spacings: 1.22 m (4 ft), 0.91 m (3 ft), 0.61 m (2 ft), and 0.30 m (1 ft) to see which would give an acceptable distribution of current across the deck. The anodes were set in grooves cut into the deck. The grooves were 10 mm (3/8 in) wide by 19 mm (3/4 in) deep.

In order to determine the applied and polarized potentials on the rebars, a series of small copper and copper sulfate half-cells were set in holes drilled into the deck. The positions of these half-cells and the anodes with reference to the rebars are shown in Figure 1. Each half-cell was connected by its own wire to a jack on the control panel (Figure 2). The applied or "instant-off" voltage could then be read at the panel by a high-impedance voltmeter.

Two zinc half-cells were installed next to the rebars (Figure 3). These half-cells with their re-

Figure 1. Anode and probe locations.

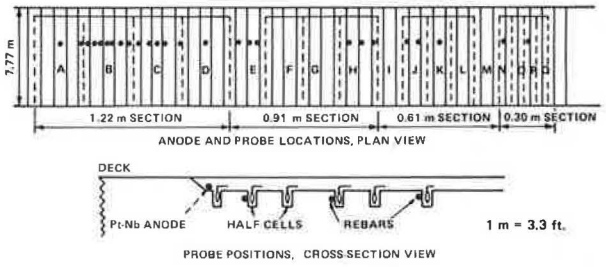

Figure 2. Control panel.

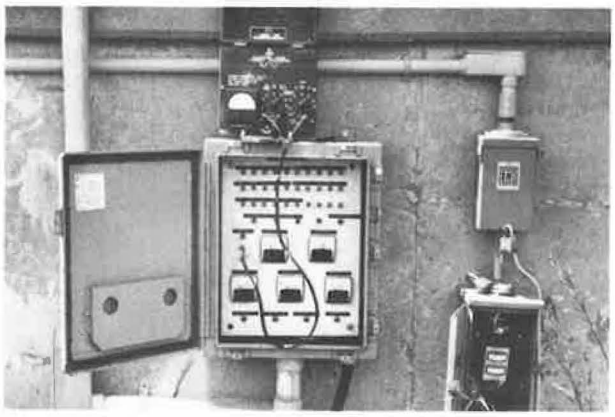

Figure 3. Deck wiring diagram.

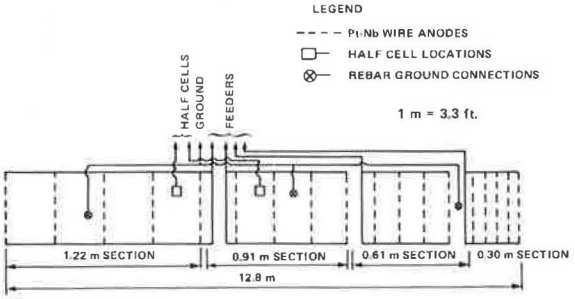

Figure 4. Laboratory test specimen.

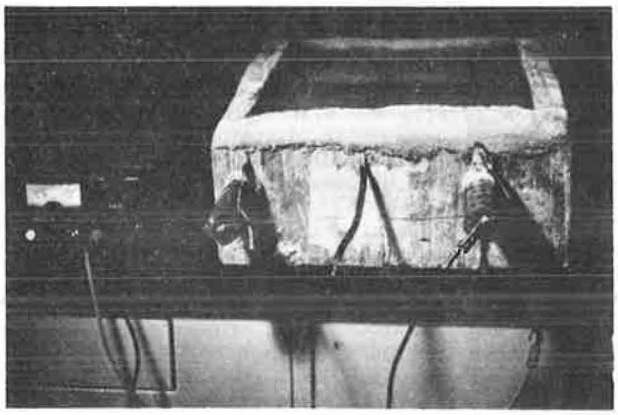

Figure 5. Voltage versus distance, 1.22-m section, applied voltage 6.0 V.

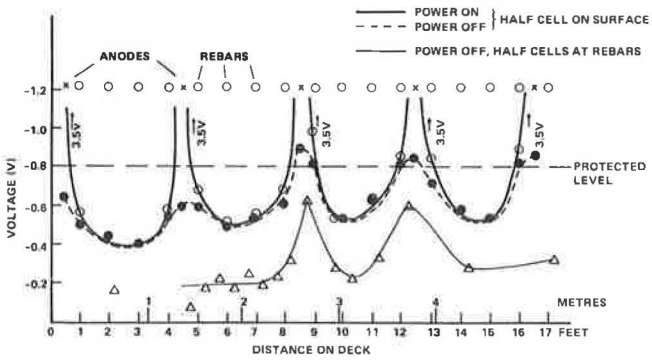

Figure 6. Voltage versus distance, 0.91-m sections, applied voltage 6.0 V.

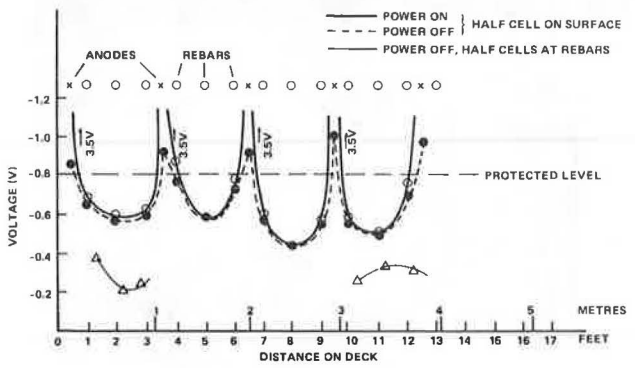

spective grounds were used to control and maintain the output voltage of the autovolt rectifier.

The anode wires were placed in their respective grooves. These grooves were then covered with a special nonshrinkable grout supplied by the supplier of the anode wire. Both ends of each anode wire were connected to the rectifier. This minimized the voltage drop due to the lengths of the narrow-gauge wire. The circuit is shown in Figure 3.

LABORATORY TEST SPECIMEN

In conjunction with the field investigation, a laboratory experiment was initiated to examine the physical and electrical properties of the platinized

Figure 7. Voltage versus distance, 0.61-m and 0.3-m sections, applied voltage 6.0 V.

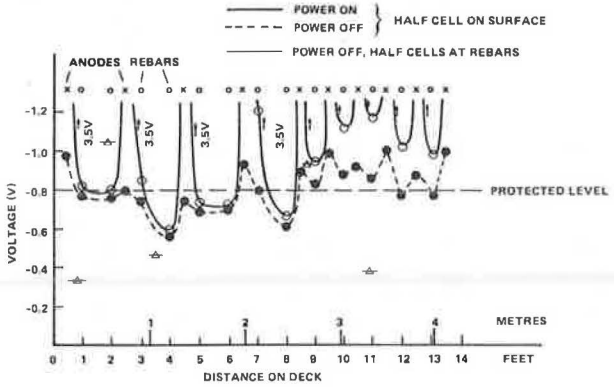

anodes and their effect on the concrete. A concrete specimen 400 mm by 300 mm by 120 mm (16 in x 12 in x 5 in) was made. This experimental specimen contained two prerusted rebars. These were set 200 mm (8 in) apart and positioned 25 mm (1 in) below the surface. The concrete used contained 2 percent salt (NaCl) by weight of the cement. Therefore, a corrosive condition existed and, at the same time, an excess of free chloride ions was present. After the specimen had been cured, three grooves were cut in its surface to a depth of 6 mm (0.25 in). Two of these grooves were directly over the rebars; the third was midway between these rebars. Platinized anode wires were placed in these grooves and covered with grout. A dyke was formed on the surface around the entire specimen. Water was ponded on the surface and cathodic protection was applied to the specimen by using a wire anode directly over one rebar. In order to get a polarized potential of 1 V on the other rebar, 7 V were required for this protection. The experimental slab and connections are shown in Figure 4.

OBSERVATIONS AND DISCUSSION

Power was applied to the platinized wire system on the bridge in January 1981. An application of 6 V DC was made, and when equilibrium had been established after several days, potential readings were taken. These readings were repeated periodically for six months and the deck surface was examined. Potential readings were taken near rebar level by means of the built-in copper and copper sulfate half-cells and on the surface by means of a copper and copper sulfate half-cell pressed on the deck surface. The on-off readings were obtained with a current interrupter in the anode circuit.

The voltage readings on the surface over the anodes were higher than those obtained at rebar level, the reason being that the anode wires were closer to the surface than to the imbedded half-cells. Samples of the series of readings taken are shown in Figures 5, 6, and 7. The on-instant-off readings are shown for those taken on the surface and only the instant-off readings for the subsurface half-cells. The on readings for these were very close to the off readings.

Figures 5 and 6 show that readings taken near the anodes were high but dropped off rapidly as the distance from the anode increased. In the 1.22-m (4-ft) section (Figure 5), the potential midway between two anodes was approximately 20 percent of the value obtained over the anode. This midpoint potential was not sufficient to protect the rebars. A minimum value of -0.8 V is required. To achieve

proper protection, the rectifier would have to operate at a higher potential than the 6 V used here. Such a high potential could cause disbonding of the concrete from the rebars in areas close to the anodes (5). Sufficient potential for protection was not achieved in either the 0.9-m (3-ft) or the 0.61-m (2-ft) section, as is shown in Figures 6 and 7.

The instant-off voltage was higher and more acceptable only in the 0.3-m (1-ft) spacing section (Figure 7). However, this spacing was not acceptable since it would greatly add to both the material and construction costs of the installation and would be too labor-intensive for most applications.

The deck readings shown in Figures 5, 6, and 7 were taken just after the deck surface had dried after a rainstorm. It seemed to make no difference when the readings were taken. Just after a rainstorm and dry, dry after several days, or summer or winter, the readings were all very similar.

An examination of the deck after six months of operation showed damage occurring to the concrete over some anodes. This is discussed in the next section.

Water was ponded on the surface of the laboratory experimental specimen. Cathodic protection (7 V) was applied to the specimen by means of an anode directly over a rebar. Three days later, a cavity 6 mm long developed directly over the current-carrying anode. The other anodes were used to apply power to the specimen, and cavities appeared over these anodes. This also is discussed in the following section.

Figure 8. Acid attack over anode on laboratory specimen.

Figure 9. Five centers of acid attack in grout.

CONCRETE DAMAGE

The higher potentials necessary in the Pt-Nb wire system for cathodic protection can lead to concrete damage. The chloride ions in salt-laden concrete will migrate more rapidly to the anode areas, causing an acidic condition to develop and possibly attack the concrete. This effect has now been observed in two field installations on bridge decks and on the experimental laboratory slab.

The laboratory slab sample, which was described previously, showed some damage. The grout used to cement the wire anodes in the grooves had been attacked in three places and the bare wire exposed. Each of the three anode wires was used in turn as the powered anode, and a green stain of copper chloride formed over the concrete. The acid action also caused a build-up of yellow-green foam at the center of attack. This was caused by escaping carbon dioxide. This gas was formed as the acid attacked the carbonates in the concrete. One of the attack sites and the exposed wire are shown in Figure 8.

On the bridge, after six months of application of cathodic protection, several active centers developed. Figure 9 shows an area in which five active centers developed close together, and the Pt-Nb wire was exposed. Figure 10 shows one center in which the wire was exposed, and Figure 11 shows a de-

Figure 10. Single center of acid attack in grout.

Figure 11. Developing center of acid attack.

veloping center. This bridge is under heavy ramp traffic and no water or moisture would remain on the surface for any length of time; the traffic would remove it and hence no stains of copper chloride were visible.

If this installation was kept under power (cathodic protection), it is believed that soon more of the anode wire would be bared and little or no power would be transferred to the deck slab. In fact, the wires might be damaged and broken by traffic passing over them.

One bridge, belonging to the City of Toronto, had an experimental system of platinized wire installed on it more than two years ago. The road surface was covered with asphaltic concrete, thus concealing the anode grooves. There were two lines of grouted-in anode wire visible down the length of each sidewalk. There were many locations along each of the anode lines and the dark areas where attack was taking place (Figure 12). The concrete in some of these areas was soft and could be dug out with a knife blade. Figure 13 is a close-up of a center in which active attack on the concrete was taking place and a cavity had formed. The froth over the center was caused by escaping CO_2 gas. The moisture in the cavity was tested with pH paper. The paper stained a deep red, showing a pH of 1 or less, indicative of a high acid concentration. The wire was exposed in the bottom of the hole and the platinum color was showing; all of the copper coating had been eaten by the acid. Several such active centers were observed on the deck. Another is shown in Figure 14. Vrable (5) also reported damage to concrete when platinized wire anodes were used.

It has been shown by Scott (6) and Vrable (5) that the application of larger amounts of current, more than is needed for effective cathodic protection, can cause a weakening of the bond between the rebar and the surrounding concrete. In the normal cathodic protection system, the current is distributed evenly over the deck by a conductive asphaltic concrete layer from which it flows to the rebars. In the wire system, there are points at which the current is concentrated and others at which the flow is considerably smaller. This can be seen by an examination of Figure 15. Here the Pt-Nb wires were

Figure 12. Municipal bridge: centers of acid attack along anode wires in sidewalk.

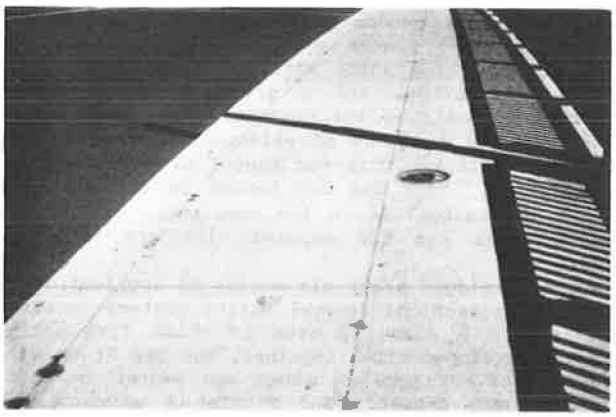

Figure 13. Municipal bridge: acid attack center, CO_2 foam and pH < 1.

Figure 14. Municipal bridge: acid attack center.

Figure 15. Circuit diagram for cathodic protection with Pt-Nb wire.

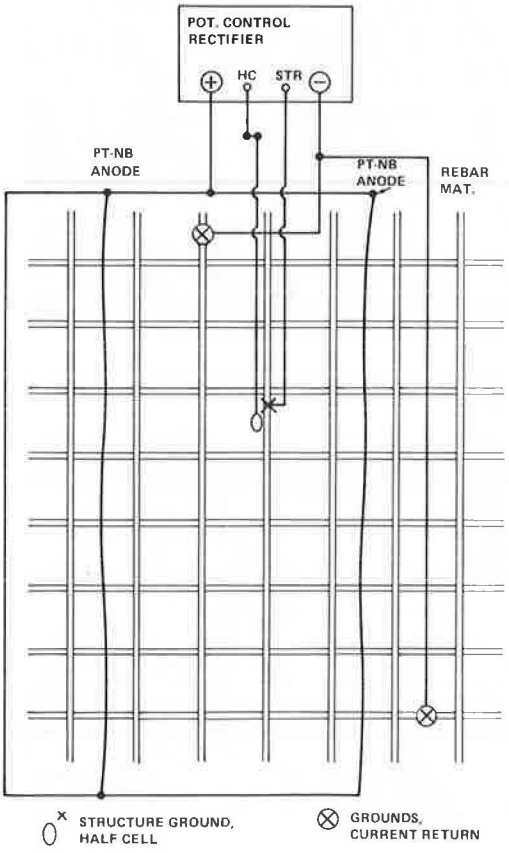

stretched and grouted in grooves 19 mm (0.75 in) deep midway between the transverse rebars. They were thus 152 mm (6 in) from each transverse bar. Where they crossed the longitudinal bars, however, they were only about 55 mm (2 in) above them. There would be, then, three times the current density flowing at each longitudinal rebar crossing as was flowing to each point on the transverse rebars. This concentrated current could weaken the bond between the rebar and the concrete after a period of time. This loss of strength might not be too serious in a slab bridge deck where the deck is supported on beams. It could, however, be a serious matter if the system were applied to, say, a parking garage floor in which there are no supporting beams between the pillars or to a support system under a bridge deck.

In the preceding section, it was shown that in order to get the necessary polarized voltage on the rebars, it would be necessary to use a 300-mm spacing of the wires. There would then be many points on each crossing rebar where the bond would be weakened, thus reducing the strength of the structure to which it was applied, whether it was a deck, parking garage floor, or a supporting structure for a bridge.

CONCLUSIONS

The conductivity of concrete is too low to permit an even distribution of power to the rebars by using a wire anode system without a conductive surface layer. The high DC voltages necessary to achieve the minimum polarized protection level of -0.8 V (with respect to the copper and copper sulfate half-cell) will overprotect some areas and could cause disbonding of the concrete from the rebars and reduce the strength of the structure.

The high DC voltages applied to the rebars attract chloride ions and cause an acid situation to develop. The acid attacks and destroys the concrete grout surrounding the wire and bares it. This reduces electrical contact with the concrete structure and reduces still further the passage of current into the structure.

The wire anode system is a good method for applying the current necessary for cathodic protection of bridge substructures, but it will have to be used in conjunction with a conductive surface layer. This is necessary so that a low applied potential can be used and still obtain an even distribution of current across the structure.

REFERENCES

1. H.J. Fromm. Bridge Rebar Corrosion--The Canadian Picture. Presented at Annual Meeting, National Association of Corrosion Engineers, Atlanta, GA, 1979.
2. F.B. Holt and D.G. Manning. Deterioration of Bridge Substructures--Phase 1. Ontario Ministry of Transportation and Communications, Downsview, Preliminary Rept., Jan. 1980.
3. J.P. Nickolson. New Approach to Cathodic Protection of Bridge Decks and Concrete Structures. TRB, Transportation Research Record 762, 1980, pp. 13-17.
4. T.H. Lewis, Jr. Platinized Anode in Carbonaceous Backfill--An Evaluation. Presented at Annual Meeting, National Association of Corrosion Engineers, Atlanta, GA, Paper 194, 1979.
5. J.B. Vrable. Cathodic Protection for Reinforced Concrete Bridge Decks. NCHRP, Rept. 180, 1977.
6. G.N. Scott. Corrosion Protection Properties of Portland Cement. Journal of the American Water Works Association, Vol. 57, No. 8, Aug. 1965.

Publication of this paper sponsored by Committee on Corrosion.

Scanning Rust Crystals and Salt Crystals with Electron Microscope

CARL F. CRUMPTON AND G.P. JAYAPRAKASH

Corrosion of reinforcing steel in concrete can create expansion pressures of 4700 psi. At 0° C, salt (halite) crystal growths can create pressures of 8140 psi at a supersaturation ratio of 2. Scanning electron micrographs of rust from corroding reinforcing steel in concrete show crystal laths and fretwork or boxwork crystals that eventually fill in and build up in layers. X-ray diffraction showed goethite and magnetite in the layers. Limonite, which is noncrystalline and does not show in X-rays, was also present. Halite crystal forms observed in air voids were fibers, columns, spirals, and ribbons. Entrained air voids help prevent or reduce salt crystal growth damage to concrete by providing empty space for the crystals to grow into. Scanning electron micrographs of the rust crystals and salt crystals are included.

Kansas salt corrosion studies of concrete reinforcing steel were done to see how volume increases of up to 13 times (1) and expansion pressures of as much as 4700 psi (2) could occur from the corrosion process. Studies were made on the scanning electron microscope at Kansas State University with some concrete taken from as near a freshly corroding rebar as possible. Swordlike laths of rust were found growing into the concrete near the steel as seen in Figure 1. Concrete petrographers can recognize the potential for one-dimensional growth here and also see the shape similarity to minerals such as ettringite, the growth of which in hardened concrete is known to be detrimental (3).

Another form of rust observed was a boxwork (Figure 2) or a fretwork of thin, apparently triangular-shaped walls with one of the points of the triangles growing away from the reinforcing steel such as that shown in Figure 3. Eventually both the lathlike and the fretwork structures become filled in with massive rust as seen in Figure 4, in which a few laths can still be seen around the edges of the glob of massive rust. Eventually reddish-, brownish-, and blackish-hued layers of such rust build up. These often contain what appears to be drying shrinkage cracks as shown in Figure 5.

Through X-ray diffraction studies of the layered rust we found the minerals goethite and magnetite.

Figure 1. Lathlike crystals of rust from corroding reinforcing bar protruding into concrete void (scale = 1μ).

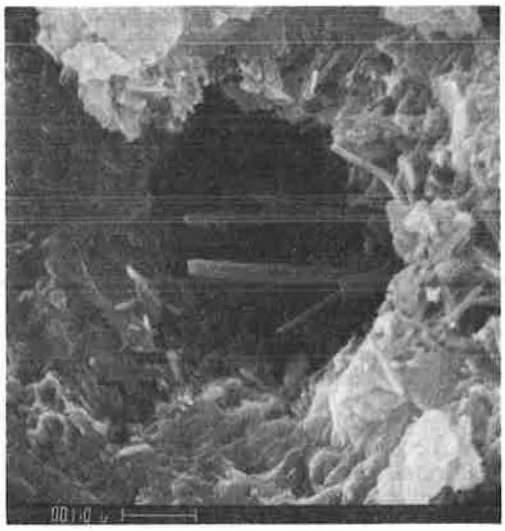

Figure 2. Boxwork of rust crystals in concrete (scale = 10μ).

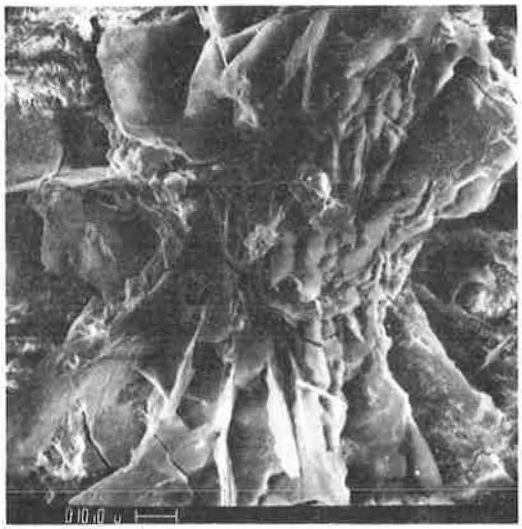

Figure 3. Fretwork of triangular rust crystals (scale = 1μ).

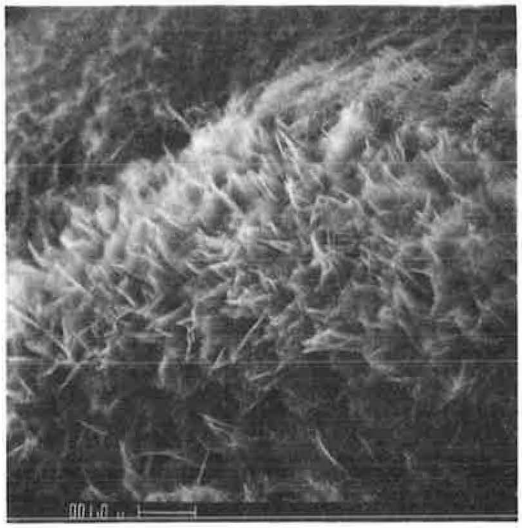

The lathlike and fretwork crystal forms shown in Figures 1, 2, and 3 are common forms for goethite (4). The bulk of the massive or globular rust seems to be limonite, which would not show up in the X-ray because limonite is noncrystalline. The rust laths were found in rusty spots at the surface of concrete as much as 2 in above the corroding reinforcing steel. Figure 6 was made at such a location.

From these studies and pictures, it began to be apparent how, as Spellman and Stratfull reported, the metal loss from a corrosion pit of less than 1-mil depth can produce sufficient corrosion products to crack a concrete cover of 875-mil thickness (5).

Growth of salt crystals in rock due to evaporation concentration precipitation can result in pressures that are capable of dislodging flakes of rock or of shattering objects (6). Calculations of the crystallization pressure of halite (NaCl) show that it can be more than 8140 psi at a supersaturation ratio of 2 and at a temperature of 0°C. At higher temperatures or higher supersaturation ratios, the pressure increases (7).

Another salt-related mechanical weathering process is due to the volume expansion of hydrating

Figure 4. Cluster of rust crystal laths being filled in with more massive rust.

Figure 5. Built-up layer of massive rust obliterating original crystal forms.

salt minerals (6). A well-defined hydrate of common salt, hydrohalite ($NaCl \cdot 2H_2O$), is known and is stable at or below 0°C (8). Since millions of tons of salt are used nationwide as a deicing chemical (9), the probability of hydrohalite formation and of damaging evaporation concentration precipitation of salt crystals in concrete is high. The formation of salt crystals has been suggested to contribute to the scaling type of concrete deterioration (10,11).

Helectites, stalactites, stalagmites, columns, crusts, and euhedral cubic crystals of common salt have been reported from caves in limestone and tubes in lava (12). In these studies, salt crystals were observed to grow in some of the salt-treated concrete as it dried. The salt crystals were first seen in air voids with a stereomicroscope but were studied in more detail with the scanning electron microscope. Sawed and polished faces of concrete cannot be used because the wet-preparation process would dissolve and wash away the salt crystals. Just as they do in caves, the halite crystals in concrete exhibit a wide variety of shapes, including fibers (Figure 7), columns (Figure 8), and spirals and ribbons (Figure 9). Similar fibers composed of calcite ($CaCO_3$), called needle and thread calcite growths, have been observed in the pores of Kansas loess (13).

In a few instances, concrete particles and quartz grains were observed at the free end of the salt fibers. Some of the salt crystals, such as those shown in Figure 10, look as though they were extruded from the concrete pores. Closer views show surface structures that suggest some growth by accretion and the bundle of fibers does not appear to extend down into the concrete but rests on its surface (Figure 11). To verify this, a cluster of salt fibers was dislodged with a micromanipulator. The area below the salt showed quite small pores in the concrete (Figure 12). The pores were much smaller than the salt crystals, as can be seen by comparing Figures 10 and 12. This indicates that the salt crystals grew by accretion from their base at the concrete surface rather than being extrusions from concrete pores.

No hydrohalite was found, but it is unstable at temperatures above 0°C. The concrete was not kept frozen before being examined; therefore, it is not known whether any hydrohalite had formed, nor is it

Figure 6. Rust crystal laths found at surface of concrete 2 in above corroding reinforcing steel.

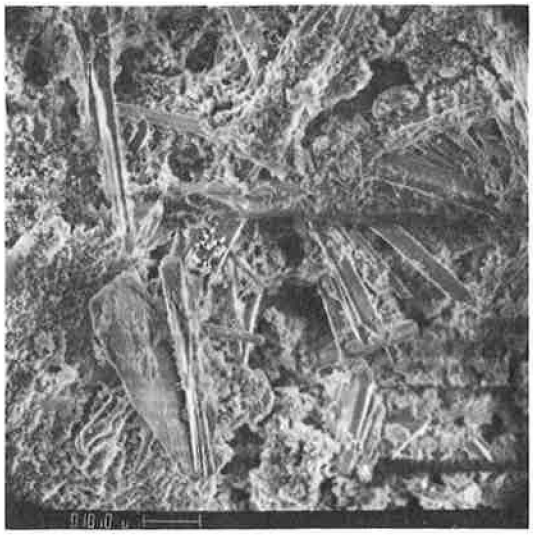

Figure 7. Fibrous crystal growths of salt (halite) in air void in concrete.

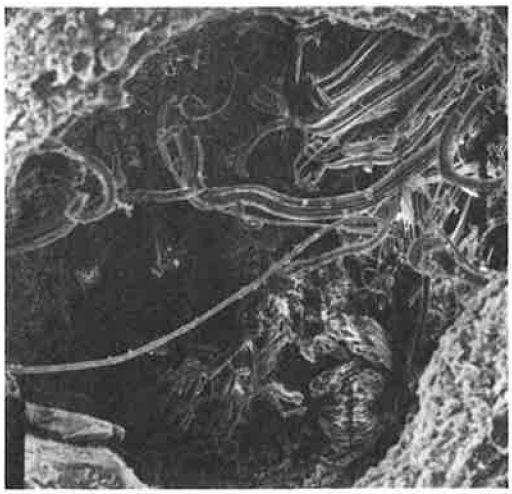

Figure 8. Columnar crystal growths of halite in concrete.

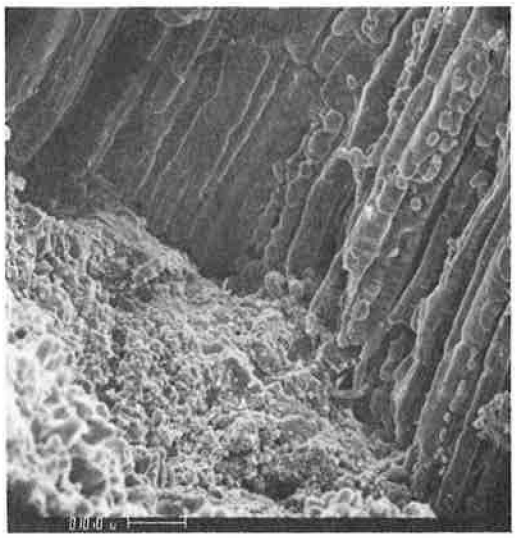

Figure 9. Spiral, ribbon, and fiber crystal growths of halite in concrete.

Figure 10. Ropelike cluster of halite fibers that look almost like extrusion from concrete pores (arrow points to same spot as arrow in Figures 11 and 12).

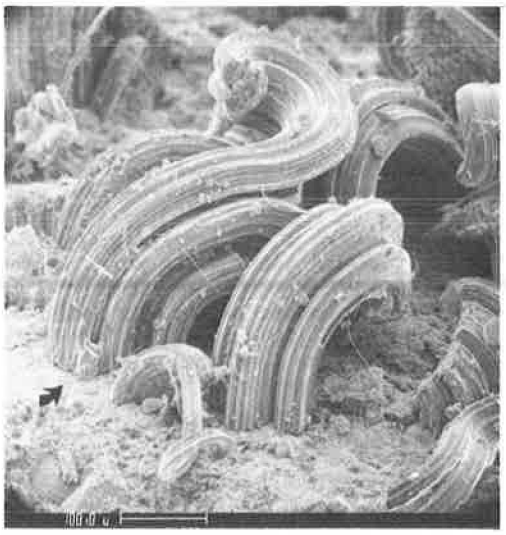

Figure 11. Enlarged view of interface of cluster of halite fibers with concrete at same location shown by arrow in Figure 10.

known whether other hydrated salts might have formed. As pointed out by Holden and Singer, any salt in which more than one state of hydration can form the higher hydrate always occurs at lower temperatures (14).

As early as 1905, it was demonstrated that crystal growth can exert a linear force (15,16). Hence the crystallization of salt similar to some of the forms shown can develop sufficient pressure to cause concrete deterioration. If one considers that one-dimensional growth of salt crystals and rust crystals might go on synergistically along with the formation of ice, it is easy to imagine what the combined effects on the concrete could be. The deterioration of bridge decks is good testimony to such destructive forces. The illustrations used here also show the importance of entrained air voids in helping prevent salt crystal growth damage. In the same way that they do for ice crystals, air voids provide empty space in the concrete for salt crystals to grow into.

Figure 12. Cluster of salt fibers removed with micromanipulator (same scale as Figure 10).

ACKNOWLEDGMENT

Garrett Morrison and William Gilliland, former research geologists, and John E. Bukovatz, concrete research engineer, who is currently the principal investigator on the project, were all involved in the work and their efforts are especially appreciated. The work was funded under the Highway Planning and Research Program; the assistance of the Kansas Department of Transportation and the Federal Highway Administration is appreciated. We thank John Krehma, Kansas State University, for his help and suggestions in obtaining the scanning electron microscope photographs. Mary Remboldt typed the original copy and made changes as we asked for them. Without her willing help, we could not have met the deadlines and we thank her for all her efforts.

The views, findings, and conclusions expressed here are ours and not necessarily those of the sponsoring agencies.

REFERENCES

1. J.R. Castelberry. Corrosion Prevention of Concrete and Metal Reinforcing in the Construction Industry. Materials Protection, March 1968, pp. 21-28.
2. J.P. Callahan, C.P. Siess, and C.E. Lesler. Effect of Stress on Freeze-Thaw Durability of Concrete Bridge Decks. NCHRP, Rept. 101, 1970.
3. P.K. Mehta and A. Klein. The Formation of Ettringite in Pastes Containing Calcium Alumino-Ferrite and Gypsum. HRB, Highway Research Record 192, 1967, pp. 32-45.
4. W.E. Ford. Dana's Textbook of Mineralogy. 4th ed., John Wiley and Sons, New York, NY, 1949.
5. D.L. Spellman and R.F. Stratfull. Chlorides and Bridge Deck Deterioration. HRB, Highway Research Record 328, 1970, pp. 38-49.
6. P.W. Berkland and E.E. Larson. Putnam's Geology. Oxford Univ. Press, New York, NY, 1978.
7. E.M. Winkler and P.E. Singer. Crystallization Pressure of Salts in Stone and Concrete. Geological Society of America Bulletin, Vol. 83, Nov. 1972, pp. 3509-3514.
8. W.A. Deer, R.A. Howie, and J. Zussman. Rock Forming Minerals. Longmans, Green, London, 1963, Vol. 5.

. U.S. Will Need 11 Million Tons of Salt for 1981-1982 Winter. Better Roads, Dec. 1981, pp. 14-15.
. W.A. Cordon. Freezing and Thawing of Concrete-Mechanisms and Control. American Concrete Institute, Detroit, MI, ACI Monograph 3, 1966.
1. W.C. Hansen. Crystal Growths as a Source of Expansion in Portland Cement Concrete. Proc. ASTM, Vol. 63, 1963, pp. 932-945.
2. C.A. Hill. Cave Minerals. National Speleological Society, Huntsville, AL, 1976.
3. C.F. Crumpton and W.A. Badgley. A Study of the Clay Mineralogy of Loess in Kansas in Relation to Its Engineering Properties. State Highway Commission of Kansas, Topeka, and U.S. Bureau of Public Roads, 1965. NTIS: PB 173038.
14. A. Holden and P. Singer. Crystals and Crystal Growing. Doubleday, Garden City, NY, 1960.
15. G.F. Becker and A.L. Day. The Linear Force of Growing Crystals. Proc., Washington Academy of Sciences, Vol. 7, 1905, pp. 283-288.
16. S. Taber. The Growth of Crystals Under External Pressure. American Journal of Science, Vol. 41, 1916, pp. 532-556.

Publication of this paper sponsored by Committee on Corrosion.